NEDERL. AKADEMIE VAN WETENSCHAPPEN

PROCEEDINGS

VOLUME XLV

No. 6

President: J. VAN DER HOEVE

Secretary: M. W. WOERDEMAN

CONTENTS

K 244

Geophysics. — *On Surface Waves in a Stratisfied Medium.* III. By J. G. SCHOLTE.
(Communicated by Prof. J. D. VAN DER WAALS.)

(Communicated at the meeting of March 28, 1942.)

Putting these results otherwise: if $\mathfrak{V}_2 > \mathfrak{V}_1 > S_2$ there exists for every value of μ_2/μ_1 and N a completely damped wave system; for some values of N and μ_2/μ_1 a second damped system is possible.

It is to be observed that, if $\mathfrak{V}_1 < \mathfrak{V}_2$, no other superficial waves are possible than those which correspond to the roots ζ, the existence of which we have just discussed. Such waves must always be damped in the semi-infinite medium 1, $\cos r_1$ being imaginary; hence $\sin r_1 > 1$; and as $\mathfrak{V}_2 > \mathfrak{V}_1$ r_1 is the smallest of the occurring angles r_1, i_1, r_2, i_2, so that all sines are >1; therefore all cosines are imaginary, *i.e.* all waves are damped.

The matter is not so simple in the opposite case: $\mathfrak{V}_1 > \mathfrak{V}_2$. Here the waves in medium 1 are of course also damped, but the amplitude-distribution in the layer can be sinusoidal, exponential and semi-sinusoidal, as $\cos r_2$ and $\cos i_2$ can be both real, or both imaginary or $\cos i_2$ imaginary and $\cos r_2$ real.

As we have already mentioned, in this paper we shall only deal with the wave system which is also damped in the superficial layer.

B. $\omega > 1$ ($\mathfrak{V}_1 > \mathfrak{V}_2$).

In this case the roots of equation (1) have to be smaller than $1/\omega$; therefore this equation has a single root if its left-hand side is greater than the right-hand side for $\zeta = 1/\omega$. That is, if

$$\left\{\left(2-\frac{1}{\omega}-\frac{\mu_2}{\mu_1}\right)^2-\left(2-\frac{\mu_2}{\mu_1}\right)^2\sqrt{\left(1-\frac{\nu_1}{\omega}\right)\left(1-\frac{1}{\omega}\right)}\right\}.(4\varphi_2\sqrt{1-\nu_2}-N\,tgh\,\alpha_2)+$$

$$+\left\{\left(2-2\frac{\mu_2}{\mu_1}\right)^2\sqrt{\left(1-\frac{\nu_1}{\omega}\right)\left(1-\frac{1}{\omega}\right)}-\left(2-\frac{1}{\omega}-2\frac{\mu_2}{\mu_1}\right)^2\right\}.\sqrt{1-\nu_2}.(-\varphi_2)>$$

$$\frac{\mu_2}{\mu_1}.\frac{\sqrt{(1-\nu_2)\left(1-\frac{1}{\omega}\right)}}{\omega}.(4\sqrt{1-\nu_2}.tgh\,\alpha_2-N)+\frac{\mu_2}{\mu_1}.\frac{\sqrt{1-\frac{\nu_1}{\omega}}}{\omega}.(-tgh\,\alpha_2)+$$

$$+\frac{\sqrt{1-\nu_2}}{\cosh\alpha_2}.\left(4\sqrt{1-\frac{\nu_1}{\omega}\left(1-\frac{1}{\omega}\right)}-\left(2-\frac{1}{\omega}\right)^2\right)$$

or:

$$\left(\frac{\mu_2}{\mu_1}\right)^2.\left\{1-\sqrt{\left(1-\frac{1}{\omega}\right)\left(1-\frac{\nu_1}{\omega}\right)}\right\}.(8\varphi_2\sqrt{1-\nu_2}-N\,tgh\,\alpha_2)-$$

$$-\left(\frac{\mu_2}{\mu_1}\right).\left\{2\left(2-\frac{1}{\omega}-2\sqrt{\left(1-\frac{1}{\omega}\right)\left(1-\frac{\nu_1}{\omega}\right)}\right)(6\varphi_2\sqrt{1-\nu_2}-N\,tgh\,\alpha_2)+\right.$$

$$\left.+\frac{1}{\omega}\left(4(1-\nu_2)\sqrt{1-\frac{1}{\omega}}-\sqrt{1-\frac{\nu_1}{\omega}}\right)tgh\,\alpha_2-\frac{\sqrt{1-\frac{1}{\omega}}}{\omega}N\sqrt{1-\nu_2}\right\}+$$

$$+\left\{\left(2-\frac{1}{\omega}\right)^2-4\sqrt{\left(1-\frac{1}{\omega}\right)\left(1-\frac{\nu_1}{\omega}\right)}\right\}(4\varphi_2\sqrt{1-\nu_2}-N\,tgh\,\alpha_2+\sqrt{1-\nu_2})>0 \quad (5)$$

where

$$a_2 = \frac{p\,d}{\mathfrak{B}_2}\sqrt{1-\nu_2} = N\sqrt{1-\nu_2}.$$

If this inequality is not satisfied equation (1) has no roots (or two roots).

The surface of separation between the two above mentioned parts of the $\{\omega, \mu_2/\mu_1, N\}$-space is here expressed by the equation:

$F\left(\frac{\mu_2}{\mu_1}\right) = 0$, $F\left(\frac{\mu_2}{\mu_1}\right)$ being the left-hand side of the inequality (5) ..... (6).

To determine the asymptotes of the "boundary-curves $1/\omega$" (the curves of intersection of the surface (6) with the planes ω = a constant) we put, just as in the preceding section *A*, $N = \sim$. Equation (6) becomes for $N = \sim$ the Stoneley boundary-equation.

$$\left(\frac{\mu_2}{\mu_1}\right)^2 \cdot \left\{1 - \sqrt{\left(1-\frac{1}{\omega}\right)\left(1-\frac{\nu_1}{\omega}\right)}\right\} - \left(\frac{\mu_2}{\mu_1}\right) \cdot \left\{2\left(2-\frac{1}{\omega}-2\sqrt{\left(1-\frac{1}{\omega}\right)\left(1-\frac{\nu_1}{\omega}\right)}\right) + \right.$$

$$\left. + \frac{\sqrt{1-\nu_2}}{\omega}\sqrt{1-\frac{1}{\omega}}\right\} + \left\{\left(2-\frac{1}{\omega}\right)^2 - 4\sqrt{\left(1-\frac{1}{\omega}\right)\left(1-\frac{\nu_1}{\omega}\right)}\right\} = 0.$$

This curve was discussed in our paper on STONELEY-waves [5]) — the second curve of figure 5 ($\omega > 1$) is its graphic representation.

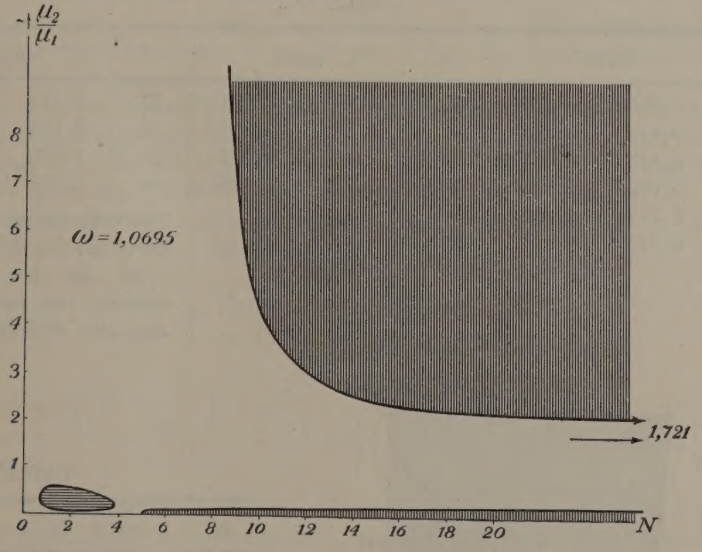

Fig. 11

TABLE VIII.

N	μ_2/μ_1		N	μ_2/μ_1		N	μ_2/μ_1	
0.75	0.476	0.343	3.5	0.402	0.119	9	7.013	0.0872
0.8	0.542	0.281	3.8	0.296	0.141	10	4.367	0.0876
1	0.642	0.191	4	0.205	0.171	12	3.027	0.0880
1.5	0.690	0.133	5	−0.1003	0.0230	14	2.603	0.0883
2	0.662	0.117	6	−1.023	0.0748	20	2.167	0.0884
3	0.520	0.113	7	−3.81	0.0805	$\sim$	1.721	0.0889
3.2	0.471	0.116	8	$\sim$	0.0849			

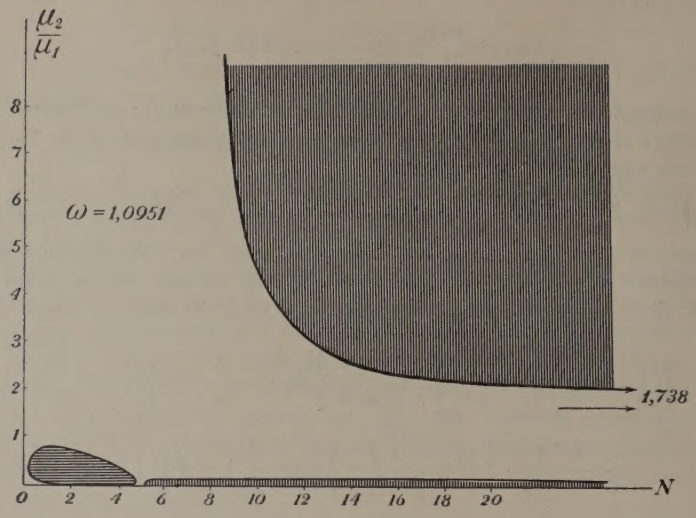

Fig. 12

TABLE IX.

N	μ_2/μ_1		N	μ_2/μ_1		N	μ_2/μ_1	
0.125	0.368	0.129	3	0.556	0.001	12	3.118	
0.150	0.421	0.093	4	0.298	9.002	14	2.654	
0.200	0.478	0.037	4.7	0.067	0.002	20	2.196	
0.500	0.760	0.005	4.8	0.026	0.002	$\sim$	1.738	0.0014
1	0.772	0.002	9	7.021				
2	0.713	0.001	10	4.500				

(the ordinates of the second curve are for $N > 5$ very small and are therefore omitted; this curve nearly coincides with the N-axis).

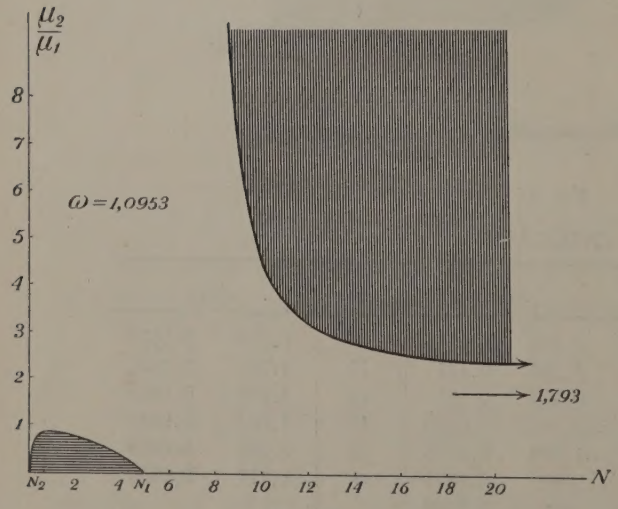

Fig. 13

TABLE X.

N	μ_2/μ_1	N	μ_2/μ_1	N	μ_2/μ_1
$\sim$	1.793	4.8	0.0272	0.5	0.81
20	2.263	4.5	0.178	0.2	0.69
16	2.498	4	0.380	0.1	0.45
12	3.203	3	0.590	0.051	0.00
10	4.615	2	0.732		
9	7.438	1	0.827		

The asymptotes parallel to the N-axis of the boundary-curves $1/\omega$ are $N = a_1$ and $N = a_2$, a_1 and a_2 being the roots of the last quadratic. At increasing value of ω a_2 diminishes, as will be seen from fig. (5); this root is equal to zero if $\omega = \left(\frac{\mathfrak{B}_1}{S_1}\right)^2$ or $S_1 = \mathfrak{B}_2$, and for still larger values of ω ($S_1 > \mathfrak{B}_2$) it is negative. The other root (a_1) increases with growing value of ω and approaches a certain finite value, if ω tends to infinite.

To obtain the asymptotes parallel to the μ_2/μ_1 axis we put $\mu_2/\mu_1 = \sim$; equation (6) reduces then to:

$$8\,\varphi_2\sqrt{1-\nu_2} - N\,tgh\,a_2 = 0.$$

As this equation is independent of ω its root remains the same at every value of ω; at $\omega = 1$ this root appeared to be $N = N_0$, (see fig. 4 and 9), therefore it is always $N = N_0$, if $\omega > 1$. Consequently the line $N = N_0$ is an asymptote of every boundary-curve $1/\omega$.

Again it will be obvious that the boundary-curves $1/\omega$ meet the N-axis for every value of ω (> 1) in the same point $N = N_1$, N_1 being the root of

$$4\,\varphi_2\sqrt{1-\nu_2} - N\,tgh\,a_2 + \sqrt{1-\nu_2} = 0.$$

This has an important bearing on the further analysis of these curves.

Considering only the asymptotes, we should expect two boundary-curves if $S_1 < \mathfrak{B}_2$; one going from $N = \sim$, $\mu_2/\mu_1 = a_1$, towards $N = N_0$, $\mu_2/\mu_1 = \sim$, and the other going from $N = \sim$, $\mu_2/\mu_1 = a_2$, towards $N = N_0$, $\mu_2/\mu_1 = -\sim$. If S_1 approaches the value $\mathfrak{B}_2$ this second curve draws near to the N-axis; if $S_1 = \mathfrak{B}_2$, it coincides with this axis and if $S_1 > \mathfrak{B}_2$, it disappears wholly to negative values of μ_2/μ_1.

This, however, is impossible: equation (6) is quadratic with respect to μ_2/μ_1 and should therefore always have two roots. Consequently, if $S_1 = \mathfrak{B}_2$, a third curve must exist between $N = N_0$ and $N = o$. This curve can not completely be lying unter the N-axis, as it meets this line at $N = N_1$.

Except the asymptote $N = N_0$ this curve also has the asymptote $N = o$, as can be seen by taking N very small; then equation (6) changes into:

$$\left(\frac{\mu_2}{\mu_1}N\right)^2 \cdot \left\{1 - \sqrt{\left(1-\frac{1}{\omega}\right)\left(1-\frac{\nu_1}{\omega}\right)}\right\}(3-4\nu_2) -$$

$$-\left(\frac{\mu_2}{\mu_1}N\right) \cdot \frac{(3-4\nu_2)\sqrt{1-\frac{1}{\omega}} - \sqrt{1-\frac{\nu_1}{\omega}}}{\omega} + \left\{\left(2-\frac{1}{\omega}\right)^2 - 4\sqrt{\left(1-\frac{1}{\omega}\right)\left(1-\frac{\nu_1}{\omega}\right)}\right\} = 0.$$

If $S_1 = \mathfrak{B}_2$ the last term of this equation is equal to zero, therefore one of its roots $\mu_2/\mu_1 = o$ and the other is very large, $N \times \mu_2/\mu_1$ remaining finite. The third curve, therefore, goes from $\mu_2/\mu_1 = -\sim$ ($N = N_0$) to $\mu_2/\mu_1 = +\sim$ ($N = o$), meeting the N-axis in the point $N = N_1$.

At larger values of ω ($S_1 > \mathfrak{B}_2$) this new branch of the boundary-curve $1/\omega$ does not very much alter its shape, as its asymptotes ($N = o$ and $N = N_0$) and the point of intersection $N = N_1$ with the N-axis remain the same if ω varies.

Lastly we observe that it is necessary for this third curve to arise continuously from the curves which exist in the case $S_1 < \mathfrak{B}_2$. Some consideration shows that in that case a loop occurs which increases in length at increasing value of ω, so that in the limiting case $S_1 = \mathfrak{B}_2$ this loop splits up into the N-axis and a curve which has the μ_2/μ_1 axis as an asymptote.

With some numerical computation the shape of the curves (6) at various values of ω can be easily determined (fig. 11—15).

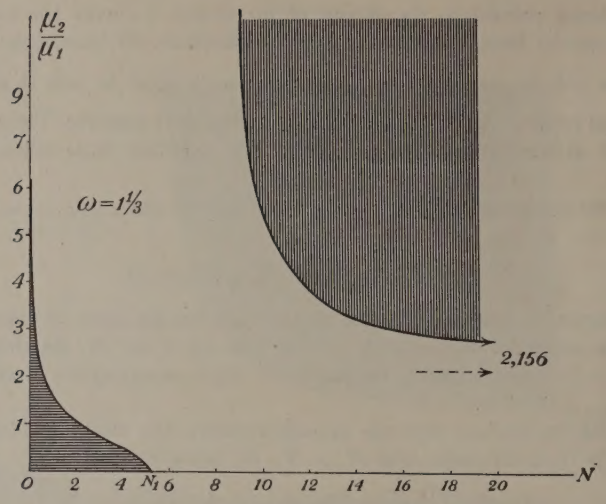

Fig. 14

TABLE XI.

N	μ_2/μ_1	N	μ_2/μ_1	N	μ_2/μ_1
$\sim$	2.156	9	8.656	3	0 808
20	2.698	4.9	0.032	2	1.042
14	3.238	4.8	0.092	1	1.623
12	3.781	4.5	0.262	0.5	2.098
10	5.405	4	0.489	0.2	4.492

TABLE XII.

N	μ_2/μ_1	N	μ_2/μ_1
$\sim$	2.563	4	0.590
20	3.205	3	0.983
14	3.847	2	1.279
12	4.490	1	1.828
10	6.440	0.5	2.879
9	10.27	0.2	13.66
4.5	0.317		

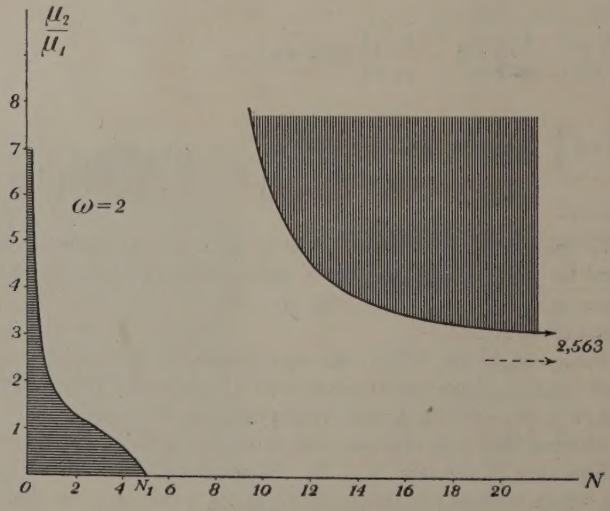

Fig. 15

Now we have to ascertain the number of roots in the two parts of the $\{\omega, \mu_2/\mu_1, N\}$-space, separated by the surface (6).

It has been pointed out by us [5]) that the STONELEY equation has no roots if $a_1 > \mu_2/\mu_1 > a_2$; further the RAYLEIGH root ζ_R satisfies equation (1). We see therefore at once that in the part of the $\{\mu_2/\mu_1, N\}$-plane which for large values of N lies between the two asymptotes $N = a_1$ and $N = a_2$, one root exists. If $S_1 < \mathfrak{V}_2$ there is no root in the area encircled by the loop, while in the remaining parts of the $\{\mu_2/\mu_1, N\}$-plane two roots are possible, which pass into ζ_R and ζ_S at large values of N. Is $S_1 > \mathfrak{V}_2$ then the just mentioned area within the loop changes into the part of the $\{\mu_2/\mu_1, N\}$-plane which lies between the μ_2/μ_1 axis and the third curve discussed above. In the remaining sections again two roots are possible.

Summarizing the results obtained in this paragraph we can roughly state, that there is always one root of equation (1), except for large values of N if $\mathfrak{V}_1 < S_2$ and for small values of N if $\mathfrak{V}_2 < S_1$. A second root is possible in some parts of the $\{\omega, \mu_2/\mu_1, N\}$-space if $\mathfrak{V}_1 > S_2$.

In the figures 6—15 the areas where no roots exist, are shaded by horizontal lines, and the areas where two roots are possible by vertical lines; in the non-shaded areas one root exists.

Par. 6. The dispersion-curves.

The waves corresponding to the roots of equation (1) are damped in the two media. The periodic factor of the wave-functions, for instance $e^{i(pt - k_1 x \sin r_1 - k_1 z \cos r_1)}$, being now $e^{i(pt - k_1 x \sin r_1)}$ or $e^{ip\left(t - \frac{x}{\mathfrak{V}_1\sqrt{\zeta}}\right)}$ it is evident that $\mathfrak{V}_1\sqrt{\zeta}$ represents the phase-velocity S of these waves; hence $\zeta = \frac{S^2}{\mathfrak{V}_1^2}$. Therefore equation (1) determines at given values of the material constants the phase-velocity as a function of the frequence p, N being equal to $\frac{pd}{\mathfrak{V}_2}$; in other words: equation (1) is the equation of the dispersion-curves.

We shall finish this paper with a problem recently discussed again by SEZAWA and KANAI, *viz.* the shape of the dispersion-curves. If the accurate shape of such a curve in a particular case is needed, it is of course necessary to solve equation (1), which can only be done by the method of trial and error. To arrive at a general survey of these curves at various values of the material constants, which is the main purpose of SEZAWA and KANAI [6, 8, 9, 10]), this method is unnecessary and somewhat laborious. This problem can be solved by using the results obtained in the preceding paragraph.

It is obvious that the roots of equation (1) have the following values:

1. at $N = 0$: $\zeta = \frac{S_1^2}{\mathfrak{V}_1^2}$ being the root of the RAYLEIGH equation for medium 1; as $\zeta = \frac{S^2}{\mathfrak{V}_1^2}$ we get $S = S_1$.
2. at $N = \infty$ one root $\zeta = \zeta_R = \frac{S_2^2}{\mathfrak{V}_1^2}$ or $S = S_2$ and the other one $= \zeta_S = \frac{S_{st}^2}{\mathfrak{V}_1^2}$; hence $S = S_{st}$, S_{st} being the phase-velocity of the STONELEY waves.
3. in any point of the boundary-curves $\zeta = 1$, one root $\zeta = 1$ or $S = \mathfrak{V}_1$.
4. in every point of the boundary-curves $1/\omega$ one root $\zeta = 1/\omega$ or $S = \mathfrak{V}_2$.

Supposing $\mu_2/\mu_1 =$ a constant c and ω increasing from small values ($S_1 < \mathfrak{V}_2$) to larger values ($S_2 < \mathfrak{V}_1$). This means that $\frac{\varrho_2}{\varrho_1}$ increases, in other words that the density of the layer increases with respect to the subjacent medium.

Choosing $c > a_1$ (fig. 6) the line $\mu_2/\mu_1 = c$ meets the boundary-curve $\zeta = 1$. The roots of equation (1) increase along this line with increasing value of N from $\zeta = \frac{S_1^2}{\mathfrak{V}_1^2}$ in $N = o$ to $\zeta = 1$ for a not very large value of N. The corresponding values of S increase from S_1 to $\mathfrak{V}_1$. At larger values of ω the course of the roots is about the same, except that the point of intersection of the line $\mu_2/\mu_1 = c$ with the boundary-curve $\zeta = 1$ occurs at a larger value of N (see curve I and II of fig. 16).

As for $\omega = \frac{S_2^2}{\mathfrak{V}_2^2}$ or $\mathfrak{V}_1 = S_2$ this point lies at $N = \sim$ the dispersion curves do not meet the line $S = \mathfrak{V}_1$ if $S_1 > \mathfrak{V}_2$. When $\mathfrak{V}_2 > \mathfrak{V}_1 > S_2$ S increases from S_1 (in $N = o$) to S_2 (in $N = \sim$). For a certain value of ω, say ω_1, S_1 is equal to S_2 (for instance this occurs at $\omega = 1$ if $\lambda_1 = \lambda_2$); then the dispersion curve has a maximum, which exists also for values of ω nearly equal to ω_1 (curve III and IV).

If $\mathfrak{V}_1 > \mathfrak{V}_2 > S_1$ there are two possibilities, as the line $\mu_2/\mu_1 = c$ meets the loop formed by the boundary-curve $1/\omega$ or lies completely above this loop. Taking the first case, the line $\mu_2/\mu_1 = c$ intersects the boundary-curve in the points $N = N_1$ and $N = N_2$. The value of S increases then from S_1 (at $N = o$) to $\mathfrak{V}_2$ (at $N = N_1$) and is again equal to $\mathfrak{V}_2$ at $N = N_2$; therefore between N_1 and N_2 the dispersion curve must show a maximum. This part of the dispersion curve relates to wave systems which are not completely damped. For values of $N > N_2$ S diminishes towards S_2 (at $N = \sim$) (curve V and VI).

At still larger values of ω S_1 is larger than $\mathfrak{V}_2$; the line $\mu_2/\mu_1 = c$ meets the first branch of the boundary-curve $1/\omega$ in one point $N = N_1$. Then $S = S_1$ at $N = o$, $S = \mathfrak{V}_2$ at $N = N_1$, and $S = S_2$ at $N = \sim$; for $N < N_1$ the wave system is semi-exponential or periodical (curve VII and VIII).

If $\mu_2/\mu_1 = c$ does not intersect the loop the part $N_1 < N < N_2$ of the dispersion curves where a damped wave system is impossible, does not occur; for the rest the shape of the dispersion curves differ but slightly from the curves described above.

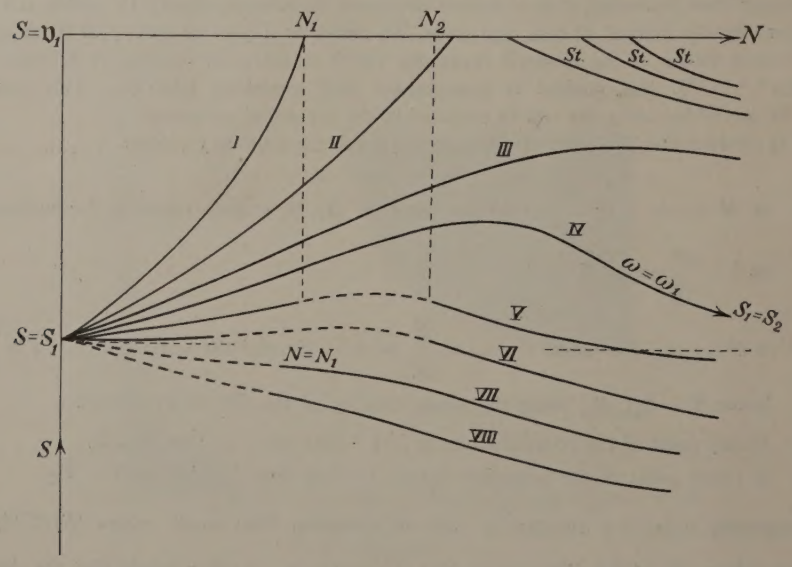

Fig. 16
Dispersion curves at various values of ω (qualitatively determined).

A second dispersion curve appears at a certain value of $\omega > \left(\frac{S_2}{\mathfrak{V}_2}\right)^2$, as the line $\mu_2/\mu_1 = c$ must intersect the boundary-curve $\zeta = 1$ (fig. 7—10) and consequently lies partly in the part of the $\{\omega, \mu_2/\mu_1, N\}$-space where two damped wave systems are possible. The value of S increases from S_{St} at $N = \sim$ to $S = \mathfrak{V}_1$ at a certain finite value of N. This value of N decreases with growing value of $\omega < 1$ and increases again if $\omega > 1$; if μ_2/μ_1 is not very large this dispersion-curve disappears finally. It is, however, possible that this curve exists for every value of $\omega > 1$, namely if μ_2/μ_1 is larger than the limiting value of a_2 (the ordinate of the asymptote of the boundary-curve $1/\omega$) for large values of ω (see fig. 5 where this limiting value of a_2 is equal to 3,268).

Par. 7. *Summary.*

By means of the simple theory of reflection and refraction of elastic waves all damped wave systems possible in a stratisfied medium have been determined in this paper. About one of these systems — the LOVE wave system — no further discussion is given here, as its properties are very well known. The remaining system, consisting of generalized RAYLEIGH and STONELEY waves, has been investigated. It appears that this system is only possible for certain values of the material constants; these values have been determined by an analysis of the period equation corresponding to these waves. As the results are not essentially altered by a special assumption, the numerical calculations have been carried out for incompressible media (these results can be read in our tables 3—12). The dispersion curves relating to these wave systems are discussed and their general shape has been qualitatively ascertained.

In conclusion I wish to express my sincere thanks to Prof. J. D. VAN DER WAALS for his great interest taken in this paper.

LITERATURE.

1. H. LAMB, „On the propagation of tremors". Phil. Trans. Roy. Soc. London, **203** (1904).
2. A. E. H. LOVE, „Some problems of Geodynamics" (1911).
3. BROMWICH, „On the influence of Gravity on elastic waves". Proc. Math. Soc. London, **30** (1899).
4. A. STONELEY, „Elastic waves at the surface of separation of two solids". Proc. Roy. Soc. London, **106** (1924).
5. J. G. SCHOLTE, „On the Stoneley-wave equation". Proc. Ned. Akad. v. Wetensch., Amsterdam, **45**, 20, 159 (1942).
6. K. SEZAWA and K. KANAI, „The range of possible existence of Stoneley-waves". Bull. Earthq. Res. Inst. Tokyo, 1, **17** (1939).
7. A. STONELEY, „The transmission of Rayleigh waves". M.N.R.A.S. Geoph. Suppl., 222, **3** (1936).
8. K. SEZAWA, „Dispersion of Elastic Waves". Bull. Earthq. Res. Inst., Tokyo, 1, **3** (1927).
9. K. SEZAWA and K. KANAI, „Anomalous dispersion of elastic Surface waves". Bull. Earthq. Res. Inst. Tokyo, 226, 683, **16** (1938).
10. ———— „Discontinuity in the dispersion curves of Rayleigh waves", ibid., 237, **13** (1935).
11. H. LAMB, „On waves in an elastic plate". Proc. Roy. Soc. London, 114, **93** (1917).
12. H. JEFFREYS, „The Earth" (1928).

Correction. In part I of this paper (Proceedings page 385) the expression

$$P = \left(1 - 2\frac{\mu_2}{\mu_1} + \frac{\varrho_2}{\varrho_1}\zeta\right)^2$$

should be replaced by

$$P = \left(2 - \zeta - 2\frac{\mu_2}{\mu_1} + \frac{\varrho_2}{\varrho_1}\zeta\right)^2.$$

Applied Mechanics. — *On the state of stress in perforated strips and plates.* (4th Communication.) By K. J. SCHULZ. (Communicated by Prof. C. B. BIEZENO.)

(Communicated at the meeting of May 30, 1942.)

7b. *The symmetrical strip with one row of holes under tension (Continuation.)*
Let the result of the ith iteration be represented by the stresses

$$\sigma_r = -C_0^{(i)} - \sum_{n=1}^{\infty} C_{2n}^{(i)} \cos 2n\varphi, \qquad \tau_{r\varphi} = -\sum_{n=1}^{\infty} D_{2n}^{(i)} \sin 2n\varphi \quad . \quad (14)$$

at the hole-boundaries I and by the stresses

$$\sigma_z = -\sum_{n=1}^{\infty} C_n^{\prime(i)} \cos 2\pi n \frac{y}{b}, \qquad \tau_{yz} = \mp \sum_{n=1}^{\infty} D_n^{\prime(i)} \sin 2\pi n \frac{y}{b} \quad . \quad (15)$$

at the straight boundaries II and III.

Upon this system of stresses an other one is superposed, which is due to the stress-function

$$F^{(i)} = C_0^{(i)} U_{\sigma 0} + \sum_{s=1}^{\infty} (C_{2s}^{(i)} U_{\sigma, 2s} + D_{2s}^{(i)} U_{\tau, 2s}) \quad . \quad . \quad . \quad . \quad (16)$$

relating to the holes of the strip, and to the two stress-functions

$$F^{\prime(i)} = \sum_{s=1}^{\infty} (C_s^{\prime(i)} F_{\sigma s}^{\prime} + D_s^{\prime(i)} F_{\tau s}^{\prime}) \quad . \quad . \quad . \quad . \quad . \quad . \quad (17)$$

relating to the two straight boundaries II and III. These stress functions are built up in such a way, that the main or principal terms of (16) — comp. section **3** — exactly cancel the stresses (14), whereas the stress functions (17) annul the stresses (15) of their "own" boundary. If in (2) and (3) we replace the constants C_{2n}, D_{2n} by $C_{2n}^{(i)}$, $D_{2n}^{(i)}$, we get the stresses at the boundaries I, II, III, caused by the stress-function (16); if in (5), (6) and (7) we replace the constants $C_n^{\prime}$, $D_n^{\prime}$ by $C_n^{\prime(i)}$, $D_n^{\prime(i)}$ we get the stresses at the same boundaries, caused by the stress functions (17). If then we add the modified stresses (2) and (7) to (14) respectively the modified stresses (3), (5) and (6) to (15), the new sets of stresses along the boundaries I, II and III are obtained. The expansion of these stresses into series analogous to (14) and (15), wherein i is replaced by $(i+1)$, leads to the following set of equations for the new constants $C_{2n}^{(i+1)}$, $D_{2n}^{(i+1)}$, $C_n^{\prime(i+1)}$, $D_n^{\prime(i+1)}$

$$\left.\begin{aligned}
C_{2n}^{(i+1)} &= -[C_0^{(i)} h_{2n}^{0} + \sum_{s=1}^{\infty} (C_{2s}^{(i)} h_{2n}^{2s} + D_{2s}^{(i)} i_{2n}^{2s}) + \sum_{s=1}^{\infty} (C_s^{\prime(i)} p_{2n}^{s} + D_s^{\prime(i)} q_{2n}^{s})] \quad (n \geqq 0),\\
D_{2n}^{(i+1)} &= -[C_0^{(i)} j_{2n}^{0} + \sum_{s=1}^{\infty} (C_{2s}^{(i)} j_{2n}^{2s} + D_{2s}^{(i)} k_{2n}^{2s}) + \sum_{s=1}^{\infty} (C_s^{\prime(i)} r_{2n}^{s} + D_s^{\prime(i)} t_{2n}^{s})] \quad (n \geqq 1),\\
C_n^{\prime(i+1)} &= -[C_0^{(i)} h_n^{\prime 0} + \sum_{s=1}^{\infty} (C_{2s}^{(i)} h_n^{\prime 2s} + D_{2s}^{(i)} i_n^{\prime 2s}) + C_n^{\prime(i)} p_n^{\prime} + D_n^{\prime(i)} q_n^{\prime}] \quad (n \geqq 1),\\
D_n^{\prime(i+1)} &= -[C_0^{(i)} j_n^{\prime 0} + \sum_{s=1}^{\infty} (C_{2s}^{(i)} j_n^{\prime 2s} + D_{2s}^{(i)} k_n^{\prime 2s}) + C_n^{\prime(i)} r_n^{\prime} + D_n^{\prime(i)} t_n^{\prime}] \quad (n \geqq 1),
\end{aligned}\right\} \quad (18)$$

by which the iteration process is defined. As a matter of fact the starting set of constants consists of the constants $C_{2n}^{(0)}$, $D_{2n}^{(0)}$, $C_n^{\prime(0)}$, $D_n^{\prime(0)}$ (11), (13).

The ultimate solution of the equations (10) — the convergence of the iteration process being assumed — is represented by

$$\left.\begin{aligned} C_{2n} &= \sum_{i=0}^{\infty} C_{2n}^{(i)}\ (n \geqq 0),\quad D_{2n} = \sum_{i=0}^{\infty} D_{2n}^{(i)}\ (n \geqq 1), \\ C_n' &= \sum_{i=0}^{\infty} C_n'^{(i)},\quad D_n' = \sum_{i=0}^{\infty} D_n'^{(i)}\ (n \geqq 1). \end{aligned}\right\} \quad . \quad . \quad . \quad (19)$$

It would carry us to far to discuss here other methods of iteration and to raise the question what can be done, if the iteration (18) diverges. As to this question, we refer to "*A*" **7**, where a train of thought is to be found which, with suitable alterations, would serve our aim.

We now pass to the determination of the stresses, especially of the normal ones, occurring at the boundaries in the tangential direction. The normal stress σ_{τ}, occurring at the hole-boundaries I consists of $\sigma_{\tau}^{(0)}$ and the stresses given by (2) and (7); the normal stress σ_y, occurring at the straight edges II and III is composed of $\sigma_y^{(0)}$ and the stresses (3), (5), (6). The double series in which they are expressed, can be reduced to a single FOURIER series by using the equations (10). The result is given by

$$\sigma_{\tau} = \sigma_{\tau}^{(0)} + C_0^{(0)} - 2\,C_0 + \sum_{n=1}^{\infty} (C_{2n}^{(0)} + 2\,D_{2n}^{(0)} - 4\,D_{2n}) \cos 2n\varphi,$$

$$\sigma_y = \sigma_y^{(0)} + \sum_{n=1}^{\infty} (C_n'^{(0)} - 2\,D_n'^{(0)} + 4\,D_n') \cos 2\pi n \frac{y}{b},$$

which, in view of (11), (12) and (13) again can be simplified to

$$\left.\begin{aligned} \sigma_{\tau} &= -2\,C_0 - 4 \sum_{n=1}^{\infty} D_{2n} \cos 2n\varphi, \\ \sigma_y &= p' + 4 \sum_{n=1}^{\infty} D_n' \cos 2\pi n \frac{y}{b}. \end{aligned}\right\} \quad . \quad . \quad . \quad . \quad . \quad (20)$$

Double series cannot be avoided if for an *arbitrary* point of the field the stresses should be required. In such a case the calculation of the stresses due to the stress function (1) can be performed either by using the expansions (**3**, 13) of the elementary stress functions U_0, U_{2s}, U_{2s}^* (the stresses of which are explicitely given in ("*A*", **9**, 14), ("*A*", **9**, 15) and ("*A*", **9**, 16)) or by using the stresses (**4**, 7) and (**4**, 15) which are due to the stress functions $U_{\sigma,0}$, $U_{\sigma,2s}$, $U_{\tau,2s}$.

The first method gives the stresses in polar coordinates and furnishes the required result the more rapidly as the point lies nearer to the boundary of the circular holes. It converges slowly for values of $b > r > b/2$ and diverges for $r \geqq b$. The second method — as already stated — fails in all points of the y-axis; the greater the distance of the point under consideration to this axis, the better its convergence.

The stresses due to the stress functions F' (**4**) can be calculated from (**5**, 6). Neither theoretical difficulties nor double series do arise; the only fact which has to be regarded is the relative position of the different systems of coordinates which come into play. The convergence of the series to be employed increases with the distance of the point under consideration to the corresponding boundary.

There remains to discuss one difficulty, due to the fact that all constants C_{2n}, D_{2n}, C_n', D_n', and consequently all stresses are expressed in terms of the uniform tension p', to which the infinite plate initially has been subjected. Obviously this quantity p' lacks every technical significance with relation to the strip of finite width, for which

all related quantities ought to be expressed in terms of the total longitudinal force P to which it is subjected. This longitudinal force can be found by integrating the normal forces acting on a cross-section $y = \text{const.}$ of the strip. We choose the section $y = 0$ and find

$$P = 2\,(c-a)\,p' + 2\int_a^c \sigma_{yI}\,dz_I + 2\int_{-2c}^{0} \sigma_{yII}\,dz_{II} - 2\int_{-(c+a)}^{-(c-a)} \sigma_{yII}\,dz_{II}. \quad (21)$$

The first right hand term represents the contribution of the uniform tension p'. In the second term σ_{yI} represents the stress σ_y due to the stress function (1) whereas z_I designs the distance to the longitudinal axis of the strip. Analogously σ_{yII} in the last two integrals represents the stress σ_y corresponding to the stress function (4) and z_{II} the distance of a point to the boundary II. The factor 2 of the first integral in (21) obviously accounts for the fact that the cross section $y = 0$ consists of two equal parts of width $(c-a)$; the factor 2 of the other integrals accounts for the fact that two different functions F' give a contribution of equal amount.

If we introduce the "mean" stress p over the width of the strip by putting $P = 2cp$, formula (21) can be written as follows

$$\frac{p}{p'} = 1 - \mu + \frac{1}{cp'}\left[\int_a^c \sigma_{yI}\,dz_I + \int_{-2c}^{0} \sigma_{yII}\,dz_{II} - \int_{-(c+a)}^{-(c-a)} \sigma_{yII}\,dz_{II}\right]. \left(\frac{a}{c} = \mu\right). \quad (22)$$

From (4, 7) and (4, 15) it follows that, with $\eta = 0$ and $\zeta > 0$, σ_y is represented by

$$\sigma_{yI} = -4\pi^2\lambda^2 C_0 \sum_{n=1}^{\infty} n e^{-n\zeta} + \sum_{s=1}^{\infty} \frac{1}{2}\frac{(-1)^s (2\pi\lambda)^{2s}}{(2s-1)!} \sum_{n=1}^{\infty} n^{2s-1} e^{-n\zeta}.$$

$$\cdot\left\{C_{2s}\left[\frac{4\pi^2\lambda^2 n^2}{2s+1} + 2s + 2 - 2n\zeta\right] - D_{2s}\left[\frac{4\pi^2\lambda^2 n^2 (2s+2)}{2s(2s+1)} + 2s + 2 - 2n\zeta\right]\right\},$$

so that we have to deal with the integrals

$$\int_a^c e^{-n\zeta}\,dz = \frac{b}{2\pi}\int_{2\pi\lambda}^{2\pi\frac{\lambda}{\mu}} e^{-n\zeta}\,\delta\zeta = -\frac{b}{2\pi n}\left(e^{-2\pi n\frac{\lambda}{\mu}} - e^{-2\pi n\lambda}\right)$$

and

$$\int_a^c 2n\zeta e^{-n\zeta}\,dz = \frac{b}{2\pi}\int_{2\pi\lambda}^{2\pi\frac{\lambda}{\mu}} 2n\zeta e^{-n\zeta}\,d\zeta =$$

$$= -\frac{b}{2\pi n}\left[\left(4\pi n\frac{\lambda}{\mu} + 2\right) e^{-2\pi n\frac{\lambda}{\mu}} - (4\pi n\lambda + 2)\, e^{-2\pi n\lambda}\right].$$

If the indefinite integral $\int \sigma_{yI}\,dz_I$ be represented by I, so that $\int_a^c \sigma_{yI}\,dz_I$ can be written as:

$$\int_a^c \sigma_{yI}\,dz_I = I_c - I_a, \quad . \quad . \quad . \quad . \quad . \quad . \quad . \quad . \quad (23)$$

it easily can be checked, that

$$I_c = +\frac{b}{2\pi}\sum_{n=1}^{\infty}\frac{1}{n}\left[C_0 j_n'^0 + \sum_{s=1}^{\infty}(C_{2s} j_n'^{2s} + D_{2s} k_n'^{2s})\right] \quad . \quad . \quad (24)$$

and

$$I_a = a\left\{2\pi\lambda C_0 \sum_{n=1}^{\infty} e^{-2\pi n\lambda} - \sum_{s=1}^{\infty}\frac{1}{2}\frac{(-1)^s(2\pi\lambda)^{2s+1}}{(2s+1)!}[2sC_{2s}-(2s+2)D_{2s}]\sum_{n=1}^{\infty} n^{2s} e^{-2\pi n\lambda} - \right.$$
$$\left. - \sum_{s=1}^{\infty}\frac{1}{2}\frac{(-1)^s(2\pi\lambda)^{2s-1}}{(2s-1)!}(C_{2s}-D_{2s})\sum_{n=1}^{\infty} n^{2s-2}(2s-4\pi n\lambda) e^{-2\pi n\lambda}\right\} \quad (25)$$

if due attention is given to the abbreviations (**4**, 19).

The latter expression can greatly be simplified by observing that the different expansions (**4**, 5, 10, 12) and (**3**, 13) for U_0, U_{2s} and U_{2s}^* as well as their derivatives may be identified for all points (particularly for all points of the z-axis) in which these series converge simultaneously. If then in (**4**, 5, 10,12) we put $\eta = 0$, and in (**3**, 13) $\varphi = \pi/2$, $r = z$, and if furthermore the first derivatives are identified for $z = a$, the following identities are found:

$$\left(\frac{dU_0}{dz}\right)_{\substack{y=0,\\ z=a}} = \frac{\pi}{b} + \frac{2\pi}{b}\sum_{n=1}^{\infty} e^{-2\pi n\lambda} = \frac{1}{a} - \frac{1}{a}\sum_{n=1}^{\infty} 2(-1)^n \sigma_{2n}\lambda^{2n},$$

$$\left(\frac{dU_{2s}}{dz}\right)_{\substack{y=0,\\ z=a}} = -\frac{(-1)^s(2\pi)^{2s+1}}{(2s-1)!\,b^{2s+1}}\sum_{n=1}^{\infty} n^{2s} e^{-2\pi n\lambda} =$$

$$= -\frac{(-1)^s \cdot 2s}{a^{2s+1}} + \frac{2s(2s+1)}{a^{2s+1}}\sum_{n=1}^{\infty}\frac{(-1)^n}{2n-1} 2\binom{2n+2s-1}{2n-2}\sigma_{2n+2s}\lambda^{2n+2s} \quad (s \geqq 1),$$

$$\left(\frac{dU_2^*}{dz}\right)_{\substack{y=0,\\ z=a}} = -\frac{2\pi}{b} - \frac{2\pi}{b}\sum_{n=1}^{\infty}(2-4\pi n\lambda) e^{-2\pi n\lambda} =$$

$$= -\frac{1}{a}\left\{4\sigma_2\lambda^2 - \sum_{n=1}^{\infty} 2(-1)^n [2n\sigma_{2n} - (2n+2)\sigma_{2n+2}\lambda^2]\lambda^{2n-2}\right\}, \quad . \quad (26)$$

$$\left(\frac{dU_{2s}^*}{dz}\right)_{\substack{y=0,\\ z=a}} = +\frac{(-1)^s(2\pi)^{2s-1}}{(2s-2)!}\frac{1}{b^{2s-1}}\sum_{n=1}^{\infty} n^{2s-2}(2s-4\pi n\lambda) e^{-2\pi n\lambda} =$$

$$= -\frac{(-1)^s(2s-2)}{a^{2s-1}} - \frac{2s-1}{a^{2s-1}}\left\{4\sigma_{2s}\lambda^{2s} - \right.$$

$$\left. - \sum_{n=1}^{\infty} 2(-1)^n\left[\binom{2n+2s-2}{2n-1}\sigma_{2n+2s-2} - \frac{2n+2}{2n+1}\binom{2n+2s-1}{2n}\sigma_{2n+2s}\lambda^2\right]\lambda^{2n-2}\right\} (s > 1).$$

They give us the infinite sums over n occurring in (25) and consequently this latter formula can be written in the form:

$$= a\left\{-\pi\lambda(C_0 + C_2 - D_2) + C_0 - \sum_{n=1}^{\infty}\frac{(-1)^n}{4n^2-1}(C_{2n} - 2nD_{2n}) - C_0\sum_{n=1}^{\infty} 2(-1)^n\sigma_{2n}\lambda^{2n} + \right.$$

$$\frac{1}{2}\sum_{s=1}^{\infty}[2sC_{2s} - (2s+2)D_{2s}]\sum_{n=1}^{\infty}\frac{2(-1)^n}{2n-1}\binom{2n+2s-1}{2n-2}\sigma_{2n+2s}\lambda^{2n+2s} + \frac{1}{2}\sum_{s=1}^{\infty}(C_{2s} - D_{2s})\left\{4\sigma_{2s}\lambda^{2s} - \right.$$

$$\left. \left. - \sum_{n=1}^{\infty} 2(-1)^n\left[\binom{2n+2s-2}{2n-1}\sigma_{2n+2s-2} - \frac{2n+2}{2n+1}\binom{2n+2s-1}{2n}\sigma_{2n+2s}\lambda^2\right]\lambda^{2n-2}\right\}\right\}.$$

If out of all terms with λ^{2n} those with C_0, C_{2s}, D_{2s} are collected, it becomes possible to express the coefficients of these latter constants in the quantities (3, 17) and (3, 19). These different steps lead to

$$I_a = -a\pi\lambda(C_0 + C_2 - D_2) + a\left\{C_0 - \sum_{n=1}^{\infty}\frac{(-1)^n}{4n^2-1}(C_{2n} - 2nD_{2n}) + C_0 h_0^0 + \right.$$
$$+ \sum_{s=1}^{\infty}(C_{2s} h_0^{2s} + D_{2s} i_0^{2s}) + \sum_{n=1}^{\infty}\frac{(-1)^n}{4n^2-1}\left(2n\left[C_0 j_{2n}^0 + \sum_{s=1}^{\infty}(C_{2s} j_{2n}^{2s} + D_{2s} k_{2n}^{2s})\right] - \right. \quad (27)$$
$$\left.\left. - \left[C_0 h_{2n}^0 + \sum_{s=1}^{\infty}(C_{2s} h_{2n}^{2s} + D_{2s} i_{2n}^{2s})\right]\right)\right\}.$$

The evaluation of the other integrals in (22) gives no difficulties. To calculate the second one we use (5, 3); integrating term by term and paying attention to the abbreviations (5, 8) we find

$$\int_{-2c}^{0} \sigma_{yII}\, dz_{II} = \frac{b}{2\pi}\sum_{n=1}^{\infty}\frac{1}{n}[D'_n + C'_n r'_n + D'_n t'_n]. \quad . \quad . \quad . \quad (28)$$

The evaluation of the third integral depends on the series (6, 7) and (6, 8). It must, however, be kept in mind that the integral has to be related to the yz system, connected with the holes of the strip. By putting $z_{II} = z_I - c$ the integral is transformed into $\int_{-a}^{+a} \sigma_{yII}\, dz_I$. The stress σ_{yII}, occurring in this integral is found by providing the stresses (6, 7) with the constants C'_s, and the stresses (6, 8) with the constants D'_s, by summing up over the index s and furthermore by replacing r by z and φ by $\pi/2$. Terms with odd powers of z do not contribute to the integral, so that

$$\int_{-(c+a)}^{-(c-a)} \sigma_{yII}\, dz_{II} = 2\int_0^a \sum_{s=1}^{\infty} e^{-2\pi s\frac{\lambda}{\mu}}\left\{C'_s + D'_s + \right.$$
$$+ \frac{1}{2}\sum_{n=1}^{\infty}\frac{(2\pi s)^{2n-2}}{(2n-2)!}\left(\frac{z}{b}\right)^{2n-2}\left[C'_s\left(\frac{4\pi^2 s^2 (2n+2)}{2n(2n-1)}\frac{z^2}{b^2} + 2n - 2 - 4\pi s\frac{\lambda}{\mu}\right) + \right.$$
$$\left.\left. + D'_s\left(\frac{4\pi^2 s^2 (2n+2)}{2n(2n-1)}\frac{z^2}{b^2} + 2n - 4\pi s\frac{\lambda}{\mu}\right)\right]\right\} dz.$$

Integration leads to — comp, the abbrevations (6, 10) —

$$\int_{-(c+a)}^{-(c-a)} \sigma_{yII}\, dz_{II} = a\left\{\sum_{s=1}^{\infty}(C'_s p_0^s + D'_s q_0^s) + \right.$$
$$\left. + \sum_{n=1}^{\infty}\frac{(-1)^n}{4n^2-1}\sum_{s=1}^{\infty}[2n(C'_s r_{2n}^s + D'_s t_{2n}^s) - (C'_s p_{2n}^s + D'_s q_{2n}^s)]\right\}. \quad (29)$$

If (24) and (27) are substituted into (23) and then (23), (28), (29) into (22), we find with regard to (10):

$$\frac{p}{p'} = 1 - \mu + \frac{1}{cp'}\left\{\frac{b}{2\pi}\sum_{n=1}^{\infty} D_n^{'(0)} + a\pi\lambda(C_0 + C_2 - D_2) - a\left[C_0^{(0)} + \sum_{n=1}^{\infty}\frac{(-1)^n}{4n^2-1}(2nD_{2n}^{(0)} - C_{2n}^{(0)})\right]\right\}.$$

TABLE 1. The coefficients of the stress functions expressed in terms of the uniform auxiliary tension p'.

	$\mu=0$			$\mu=0.20$			$\mu=0.40$			$\mu=0.60$	
	$\lambda=0.10$	$\lambda=0.20$	$\lambda=0.30$	$\lambda=0.10$	$\lambda=0.20$	$\lambda=0.30$	$\lambda=0.10$	$\lambda=0.20$	$\lambda=0.30$	$\lambda=0.15$	$\lambda=0.30$
C_0/p'	−0.47006	−0.40545	−0.34197	−0.46351	−0.40530	−0.34196	−0.42033	−0.37987	−0.33690	−0.31967	−0.29027
C_2/p'	−0.45488	−0.35594	−0.25666	−0.46980	−0.35635	−0.25667	−0.54094	−0.39732	−0.26333	−0.59440	−0.32639
C_4/p'	+0.00146	+0.01716	+0.05494	+0.00356	+0.01745	+0.05494	+0.02840	+0.04147	+0.06637	+0.12201	+0.13462
C_6/p'	+0.00003	+0.00140	+0.00831	-0.00001^{4}	+0.00137	+0.00832	−0.00270	−0.00053	+0.00570	−0.02406	−0.00840
C_8/p'	—	+0.00009	+0.00094	—	$+0.00009^{5}$	+0.00095	+0.00020	$+0.00020^{5}$	+0.00113	+0.00364	+0.00300
C_{10}/p'	—	$+0.00000^{6}$	+0.00009	—	$+0.00000^{6}$	$+0.00007^{7}$	-0.00001^{0}	$+0.00000^{2}$	$+0.00006^{0}$	−0.00047	−0.00039
C_{12}/p'	—	—	$+0.00000^{2}$	—	—	$+0.00000^{3}$	—	—	$+0.00000^{1}$	$+0.00006^{1}$	$+0.00005^{3}$
C_{14}/p'	—	—	—	—	—	—	—	—	—	-0.00000^{7}	-0.00000^{9}
D_2/p'	+0.45548	+0.36338	+0.28345	+0.46926	+0.36374	+0.28346	+0.52375	+0.39201	+0.28852	+0.51274	+0.30765
D_4/p'	−0.00144	−0.01670	−0.05155	−0.00351	−0.01700	−0.05155	−0.02615	−0.03899	−0.05952	−0.09858	−0.11496
D_6/p'	−0.00003	−0.00137	−0.00793	$+0.00001^{3}$	−0.00134	−0.00793	+0.00252	+0.00046	−0.00634	+0.01972	+0.00585
D_8/p'	—	−0.00009	−0.00091	—	-0.00009^{4}	−0.00091	−0.00018	-0.00019^{4}	−0.00095	−0.00298	−0.00253
D_{10}/p'	—	-0.00000^{6}	−0.00008	—	-0.00000^{6}	-0.00007^{5}	$+0.00001^{0}$	-0.00000^{2}	-0.00005^{5}	+0.00039	+0.00033
D_{12}/p'	—	—	-0.00000^{2}	—	—	-0.00000^{2}	—	—	-0.00000^{2}	-0.00004^{8}	-0.00004^{3}
D_{14}/p'	—	—	—	—	—	—	—	—	—	$+0.00000^{6}$	$+0.00000^{8}$
C'_1/p'	0	0	0	−0.04004	−0.01144	−0.00137	−0.08046	−0.12242	−0.06397	−0.18874	−0.21060
C'_2/p'	0	0	0	−0.00749	-0.00008^{7}	—	−0.08476	−0.02194	−0.00272	−0.18275	−0.04823
C'_3/p'	0	0	0	-0.00072^{6}	—	—	−0.03999	−0.00210	-0.00006^{4}	−0.08587	−0.00637
C'_4/p'	0	0	0	-0.00005^{4}	—	—	−0.01434	-0.00016^{4}	-0.00000^{1}	−0.03246	−0.00066
C'_5/p'	0	0	0	-0.00000^{4}	—	—	−0.00449	-0.00001^{1}	—	−0.01127	-0.00006^{0}
C'_6/p'	0	0	0	—	—	—	−0.00130	—	—	−0.00378	-0.00000^{5}
C'_7/p'	0	0	0	—	—	—	−0.00036	—	—	−0.00124	—
C'_8/p'	0	0	0	—	—	—	−0.00009	—	—	−0.00041	—
C'_9/p'	0	0	0	—	—	—	-0.00002^{3}	—	—	-0.00013^{2}	—
C'_{10}/p'	0	0	0	—	—	—	-0.00000^{5}	—	—	-0.00004^{2}	—
D'_1/p'	0	0	0	−0.02412	−0.00928	−0.00120	+0.00390	−0.06747	−0.04402	+0.01425	−0.09087
D'_2/p'	0	0	0	−0.00610	-0.00007^{9}	—	−0.04819	−0.01678	−0.00224	−0.08787	−0.03162
D'_3/p'	0	0	0	-0.00063^{5}	—	—	−0.02831	−0.00174	-0.00005^{5}	−0.05177	−0.00455
D'_4/p'	0	0	0	-0.00004^{8}	—	—	−0.01103	-0.00013^{9}	-0.00000^{1}	−0.02113	−0.00048
D'_5/p'	0	0	0	-0.00000^{4}	—	—	−0.00360	-0.00001^{0}	—	−0.00761	-0.00004^{2}
D'_6/p'	0	0	0	—	—	—	−0.00106	—	—	−0.00261	-0.00000^{4}
D'_7/p'	0	0	0	—	—	—	−0.00030	—	—	−0.00089	—
D'_8/p'	0	0	0	—	—	—	−0.00008	—	—	−0.00029	—
D'_9/p'	0	0	0	—	—	—	-0.00002^{0}	—	—	-0.00009^{6}	—
D'_{10}/p'	0	0	0	—	—	—	-0.00000^{5}	—	—	-0.00003^{2}	—

Finally the constants $C^{(0)}$ and $D^{(0)}$ can be replaced by their values (11) and (13), which leads to the strikingly simple endresult

$$\frac{p}{p'} = 1 + \pi\mu\lambda\,\frac{C_0 + C_2 - D_2}{p'} \quad . \quad . \quad . \quad . \quad . \quad . \quad (30)$$

It must be remembered that C_0, C_2 and D_2 are expressed in terms of p', so that the right hand member of equation (30) must be looked upon as a wellknown, calculable number.

We conclude from (30) that in both limiting cases, $\mu = 0$ (the infinite plate with one

TABLE 2.

The multiplying factor p'/p.

λ \ μ	0	0.20	0.40	0.60
0	1.00000	1.00000	1.00000	1.00000
0.10	1.00000	1.09665	1.22942	1.67622 *)
0.20	1.00000	1.16471	1.41613	
0.30	1.00000	1.19943	1.50386	2.09500

*) This value corresponds to $\lambda = 0{,}15$.

TABLE 3.

The normal stress σ_φ in points of the boundary I.

σ_φ/p	$\mu = 0$				$\mu = 0.20$		
φ	$\lambda = 0$	$\lambda = 0.10$	$\lambda = 0.20$	$\lambda = 0.30$	$\lambda = 0.10$	$\lambda = 0.20$	$\lambda = 0.30$
0°	−1.0000	−0.8759	−0.5700	−0.2080	−1.0265	−0.6646	−0.2495
10°	−0.8794	−0.7675	−0.5010	−0.2071	−0.9059	−0.5844	−0.2485
20°	−0.5321	−0.4546	−0.2941	−0.1684	−0.5575	−0.3438	−0.2020
30°	0	+0.0262	+0.0451	−0.0194	−0.0203	+0.0508	−0.0234
40°	+0.6527	+0.6183	+0.4933	+0.2805	+0.6447	+0.5727	+0.3364
50°	+1.3473	+1.2512	+1.0035	+0.7055	+1.3596	+1.1674	+0.8462
60°	+2.0000	+1.8483	+1.5096	+1.1775	+2.0381	+1.7578	+1.4123
70°	+2.5321	+2.3368	+1.9384	+1.6010	+2.5961	+2.2588	+1.9203
80°	+2.8794	+2.6565	+2.2253	+1.8922	+2.9627	+2.5942	+2.2695
90°	+3.0000	+2.7677	+2.3261	+1.9956	+3.0905	+2.7121	+2.3936

σ_φ/p	$\mu = 0.40$			$\mu = 0.60$	
φ	$\lambda = 0.10$	$\lambda = 0.20$	$\lambda = 0.30$	$\lambda = 0.15$	$\lambda = 0.30$
0°	−1.4251	−0.9253	−0.3207	−1.8197	−0.4287
10°	−1.2943	−0.8427	−0.3233	−1.7148	−0.4889
20°	−0.9118	−0.5865	−0.2788	−1.3975	−0.5845
30°	−0.3067	−0.1428	−0.0743	−0.8565	−0.5172
40°	+0.4723	+0.4849	+0.3610	−0.0671	−0.0982
50°	+1.3545	+1.2535	+1.0014	+0.9985	+0.7522
60°	+2.2443	+2.0726	+1.7372	+2.3195	+1.9657
70°	+3.0219	+2.8129	+2.4190	+3.7325	+3.3113
80°	+3.5586	+3.3332	+2.9004	+4.8774	+4.4042
90°	+3.7510	+3.5210	+3.0741	+5.3256	+4.8310

TABLE 4.

The normal stress σ'_y in points of the boundaries II and III.

σ_y/p	$\mu = 0.20$			$\mu = 0.40$			$\mu = 0.60$	
y/b	$\lambda = 0.10$	$\lambda = 0.20$	$\lambda = 0.30$	$\lambda = 0.10$	$\lambda = 0.20$	$\lambda = 0.30$	$\lambda = 0.15$	$\lambda = 0.30$
0.0	+0.9611	+1.1211	+1.1937	+0.7933	+0.9282	+1.2253	+0.6166	+1.0260
0.1	+1.0038	+1.1296	+1.1948	+1.2807	+1.0813	+1.2856	+1.8589	+1.4124
0.2	+1.0878	+1.1517	+1.1977	+1.5050	+1.3826	+1.4332	+2.3690	+2.1033
0.3	+1.1487	+1.1784	+1.2012	+1.3011	+1.6030	+1.5963	+1.8411	+2.5130
0.4	+1.1733	+1.1996	+1.2041	+1.1275	+1.6935	+1.7138	+1.3853	+2.6203
0.5	+1.1783	+1.2076	+1.2052	+1.0719	+1.7124	+1.7555	+1.2350	+2.6260

TABLE 5.

The stresses in points of the y- and z-axis; $\lambda = 0.20$, $\mu = 0.40$.

r/b		0.2	0.3	0.4	0.5
points of the y-axis	σ_y/p	0	+0.1175	+0.3198	+0.3830
	σ_z/p	−0.9251	+0.0114	+0.1952	+0.2085
points of the z-axis	σ_y/p	+3.5210	+1.7259	+1.3152	+0.9283
	σ_z/p	0	+0.3153	+0.1122	0

TABLE 6.

The maximum stresses in terms of the average stress $p = P/2c$.

λ \ μ	0	0.20	0.40	0.60
0	+3.0000			
0.10	+2.7677	+3.0905	+3.7510	+5.3256 *)
0.20	+2.3261	+2.7121	+3.5210	
0.30	+1.9956	+2.3936	+3.0741	+4.8310

*) This value corresponds to $\lambda = 0.15$.

TABLE 7.

The maximum stresses in terms of the average stress $\bar{p} = P/2(c\text{-}a)$ of the section $y = 0$.

λ \ μ	0	0.20	0.40	0.60
0	+3.0000			
0.10	+2.7677	+2.4724	+2.2506	+2.1302 *)
0.20	+2.3261	+2.1697	+2.1126	
0.30	+1.9956	+1.9149	+1.8445	+1.9324

*) This value corresponds to $\lambda = 0.15$.

row of holes) and $\lambda = 0$ (strip of finite width with one single hole) the effective average tension p is equal to the auxiliary tension p' as was to be expected.

All stresses, which up to now were written as a multiple m of p', can be expressed in p, by writing them as $(mp'/p) \cdot p$.

Before proceeding to the numerical evaluation of these stresses we deduce an expression

for the elongation of the strip. To this end we consider the strip — as in the beginning of this section — as a part of the infinite plate, subjected simultaneously to the uniform tension p' and the stress functions F and F', which annul the stresses σ_r, $\tau_{r\varphi}$, σ_z, τ_{yz} along the lines I, II, III. Evidently two lines $y = 0$ and $y = b$ drawn on this plate remain parallel in consequence of the symmetry and periodicity of the problem. Their change in distance can be calculated at every distance z. At sufficient great distances z, however, the state of stress depends solely on p', because of the disappearing influence of the stress functions F and F' at infinity. Therefore we find

$$\triangle b = \frac{p'}{E} b = \frac{p'}{p} \frac{pb}{E} = \frac{p'}{p} \cdot \frac{Pb}{2cE}. \quad . \quad . \quad . \quad . \quad . \quad (31)$$

The numerical work, which actually has to be done, is illustrated in the tables 1—7. Firstly the coefficients in the formulae (3, 17), (4, 19), (5, 8) and (6, 10) have to be computed, whereupon the iteration (18) can be carried out and the coefficients C_{2n}, D_{2n}, C'_n, D'_n (19) can be calculated. Then these coefficients must be checked with the aid of the equations (10). As will be seen from table 1 they have been calculated in 5 decimals. It is recommendable to start with a provisional calculation in 3 decimals, to check the results with the aid of (10) and to calculate the remaining decimals by a secondary iteration, applied to the established errors, along a scheme which has been described at full length in ("*A*", 6). In this way the first calculations can be performed without a calculating machine, whereas the total number of iterations can be reduced. Table 1 gives the results inclusive those having a bearing on the limiting cases $\mu = 0$ (comp. "*A*", 9, Table 6). The multiplying factor p'/p, by which all stresses can be expressed in terms of the mean tension p has been tabulated in table 2. The boundary stresses themselves are represented in the tables 3 and 4. Table 5 gives the principal stresses in the points of the y- and z-axis for the values $\lambda = 0{,}20$ and $\mu = 0{,}40$. The maximum boundary stresses, expressed in terms of the average stress $p = P/2c$, respectively in terms of the average stress $\bar{p} = P/2(c-a)$ over the narrowest section of the strip are reproduced in the tables 6 and 7.

Applied Mechanics. — *On the buckling and the lateral rigidity of helical compression springs.* I. By J. A. HARINGX. (Natuurkundig Laboratorium der N. V. PHILIPS' Gloeilampenfabrieken Eindhoven — Holland.) (Communicated by Prof. C. B. BIEZENO.)

(Communicated at the meeting of May 30, 1942.)

1. *Introduction.*

The buckling of helical springs has first been studied by R. GRAMMEL in a paper read before the first International Congress for Applied Mechanics [1]). Later on C. B. BIEZENO and J. J. KOCH pointed out that the results obtained in this paper did not agree with the experiments and that the reason for this discrepancy must be sought in the neglection of the "shear-elasticity" of the spring [2]). Unfortunately a mistake in the deduction of the differential equation of the problem leads the latter authors to an overestimation of this shear effect which makes itself earnestly perceptible in the end result. In this paper the correction is given and it will be seen that now full agreement between theory and experiment is established. As could be expected beforehand the new results lie between those of GRAMMEL and those of BIEZENO and KOCH (see fig. 3).

The theory is not restricted to the determination of the buckling load of helical springs under compression, but can be applied as well to springs subjected to an axial force combined with a bending moment and a lateral force, as to springs under the combined action of compression and torsion.

2. *The underlying assumption.*

If the number of coils of the helical spring is sufficiently great it may be expected that it will behave like an ordinary rod of minor elasticity if subjected to the action of end forces and end moments. From this point of view the calculation of the buckling load can be reduced to that of a rod of suitable elasticity. While, however, in the case of a normal beam the deformations caused by the normal and shearing forces are usually neglected with respect to those caused by the bending moments, here the shear action must be brought into account. Moreover, it must be observed that the compression of the spring results in an increase of the number of coils per unit of axial length, and therefore leads to a decrease of all coefficients of rigidity, as compared with those in the unloaded state.

Finally we assume, as usual, that the normal and shearing forces as well as the bending and torsional moments acting upon the end sections of a rod element give independently from each other rise to well defined deformations of the element.

If the coefficients of elastic rigidity with respect to bending, shear, compression and torsion, as defined per unit of axial length of the deformed spring be called respectively α, β, γ and δ, the *extra* deformation of an element dx of the deformed spring under action

---

[1]) R. GRAMMEL, Die Knickung von Schraubenfedern, Proc. of the 1st Int. Congr. for Appl. Mech. Delft 1924, p. 276—278 and Zs. f. Ang. Math. und Mech. Vol. **4**, 384—389 (1924).

[2]) C. B. BIEZENO and J. J. KOCH, Knickung von Schraubenfedern, Zs. f. Ang. Math. und Mech. Vol. **5**, 279—280 (1925). See also C. B. BIEZENO and R. GRAMMEL, Technische Dynamik, p. 548—559, Berlin 1939.

of shearing forces Q, bending moments M and torsional moments W, consists of

$$\left.\begin{aligned} &\text{the angle of bending} && d\psi = \frac{M}{\alpha}\,dx \\ &\text{the angle of torsion} && d\chi = \frac{W}{\delta}\,dx \\ &\text{the angle of shear} && \varphi = \frac{Q}{\beta} \end{aligned}\right\} \quad \ldots\ldots \quad (1)$$

Denoting by

- n the number of active coils
- D the mean spring diameter
- I the linear moment of inertia of the (circular) wire section
- l_0 the length of the unloaded spring
- l the length of the loaded spring
- E YOUNG's modulus of elasticity
- m POISSON's ratio

the various coefficients of elastic rigidity per unit of length of the unloaded spring are [3])

$$\left.\begin{aligned} \frac{1}{\alpha_0} &= \frac{n}{l_0}\frac{\pi D}{EI}\frac{2m+1}{2m} & \frac{1}{\beta_0} &= \frac{n}{l_0}\frac{\pi D^3}{8EI} \\ \frac{1}{\gamma_0} &= \frac{n}{l_0}\frac{\pi D^3}{EI}\frac{m+1}{4m} & \frac{1}{\delta_0} &= \frac{n}{l_0}\frac{\pi D}{EI}; \end{aligned}\right\} \quad \ldots\ldots \quad (2)$$

those defined per unit of length of the loaded spring are represented by

$$\alpha = \frac{l}{l_0}\alpha_0 \quad \beta = \frac{l}{l_0}\beta_0 \quad \gamma = \frac{l}{l_0}\gamma_0 \quad \delta = \frac{l}{l_0}\delta_0. \quad \ldots \quad (3)$$

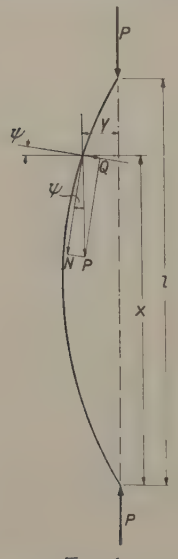

Fig. 1.
The central line of an axially loaded rod with hinged ends.

3. *The buckling load of helical compression springs.*

If the rod is loaded at its ends only by two compressive forces P, which are supposed to maintain a deflection

$$y = f(x) \quad \ldots\ldots \quad (4)$$

an arbitrary crossection of the rod will be subjected to the action of a normal force N, a bending moment M and a shearing force Q. Denoting by ψ the angle through which the crossection has rotated (fig. 1) we have

$$M = Py$$
$$Q = P\sin\psi \approx P\psi$$
$$N = P\cos\psi \approx P.$$

Substituting these expressions into the first and third of the relations (1) we find

$$\left.\begin{aligned} d\psi &= \frac{M}{\alpha}\,dx = \frac{Py}{\alpha}\,dx \\ \varphi &= \frac{Q}{\beta} = \frac{P\psi}{\beta} \end{aligned}\right\} \quad \ldots\ldots \quad (5)$$

[3]) See C. B. BIEZENO and R. GRAMMEL, Technische Dynamik, p. 549 and 552, Berlin 1939.

The slope of the deflected central line of the rod is represented by (fig. 2)

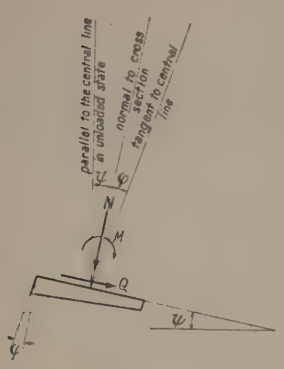

Fig. 2.
The element of the rod.

$$-\frac{dy}{dx}=\psi+\varphi=\left(1+\frac{P}{\beta}\right)\psi. \quad . \quad . \quad . \quad . \quad (6)$$

Differentiating this equation we find

$$-\frac{d^2y}{dx^2}=\left(1+\frac{P}{\beta}\right)\frac{d\psi}{dx}$$

or, with respect to (5)

$$\frac{d^2y}{dx^2}+\frac{P}{\alpha}\left(1+\frac{P}{\beta}\right)y=0 \; . \quad . \quad . \quad (7)$$

Putting

$$q^2=\frac{P}{\alpha}\left(1+\frac{P}{\beta}\right) \quad . \quad . \quad . \quad . \quad . \quad . \quad . \quad (8)$$

the solution of eq. (7) is

$$y=A\,sin\,qx+B\,cos\,qx.$$

In the simple case of hinged ends the terminal conditions — $y=0$ both at $x=0$ and $x=l$ — lead to the following equation for the smallest critical load:

$$\frac{P}{\alpha}\left(1+\frac{P}{\beta}\right)l^2=\pi^2. \quad . \quad . \quad . \quad . \quad . \quad . \quad . \quad . \quad (9)$$

If we put

$$l=(1-\xi)\,l_0 \quad . \quad . \quad . \quad . \quad . \quad . \quad . \quad . \quad . \quad (10)$$

and — in accordance with the definitions of γ_0 and γ —

$$\triangle l=l_0-l=\frac{Pl_0}{\gamma_0}=\frac{Pl}{\gamma} \quad . \quad . \quad . \quad . \quad . \quad . \quad . \quad (11)$$

we find, with regard to eqs. (3)

$$\xi\left\{1-\xi\left(1-\frac{\gamma_0}{\beta_0}\right)\right\}\frac{\gamma_0}{\alpha_0}\,l_0^2=\pi^2$$

or in consequence of the expressions (2)

$$\xi\left\{1-\frac{m+2}{2\,(m+1)}\,\xi\right\}=\pi^2\,\frac{m+1}{2\,(2\,m+1)}\left(\frac{D}{l_0}\right)^2. \quad . \quad . \quad . \quad (12)$$

Putting $m=10/3$ this equation becomes

$$\xi\,(1-0.615\,\xi)=2.790\left(\frac{D}{l_0}\right)^2. \quad . \quad . \quad . \quad . \quad . \quad (12a)$$

In fig. 3 the relative compression ξ, at which the spring buckles is plotted against the ratio l_0/D. Only that part of the graph belonging to $\xi < 1$ has practical importance. The dotted curves represent the results deduced by GRAMMEL [4]) ($\beta = \infty$) and by BIEZENO and KOCH [4]). The isolated points represent experimental results obtained with springs of various lengths ($D = 18$ mm, wire diameter 0,5 resp. 2 mm, pitch = 5 mm); a vertical arrow indicates that the spring in question did not buckle if totally compressed. As will be seen the agreement between theory and experiment is quite satisfactory. Most interes-

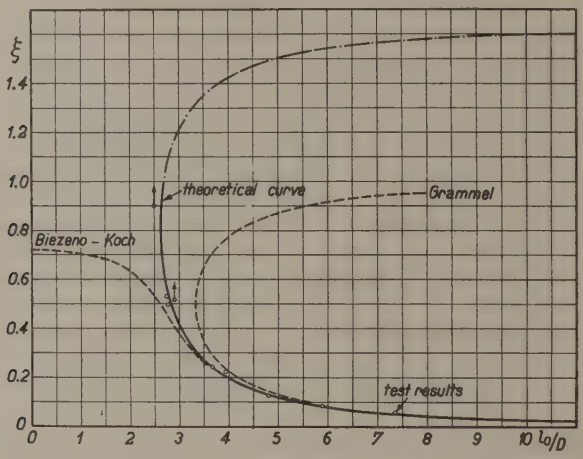

Fig. 3.

The critical relative compression ξ of a spring with hinged ends as function of ratio l_0/D. Comparison with the results of other authors and with some test results.

ting is the behaviour of a spring, the length of which is about 2.7 times its diameter. If the length exceeds this amount with some 5 % the spring buckles under a compression of about 50 %, whereas no instability at all occurs if the length is some 5 % smaller.

When other endconditions for the spring are prescribed, fig. 3 still holds true, if only the length l_0 be replaced by the so-called reduced buckling length of the spring (f.i. by $\frac{1}{2}\, l_0$ if both ends are clamped).

4. *The lateral rigidity of helical compression springs.*

We now consider a spring clamped at one end and loaded at its other free end by an axial force P, a lateral force L and a bending moment M_0. Using the same notations as before, we have (fig. 4)

$$M = Py + L(l-x) + M_0$$
$$Q = P\psi + L$$
$$N = P$$

---

[4]) Loc. cit. It may be noticed here, that the discrepancy between our results and those of the latter authors is due to the fact that they put

$$Q = P\frac{dy}{dx} \quad \text{instead of} \quad Q = P\psi .$$

and consequently

$$\left.\begin{aligned} \varphi &= \frac{Q}{\beta} = \frac{P}{\beta}\psi + \frac{L}{\beta} \\ \frac{d\psi}{dx} &= \frac{M}{a} = \frac{Py + L(l-x) + M_0}{a} \end{aligned}\right\} \quad . \quad . \quad . \quad .$$

The slope of the central line is represented by (fig. 2)

$$-\frac{dy}{dx} = \varphi + \psi = \left(1 + \frac{P}{\beta}\right)\psi + \frac{L}{\beta} \quad . \quad . \quad . \quad . \quad . \quad (14)$$

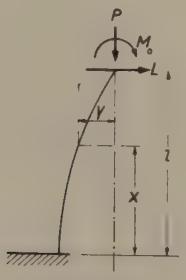

Fig. 4.

The central line of a rod subjected to the simultaneous action of an axial force, a lateral force and a bending moment.

From (13) and (14) we deduce the differential equation

$$\frac{d^2y}{dx^2} + \frac{P}{a}\left(1 + \frac{P}{\beta}\right)y = -\left(1 + \frac{P}{\beta}\right)\frac{L(l-x) + M_0}{a} \quad . \quad . \quad (15)$$

the solution of which is given by (comp. 8)

$$y = A \sin qx + B \cos qx - \frac{L(l-x) + M_0}{P} \quad . \quad . \quad . \quad . \quad (16)$$

The end conditions $\begin{matrix} x=0 \\ \psi=0 \end{matrix}$ and $\begin{matrix} x=l \\ y=0 \end{matrix}$ are fulfilled if

$$A = -\frac{L}{P}\left(1 + \frac{P}{\beta}\right)\frac{1}{q}, \quad B = \frac{M_0}{P}\frac{1}{\cos ql} + \frac{L}{P}\left(1 + \frac{P}{\beta}\right)\frac{tg\,ql}{q}.$$

The lateral displacement y_l and the slope ψ_l of the free end of the spring can now easily be calculated and it is found that

$$\left.\begin{aligned} y_l &= \frac{L}{P}l\left\{\left(1 + \frac{P}{\beta}\right)\frac{tg\,ql}{ql} - 1\right\} + \frac{M_0}{P}\left(\frac{1}{\cos ql} - 1\right) \\ \psi_l &= \frac{L}{P}\left(\frac{1}{\cos ql} - 1\right) + \frac{M_0}{P}\frac{q\,tg\,ql}{1 + P/\beta} \end{aligned}\right\} \quad . \quad . \quad (17)$$

These relations may be written in the form

$$\left.\begin{aligned} L &= c_1 y_l - c_2 \psi_l \\ M_0 &= -c_2 y_l + c_3 \psi_l \end{aligned}\right\} \quad . \quad . \quad . \quad . \quad . \quad . \quad . \quad . \quad (18)$$

With the notations

$$\left.\begin{aligned} &\xi = \triangle l/l_0,\ a = (m+2)/2(m+1),\ c_a = \frac{\gamma_0}{l_0} = \frac{4m}{m+1}\,\frac{EI}{\pi n D^3} \\ &\text{and} \\ &\tfrac{1}{2}\,q\,l = \sqrt{\frac{2m+1}{2(m+1)}}\,\frac{l_0}{D}\,\sqrt{\xi(1-a\xi)} \end{aligned}\right\} \qquad (19)$$

the coefficients c_1, c_2, c_3 are represented by

$$\left.\begin{aligned} \frac{c_a}{c_1} &= \frac{1-\xi}{\xi}\left(\frac{1-a\xi}{1-\xi}\,\frac{tg\,\frac{1}{2}\,q\,l}{\frac{1}{2}\,q\,l} - 1\right) \\ \frac{c_2}{c_1} &= \tfrac{1}{2}\,l_0\,(1-a\xi)\,\frac{tg\,\frac{1}{2}\,q\,l}{\frac{1}{2}\,q\,l} \\ \frac{c_3}{c_2} &= l_0\,(1-\xi)\,\frac{\frac{1-a\xi}{1-\xi}\,\frac{tg\,q\,l}{q\,l} - 1}{\frac{1}{\cos q\,l} - 1} \end{aligned}\right\} \quad \ldots\ldots \qquad (20)$$

In absence of an axial force ($\xi = 0$) these expressions reduce to

$$\left.\begin{aligned} \frac{c_a}{c_1} &= \frac{m}{2(m+1)}\left\{1 + \frac{2m+1}{3m}\left(\frac{l_0}{D}\right)^2\right\} \\ \frac{c_2}{c_1} &= \tfrac{1}{2}\,l_0 \\ \frac{c_3}{c_1} &= \frac{c_3}{c_2}\cdot\frac{c_2}{c_1} = \frac{m}{4(2m+1)}\,D^2\left\{1 + \frac{4(2m+1)}{3m}\left(\frac{l_0}{D}\right)^2\right\} \end{aligned}\right\} \quad \ldots \qquad (21)$$

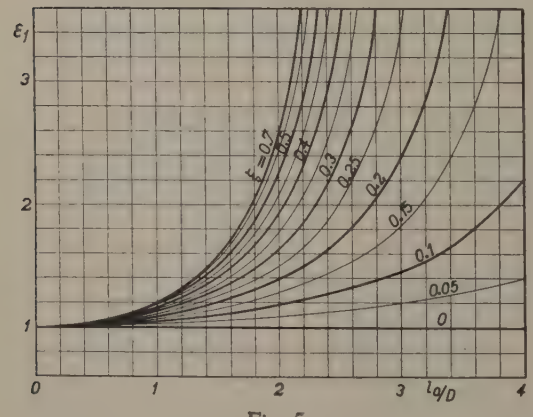

Fig. 5.

The correction factor ε_1 as function of the relative compression ξ and the ratio l_0/D.

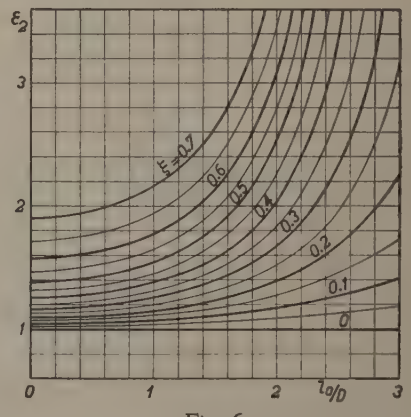

Fig. 6.

The correction factor ε_2 as function of the relative compression ξ and the ratio l_0/D.

If an axial force is present the formulae (20) can be brought in a form similar to (21) by writing

$$\left.\begin{aligned} \frac{c_a}{c_1} &= \frac{m}{2(m+1)}\left\{1+\frac{2m+1}{3m}\left(\frac{l}{D}\right)^2\right\}\cdot\varepsilon_1 = 0.3845\left\{1+0.766\left(\frac{l}{D}\right)^2\right\}\cdot\varepsilon_1 \\ \frac{c_2}{c_1} &= \tfrac{1}{2}\,l\,.\,\varepsilon_2 \qquad\qquad (m=10/3) \\ \frac{c_3}{c_1} &= \frac{m}{4(2m+1)}D^2\left\{1+\frac{4(2m+1)}{3m}\left(\frac{l}{D}\right)^2\right\}\varepsilon_3 = 0.1087\,D^2\left\{1+3.066\left(\frac{l}{D}\right)^2\right\}\cdot\varepsilon_3 \end{aligned}\right\} \quad (22)$$

Evidently the corrective coefficients ε_1, ε_2 and ε_3 are functions of $\xi = \triangle l/l_0$ and l_0/D. They have been plotted in the figs. 5, 6 and 7.

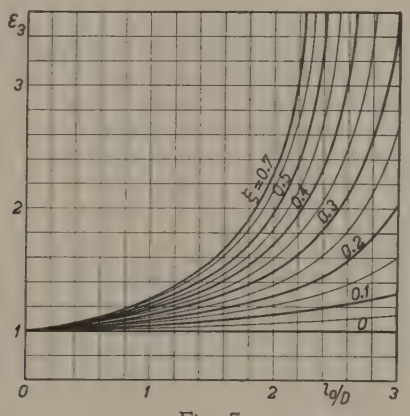

Fig. 7.

The correction factor ε_3 as function of the relative compression ξ and the ratio l_0/D.

If it is required that both ends of the spring remain parallel to each other, ψ_l must be zero. In that case the lateral rigidity, according to equation (18) is given by c_1, and therefore the ratio between the axial and lateral rigidity is represented by the first expression (22). If $M_0 = 0$ this ratio is represented by the same expression provided only that l be replaced by $2l$.

(To be continued.)

Mathematics. — *Zur projektiven Differentialgeometrie der Regelflächen im R_4.* (Zwölfte Mitteilung.) Von W. J. BOS. (Communicated by Prof. R. WEITZENBÖCK.)

(Communicated at the meeting of May 30, 1942.)

Im Anschluss an die vorige Mitteilung setzen wir hier die Besprechung der Vierpunktebenen fort.

§ 33.

Die Vermutung liegt nahe, dass die Eigenschaften der Vierpunktebenen viel Uebereinstimmung zeigen werden mit den Eigenschaften der Ebenen, die vier Geraden *a*, *b*, *c* und *d* allgemeiner Lage im R_4 schneiden. Bekanntermassen bekommt man bei dieser Figur mittels einfacher Inzidenzen die assozierte Gerade *e*. Dabei entsteht eine Konfiguration von fünfzehn Punkten und fünfzehn Geraden. Jede dieser Geraden enthält drei der Punkte und durch jeden Punkt gehen drei Geraden der Konfiguration. Weiter gibt es zehn singuläre Räume, wovon in jedem sechs der Geraden liegen.

Man kann dann Folgendes zeigen [1]):

I. Es gibt einen System von ∞^2 Ebenen S, welche *a*, *b*, *c* und *d* schneiden.

II. Diese Ebenen S schneiden auch die assozierte Gerade *e*.

III. Durch einen Punkt auf einer der fünf Geraden *a*, *b*, *c*, *d* und *e* gehen ∞^1 Ebenen S, die im Allgemeinen einen kwadratischen Hyperkegel bilden.

IV. Im Allgemeinen liegen keine zwei der Ebenen S in einem R_3. Nur die singulären Räume enthalten mehr als eine Ebene S; sie enthalten nämlich Büschel dieser Ebenen.

V. Durch einen Punkt gehen im Allgemeinen zwei Ebenen S.

VI. Die Punkte wofür diese beiden Ebenen zusammenfallen liegen auf einer Hyperfläche vierten Grades Σ mit den folgenden Eigenschaften:

a. Die fünfzehn Geraden sind Doppellinien von Σ.

b. Jeder singuläre Raum ist Tangentialraum von Σ und schneidet Σ in einer doppelt zu zählenden Quadrik.

c. Jede Ebene S schneidet Σ in einem doppelt zu zählenden Kegelschnitt.

In grosser Uebereinstimmung hiermit finden wir bei den Regelflächen die folgenden Eigenschaften der Vierpunktebenen.

I*. *Es gibt ∞^2 Vierpunktebenen.*

Wir haben nämlich sechs Beziehungen (277), (ϕ_1), (ϕ_2) und (ϕ_3) zwischen den neun homogenen Grössen λ_i aus (275).

Der Gleichung (93) entnimmt man leicht:

II*. *Die Vierpunktebenen schneiden die Beigerade g.*

Im § 32 fanden wir:

III*. *Die Vierpunktebenen durch einen Punkt der Erzeugende 0_{ik} bilden im Allgemeinen einen kwadratischen Hyperkegel.*

Analog mit IV erhielten wir weiter im § 33 den Satz:

IV*. *Nur der Tangentialraum und der Beiraum enthalten mehr als eine Vierpunktebene, in diesen Räumen liegen nämlich die Vierpunktebenen A resp. B.*

Statt der Eigenschaft V der oben betrachtete Konfiguration bekommen wir jetzt:

V*. *Durch einen Punkt im R_4 gehen im Allgemeinen zwei Vierpunktebenen.*

---

[1]) H. F. BAKER, Principles of Geometrie, Vol. IV, Ch. V, 113—130, Cambridge (1925).

Beweis: Der Punkt y liegt in der Ebene ϕ (275) wenn:

$$\left.\begin{aligned} & x_{02}(\quad\quad\quad \lambda_1 y_{03} + \lambda_2 y_{04} + \lambda_3 y_{22} + \lambda_4 y_{23}) + \\ + & x_{03}(-\lambda_1 y_{02} \quad\quad + \lambda_5 y_{04} + \lambda_6 y_{22} + \lambda_7 y_{23}) + \\ + & x_{04}(-\lambda_2 y_{02} - \lambda_5 y_{03} \quad\quad + \lambda_8 y_{22} + \lambda_9 y_{23}) + \\ + & x_{22}(-\lambda_3 y_{02} - \lambda_6 y_{03} - \lambda_8 y_{04}) + \\ + & x_{23}(-\lambda_4 y_{02} - \lambda_7 y_{03} - \lambda_9 y_{04}) \equiv 0 \ \{x\} \end{aligned}\right\} \quad . \quad . \quad (288)$$

Da die Ausdrücke x_{02}, x_{03}, x_{04}, x_{22} und x_{23} linear unabhängig sind, führt dies zu den fünf Beziehungen

$$\lambda_1 y_{03} + \lambda_2 y_{94} + \lambda_3 y_{22} + \lambda_4 y_{23} = 0 \quad . \quad . \quad . \quad . \quad (289a)$$

$$-\lambda_1 y_{02} \quad\quad + \lambda_5 y_{04} + \lambda_6 y_{22} + \lambda_7 y_{23} = 0 \quad . \quad . \quad . \quad . \quad (289c)$$

$$-\lambda_2 y_{02} - \lambda_5 y_{03} \quad\quad + \lambda_8 y_{22} + \lambda_9 y_{23} = 0 \quad . \quad . \quad . \quad . \quad (289d)$$

$$-\lambda_3 y_{02} - \lambda_6 y_{03} - \lambda_8 y_{04} = 0 \quad . \quad . \quad . \quad . \quad . \quad . \quad . \quad . \quad . \quad (289d)$$

$$-\lambda_4 y_{02} - \lambda_7 y_{03} - \lambda_9 y_{04} = 0 \quad . \quad . \quad . \quad . \quad . \quad . \quad . \quad . \quad . \quad (289e)$$

Diese Beziehungen zwischen den λ_i sind aber nicht unabhängig wenn man auch die Relationen (277) mit in Betracht zieht. Man sieht leicht, dass man, wenigstens wenn λ_8 und λ_9 ungleich Null sind, das System der Beziehungen (277) und (289) ersetzen kann durch (277), (289c) und (289e). Die Beschränkung $\lambda_9 \neq 0$ können wir hier weglassen, denn aus $\lambda_9 = 0$ folgt wegen (276a) und (ϕ_1): $\lambda_8 = 0$. Die Vierpunktebenen ϕ mit $\lambda_8 = 0$ betrachteten wir schon in der Mitteilung 11.

Wenn weiter $y_{02} \neq 0$ ist, also wenn y nicht im Tangentialraume liegt, können wir mit Hilfe von (277), (289c), (289e), (ϕ_1) und (ϕ_2) die Parameter $\lambda_i (i = 1, 2, \ldots\ldots 7)$ ausdrücken in λ_8 und λ_9. In diesem Falle hat man nämlich:

$$\left.\begin{aligned} & \lambda_7 = \frac{8}{3}\lambda_8 ; \ \lambda_4 = -\frac{y_{03}}{y_{02}}\lambda_7 - \frac{y_{04}}{y_{02}}\lambda_9 ; \\ & \lambda_5 = \frac{1}{6}\lambda_4 + \frac{2}{9}\frac{R}{Q}\lambda_8 - \frac{1}{6}\frac{S}{Q}\lambda_9 ; \ \lambda_2 = -\frac{y_{03}}{y_{02}}\lambda_5 + \frac{y_{22}}{y_{02}}\lambda_8 + \frac{y_{23}}{y_{02}}\lambda_9 ; \\ & \lambda_3 = \frac{\lambda_4 \,.\, \lambda_8}{\lambda_9} ; \ \lambda_6 = \frac{\lambda_7 \,.\, \lambda_8}{\lambda_9} ; \ \lambda_1 = \frac{\lambda_2 \,.\, \lambda_6 - \lambda_3 \,.\, \lambda_5}{\lambda_8} . \end{aligned}\right\} \quad (290)$$

Hiermit findet man aus (ϕ_3) die kwadratische Gleichung:

$$\left.\begin{aligned} & -16 y_{02}(R \,.\, y_{02} - 2Q \,.\, y_{03})\lambda_8^2 + 8(3S \,.\, y_{02}^2 - 6Q \,.\, y_{02} \,.\, y_{13} + 2Q \,.\, y_{03}^2)\lambda_8 \,.\, \lambda_9 + \\ & + 3(-\tfrac{3}{2} T \,.\, y_{02}^2 + 2S \,.\, y_{02} \,.\, y_{03} + R \,.\, y_{02} \,.\, y_{04} + 12Q \,.\, y_{02} \,.\, y_{23} + 2Q \,.\, y_{03} \,.\, y_{04})\lambda_9^2 = 0. \end{aligned}\right\} \quad (291)$$

Für jeden gegebenen Punkt y gibt uns diese Gleichung zwei Werte für $\frac{\lambda_8}{\lambda_9}$ woraus mit (290) die Gleichungen der beiden Vierpunktebenen durch y berechenbar sind. Damit ist der Satz V* bewiesen.

Man rechnet leicht nach, dass (291) auch gilt wenn der Punkt y im Tangentialraume aber nicht in der Heftebene liegt ($y_{02} = 0$, $y_{03} \neq 0$). Für diese Punkte y haben wir dann

$$8 y_{03} \,.\, \lambda_8 + 3 y_{04} \,.\, \lambda_9 = 0.$$

Die zugehörigen Werte der übrigen λ_i findet man leicht. Die zweite Vierpunktebene durch y ist hier natürlich die Vierpunktebene A durch y, d.h. die Verbindungsebene von y mit der Gerade HG. (§ 32; dabei ist $\lambda_8 = 0$.)

Auch für die Punkte y im Beiraume gibt (291) nur eine Ebene; die zweite Ebene ist hier die Vierpunktebene B durch y ($\lambda_8 = 0$).

Schreiben wir (291) in der Gestalt

$$-16\, y_{02}\,(B'\,y)\,\lambda_8^2 + 8\,(L'\,y)^2\,\lambda_8\,.\,\lambda_9 + 3\,(N'\,y)^2\,\lambda_9^2 = 0, \quad . \quad . \quad (292)$$

dann wird λ_8/λ_9 unbestimmt für die Punkte im Beiraume wofür ausserdem gilt:

$$(L'\,y)^2 = 0, \quad (N'\,y)^2 = 0.$$

Eine einfache Berechnung zeigt, dass der Beiraum die Hyperquadrik $(L'\,y)^2 = 0$ schneidet in der Heftebene und der Ebene (267) durch H und g, während die Schnittfigur des Beiraumes mit der zweiten Hyperquadrik $(N'\,y)^2 = 0$ aus der Heftebene und der Ebene durch g_{ik} und den Punkt mit Gleichung

$$2\,R\,.\,H_{u'} - Q\,.\,2_{03}\,2_{u'} = 0$$

besteht.

Hieraus sehen wir, dass *durch einen Punkt der Beigerade* g_{ik} ∞^1 *Vierpunktebenen gehen.* (Vgl. III.)

Weiter gibt uns (291), (292) analog zu VI:

VI*. *Durch den Punkt y geht nur eine Vierpunktebene (oder* ∞ *viele), wenn y gelegen ist auf der Hyperfläche* W_3^4 *vierten Grades mit der Gleichung*

$$\left.\begin{aligned} W_3^4 = (w'\,x)^4 = \{(L'\,x)^2\}^2 + 3\,.\,x_{02}\,(B'\,x)\,(N'\,x)^2 = \\ = (3S\,.\,x_{02}^2 - 6Q\,.\,x_{02}\,.\,x_{13} + 2Q\,.\,x_{03}^2)^2 + 3\,.\,x_{02}\,(R\,.\,x_{02} - 2Q\,.\,x_{03})\,. \\ (-\tfrac{3}{2}\,T\,.\,x_{02}^2 + 2S\,.\,x_{02}\,.\,x_{03} + R\,.\,x_{02}\,.\,x_{04} + 12Q\,.\,x_{02}\,.\,x_{23} + 2Q\,.\,x_{03}\,.\,x_{04}) = 0. \end{aligned}\right\} \quad (293)$$

Mit Rücksicht auf die Eigenschaft (VIa) der Hyperfläche Σ liegt es auf der Hand, dass jetzt 0_{ik}, a_{ik} und g_{ik} Doppellinien von W_3^4 sind. Da die Gerade g_{ik} aber die Verbindungsebene von 0_{ik} und a_{ik} (die Heftebene) schneidet, ist in diesem Falle die Heftebene eine singuläre Ebene von W_3^4.

Zum Beweise betrachten wir einen allgemeinen Punkt P der Heftebene und berechnen wir die Polaren von P in Bezug auf W_3^4.

Die Gleichung von P können wir schreiben:

$$P = P_{u'} = \varrho_{u'}\,\varrho_{02,03} = -\,\varrho_{u'}\,2_{0\varrho,03} = 0. \quad . \quad . \quad . \quad . \quad (294)$$

Wegen $P_{02} = 0$, $P_{03} = 0$ finden wir dann

$$\left.\begin{aligned} \triangle_{xP}\,W_3^4 = 4\,(w'\,P)\,(w'\,x)^3 = -12Q\,.\,x_{02}\,.\,P_{13}\,(L'\,x)^2 + \\ + 3\,.\,x_{02}\,(B'\,x)\,(R\,.\,x_{02}\,.\,P_{04} + 12Q\,.\,x_{02}\,.\,P_{23} + 2Q\,.\,x_{03}\,.\,P_{04}). \end{aligned}\right\} \quad (295)$$

Hier haben wir nach (255) und (256)

$$P_{04} = \varrho_{04,02,03} = -\tfrac{4}{3}\,Q\,(0^2\,\varrho^3), \quad P_{22} = \varrho_{22,02,03} = +\tfrac{2}{3}\,(a^2\,\varrho^3).$$

Weiter ist (Vgl. (245) und (95))

$$P_{13} = -\tfrac{1}{4}\,P_{04} - \tfrac{3}{4}\,P_{22} = +\tfrac{1}{3}\,Q\,(0^2\,\varrho^3) - \tfrac{1}{2}\,(a^2\,\varrho^3) = \tfrac{1}{6}\,(HG\,\varrho^3)$$

und

$$P_{23} = \varrho_{23,02,03} = -\,\varrho_{23}\,2_{0\varrho,03} = \tfrac{2}{3}\,.\,0_{23}\,2_{03}\,(02\,\varrho^3) + \tfrac{1}{9}\,R\,(0^2\,\varrho^3).$$

Damit kommt statt (295):

$$\left.\begin{aligned}\Delta_{xP} W_3^4 = &-\tfrac{3}{2} x_{02} \,.\, Q\,(HG\varrho^3)\,(L'x)^2 + \\ &+ 8Q \,.\, x_{02}\,(B'x)\,\{(3\,.\,0_{23}\,2_{03}\,(02\varrho^3) - Q\,.\,x_{03}\,(0^2\varrho^3)\}\,.\end{aligned}\right\} \quad (296)$$

Weiter wird

$$\Delta_{xP}^2 W_3^4 = 12\,(w'P)^2\,(w'x)^2 = \tfrac{9}{8} x_{02}^2 \,.\, Q^2\,\{(HG\varrho^3)\}^2 \quad . \quad . \quad (297)$$

und

$$\Delta_{xP}^3 W_3^4 = 24\,(w'P)^3\,(w'x) \equiv 0. \quad . \quad . \quad . \quad . \quad (298)$$

Die letzte Gleichung zeigt:

VIa*$_1$. *Die Heftebene ist eine Doppelebene von* W_3^4.

Weiter gibt (297):

VIa*$_2$. *Die Gerade HG (die Achse der Vierpunktebenen A) ist eine dreifache Gerade von* W_3^4.

Die Polaren $\Delta_{xP} W_3^4$ und $\Delta_{xP}^2 W_3^4$ enthalten den Faktor x_{02}, also:

VIb*$_1$. *Die Schnittfigur von* W_3^4 *mit dem Tangentialraume* $x_{02} = 0$ *der Regelfläche F ist die vierfach zu zählende Heftebene.*

Wir bestimmen weiter die Tangentialräume der Fläche W_3^4 in den Punkten von HG. Wegen $H_{02} = 0$, $H_{03} = 0$, $H_{04} = 0$, $H_{22} = 0$ und $H_{13} = 0$ finden wir für die erste Polare des Punktes H in Bezug auf W_3^4:

$$\left.\begin{aligned}\Delta_{xH} W_3^4 &= 4\,(w'H)\,(w'x)^3 = \\ &= 3\,.\,x_{02}\,(B'x)\,(12\,Q\,.\,x_{02}\,.\,0_{23,22}) = 48\,Q^2\,.\,x_{02}^2\,(B'x).\end{aligned}\right\} \quad (299)$$

Die Gleichung (245) zeigt, dass der Punkt C mit Gleichung

$$C = C_{u'} = 3_{u'}\,3_{02} = 0$$

auf der Gerade HG liegt. Berechnen wir $\Delta_{xc} W_3^4$, dann finden wir

$$\Delta_{xC} W_3^4 = -\,24\,Q^2\,.\,x_{02}\,.\,x_{03}\,(B'x). \quad . \quad . \quad . \quad . \quad (300)$$

Nach (95) erhalten wir also aus (299) und (300):

$$\Delta_{xG}\, W_3^4 = \Delta_{x,\,RH+4QC}\, W_3^4 = +\,48\,Q^2\,.\,x_{02}\,\{(B'x)\}^2 \quad . \quad . \quad (301)$$

Wir haben hiermit bewiesen, dass die drei Tangentialräume der Fläche W_3^4 in einem Punkte $\xi H + \eta G$ der Gerade HG die Räume sind mit den Gleichungen

$$x_{02} = 0, \quad (B'x) = 0, \quad \xi\,.\,x_{02} + \eta\,.\,(B'x) = 0.$$

Hieraus folgt weiter, dass die Gerade HG eine vierfache Gerade des Durchschnitts von W_3^4 mit dem Beiraume ist. Diese Schnittfigur besteht also aus der doppelt zu zählenden Heftebene und aus einem Ebenenpaar mit Achse HG. Es ist zu erwarten, und wir werden auch tatsächlich beweisen, dass dieses Ebenenpaar wieder eine Doppelebene ist, nämlich die Ebene durch H und g_{ik} (267).

Dazu genügt es zu zeigen, dass g_{ik} eine Doppellinie von W_3^4 ist.

Nun bekommen wir einen nicht-invarianten Punkt Y auf g_{ik} durch g_{ik} zu schneiden mit dem Raume mit der Gleichung $x_{22} = 0$.

Wegen

$$1_{u'}\,1_{22} = +\,\tfrac{8}{3}\,.\,2_{u'}\,2_{03}$$

lautet die Gleichung des Punktes Y (Vgl. (93).):

$$Y_{u'} = P \,.\, 0_{u'}\, 0_{22} - 8Q\,(3QS + R^2)\, 2_{u'}\, 2_{03} - 72Q^3 \,.\, 3_{u'}\, 3_{22} = 0. \quad (302)$$

Dies schreiben wir in der Gestalt

$$Y = \lambda \,.\, H + \mu \,.\, D + \nu \,.\, E = 0. \quad . \quad . \quad . \quad . \quad . \quad (303)$$

Dabei ist also:

$$\left.\begin{aligned} \lambda &= P = 2R^3 + 12\,QRS + 9\,Q^2\,T, \\ \mu &= -\,8\,Q\,(3\,QS + R^2), \\ \nu &= -\,72\,Q^3, \end{aligned}\right\} \quad . \quad . \quad . \quad . \quad (304a)$$

$$D = 2_{u'}\, 2_{03}, \quad E = 3_{u'}\, 3_{22} \quad . \quad . \quad . \quad . \quad . \quad . \quad (304b)$$

Wir werden jetzt zeigen dass

$$\tfrac{1}{24}\, \Delta^3_{xY}\, W_3^4 = (w'\,Y)^3\,(w'\,x) \equiv 0$$

und bemerken dazu erstens, dass H ein dreifacher und D ein zweifacher Punkt von W_3^4 ist, sodass wir

$$(w'\,H)^2\,(w'\,x)^2 \equiv 0$$

und

$$(w'\,D)^3\,(w'\,x) \equiv 0$$

haben.

Weiter folgt wegen $D_{02} = 0$ und $D_{03} = 0$ aus (299):

$$(w'\,H)\,(w'\,D)\,(w'\,x)^2 \equiv 0.$$

Mit Rücksicht auf diese Gleichungen haben wir also:

$$\left.\begin{aligned} (w'\,Y)^3\,(w'\,x) = 3\,\lambda\,\nu^2\,(w'\,H)\,(w'\,E)^2\,(w'\,x) + 3\mu^2\,\nu\,(w'\,D)^2\,(w'\,E)\,(w'\,x) + \\ + 3\,\mu\,\nu^2\,(w'\,D)\,(w'\,E)^2\,(w'\,x) + \nu^3\,(w'\,E)^3\,(w'\,x). \end{aligned}\right\} \quad (305)$$

Wir berechnen E_{02}, E_{03}, E_{13}, E_{04} und E_{23}:

$$\left.\begin{aligned} &E_{02} = 3_{02,\,22} = -\tfrac{4}{3}\,Q\,; \quad E_{03} = 3_{03,\,22} = -\tfrac{2}{3}\,R\,; \\ &E_{13} = 3_{13,\,22} = -\tfrac{1}{4}\,.\,3_{04,\,22} = \tfrac{1}{2}\,.\,2_{04,\,23} = -\tfrac{1}{3}\,S\,; \\ &E_{04} = 3_{04,\,22} = +\tfrac{4}{3}\,S\,; \quad E_{23} = 3_{23,\,22} = -\,2\,.\,2_{23,\,23} = 0. \end{aligned}\right\} \quad . \quad . \quad (306)$$

Dies gibt

$$(B'\,E) = RE_{02} - 2\,QE_{03} = 0. \quad . \quad . \quad . \quad . \quad . \quad . \quad (307)$$

Mit Hilfe der Ausdrücke (306) und (307) finden wir aus (299):

$$(w'\,H)\,(w'\,E)^2\,(w'\,x) = \tfrac{64}{9}\,Q^4\,(B'\,x). \quad . \quad . \quad . \quad . \quad . \quad (308)$$

Auf dieselbe Weise erhalten wir:

$$(w'\,D)^2\,(w'\,E)\,(w'\,x) = -\,8\,Q^5\,x_{02} \quad . \quad . \quad . \quad . \quad . \quad . \quad (309)$$

$$\left.\begin{aligned} (w'\,D)\,(w'\,E)^2\,(w'\,x) = \tfrac{8}{9}\,Q^3\,(R^2 + 3\,QS)\,x_{02} + \\ + \tfrac{8}{9}\,Q^4\,(9\,Sx_{02} + 4\,Rx_{03} - 12\,Qx_{13}) \end{aligned}\right\} \quad (310)$$

$$\left.\begin{aligned} (w'\,E)^3\,(w'\,x) = -\,\tfrac{8}{27}\,Q^2\,(R^2 + 3\,QS)\,(9\,Sx_{02} + 4\,Rx_{03} - 12\,Qx_{13}) + \\ + \tfrac{8}{9}\,Q^2\,(3\,QT + 2\,RS)\,(B'\,x). \end{aligned}\right\} \quad (311)$$

Einsetzung der Ausdrücke (304a) und (308) bis (311) in (305) gibt dann in der Tat:

$$(w' Y)^3 (w' x) \equiv 0.$$

VIa$_3^*$. *Die Beigerade ist also eine Doppellinie der Hyperfläche* W_3^4.

VIb$_2^*$. *Der Beiraum schneidet* W_3^4 *in einem doppelt zu zählenden Ebenenpaare, bestehend aus der Heftebene und der Ebene durch* H *und die Beigerade* g_{ik}.

Es gibt in (305) nur einen Term, worin H vorkommt und dieser Term enthält wegen (308) den Faktor $(B' x)$.

Betrachten wir also statt Y den Punkt

$$Y^* = \mu D + \nu E,$$

dann hat $(w' Y^*)^3 (w' x)$ der Faktor $(B' x)$. Y_* ist ein nicht-invarianter Punkt der Ebene durch H und g_{ik} und man sieht leicht, dass man durch Transformationen

$$t = \varphi(\tilde{t}), \quad \hat{a}_{ik} = \lambda(t) \, . \, a_{ik},$$

Y^* in jeden Punkt dieser Ebene überführen kann (ausgenommen die Punkte der Geraden HG und g). Wegen $(B' Y^*) = 0$ gibt dies also, neben einer Bestätigung des Satzes VIa$_3^*$, das Resultat:

VIa$_4^*$. *Die Ebene durch* H *und* g *liegt auf der Hyperfläche* W_3^4.

Alle Geraden der Heftebene und der Ebene Hg liegen auf W_3^4; wir können fragen ob es noch mehr Geraden auf W_3^4 gibt.

Jede solche Gerade 1 wird den Raum $x_{02} = 0$ schneiden in einem Punkte der Heftebene (VIb$_1^*$) und 1 liegt also mit der Heftebene in einem Raume r' mit der Gleichung

$$(r' x) = \xi x_{02} + \eta (B' x) = 0 \, . \, . \, . \, . \, . \, . \quad (312)$$

Dieser Raum ist aber, wie wir zeigten, Tangentialraum der Fläche W_3^4 in dem Punkte $\xi H + \eta G$ von HG. Nach VIa$_2^*$ finden wir also:

Die Schnittfigur von r' mit W_3^4 besteht aus einem kwadratischen Kegel mit Spitze $\xi H + \eta G$ und der dabei doppelt zu zählenden Heftebene. Dieser Kegel enthält die Gerade HG und ist dann und nur dann entartet wenn r' der Tangentialraum $x_{02} = 0$ oder der Beiraum $(B' x) = 0$ ist.

Alle Geraden auf W_3^4 *schneiden also* HG.

Mathematics. — *Sur l'unicité des solutions de certaines équations aux dérivées partielles du quatrième ordre.* Par H. BREMEKAMP. (Communicated by Prof. W. v. d. WOUDE.)

(Communicated at the meeting of May 30, 1942.)

A l'égard de l'équation de LAPLACE $\triangle u = 0$ on connaît le théorème de DIRICHLET, qui pour le cas de deux variables indépendantes s'énonce comme il suit: la solution est unique, si l'on se donne les valeurs de u en tous les points d'une courbe fermée et que l'on exige en outre que la solution soit valable dans tout le domaine intérieur à la courbe. Si l'on compare ce théorème au théorème de CAUCHY–KOWALEWSKI selon lequel la solution est unique si l'on se donne le long de la courbe u et $\frac{\partial u}{\partial n}$ (la solution est alors valable dans un certain domaine situé des deux côtés de la courbe), on voit que le donné $\frac{\partial u}{\partial n}$ en tous les points de la courbe est remplacé par le donné la solution est valable pour tout l'intérieur de la courbe. M. E. PICARD [1]) a démontré qu'un théorème analogue à celui de DIRICHLET vaut pour l'équation

$$\triangle u + \alpha \frac{\partial u}{\partial x} + \beta \frac{\partial u}{\partial y} + \gamma u + f = 0,$$

seulement il faut dans certains cas ajouter la condition, que le domaine intérieur à la courbe soit assez petit.

On sait très peu sur ces questions à l'égard des équations d'ordre supérieur au second. Je vais considérer dans cette note l'équation du quatrième ordre

$$\alpha \triangle\triangle u + 2\beta \triangle u + \gamma u = 0, \quad . \quad . \quad . \quad . \quad . \quad . \quad (1)$$

où α, β, γ sont des fonctions connues de x, y holomorphes dans le domaine considéré et α sans zéros. Cette équation est une généralisation de l'équation $\triangle\triangle u = 0$; sur cette dernière équation qui joue un rôle important dans la théorie de l'élasticité, MATHIEU [2]) a démontré deux théorèmes analogues au théorème de DIRICHLET, à savoir: la solution de l'équation valable dans tout l'intérieur d'une courbe fermée est uniquement déterminée, quand on se donne aux points de la courbe 1^0 u et $\triangle u$, 2^0 u et $\frac{\partial u}{\partial n}$. La démonstration de ces théorèmes est très simple et elle se fait pour les deux théorèmes à la fois.

Du théorème de GREEN

$$\int (u \triangle v - v \triangle u)\, d\sigma = \int \left(u \frac{\partial v}{\partial n} - v \frac{\partial u}{\partial n} \right) ds$$

on déduit en prenant $v = \triangle u$

$$\int u \triangle\triangle u \, d\sigma - \int (\triangle u)^2 \, d\sigma = \int u \frac{\partial \triangle u}{\partial n} \, ds - \int \triangle u \frac{\partial u}{\partial n} \, ds. \quad (2)$$

Or si u satisfait à l'équation $\triangle\triangle u = 0$ et sur la courbe à laquelle se rapportent les intégrations au second membre, $u = 0$ et, ou $\triangle u = 0$, ou $\frac{\partial u}{\partial n} = 0$, on voit, que $\int (\triangle u)^2 \, d\sigma = 0$ d'où $\triangle u = 0$ en tout point à l'intérieur de la courbe, l'application du théorème de DIRICHLET et puis un raisonnement bien connu achèvent la démonstration.

§ 1. Nous allons démontrer des théorèmes analogues pour l'équation (1). Nous ne nous efforcerons pas à supposer aussi peu que possible sur la courbe fermée C, qui porte les

---

[1]) Journal de Mathématiques pures et appliquées 4^0. Série T. VI, 1890.

[2]) Journal de Mathématiques pures et appliquées, T. XIV, 1879.

valeurs données de u et de $\triangle u$ ou $\frac{\partial u}{\partial n}$. Nous admettrons qu'elle soit fermée, sans point double et ayant une tangente déterminée en chacun de ses points. En répétant ou en imitant des raisonnements célèbres de LIAPOUNOFF et d'autres auteurs, il ne serait pas difficile d'affaiblir considérablement ces conditions. Dans quelques exemples nous admettrons un nombre limité de pointes, un cas auquel les démonstrations s'appliquent sans difficulté. Nous supposerons en outre que les suites de valeurs données sur la courbe constituent des fonctions continues de quelque paramètre définissant les points de la courbe, seulement pour ne pas trop prolonger les raissonnements. Aussi pourrait on remplacer cette condition par d'autres beaucoup moins rigoureuses.

On verra, que pour notre équation (1) on ne peut pas toujours traiter les données u et $\triangle u$ et les données u et $\frac{\partial u}{\partial n}$ sur la courbe C de la même manière et qu'il faut distinguer différents cas selon le signe de l'expression $\alpha\gamma - \beta^2$. Pour simplifier nous admettrons que ce signe est le même en tous les points intérieurs à la courbe C.

Il s'agit de démontrer qu'une fonction u satisfaisant à l'équation (1) en tout point intérieur à la courbe fermée C, si en outre en tout point de C $u = 0$ et $\triangle u = 0$, ou $u = 0$ et $\frac{\partial u}{\partial n} = 0$, est nulle en tout point intérieur à C. On verra que les démonstrations de ces deux théorèmes pour le cas $\alpha\gamma - \beta^2 < 0$ qui seront données aux §§ 2 et 3 sont beaucoup plus difficiles que pour les autres cas.

D'abord nous allons encore appliquer la formule (2). Les conditions énoncées rendent le second membre zéro et l'on trouve

$$\int (\triangle u)^2 \, d\sigma = \int u \triangle\triangle u \, d\sigma - \int u \left(2 \frac{\beta}{\alpha} \triangle u + \frac{\gamma}{\alpha} u \right) d\sigma,$$

donc

$$\int \left(\triangle u + \frac{\beta}{\alpha} u \right)^2 d\sigma + \int \frac{\alpha\gamma - \beta^2}{\alpha^2} u^2 \, d\sigma = 0 . \quad . \quad . \quad . \quad (3)$$

Premier cas: $\alpha\gamma - \beta^2 > 0$.

Dans ce cas nous tirons de l'équation (3), que dans tout le domaine considéré, $\triangle u + \frac{\beta}{\alpha} u = 0$ et $u = 0$. C'est ce dernier fait, que nous voulions démontrer. Pour $\alpha\gamma - \beta^2 > 0$ les deux théorèmes sont donc démontrés.

Deuxième cas: $\alpha\gamma - \beta^2 = 0$.

Dans ce cas nous nous occuperons d'abord des donnés $u = 0$ et $\triangle u = 0$ en tout point de C. De l'équation (3) nous tirons en ce cas

$$\triangle u + \frac{\beta}{\alpha} u = 0$$

et nous cherchons une fonction satisfaisant à cette équation, qui en tout point du contour prend la valeur zéro. D'après le théorème de PICARD, cité plus haut, nous pouvons indiquer autour de chaque point du plan un domaine tel, que $u = 0$ est la seule solution satisfaisant à cette condition, si la courbe donnée est intérieure à ce domaine. Si $\frac{\beta}{\alpha}$ est négatif partout dans la partie du plan considérée, l'assertion est vraie sans restriction. L'exemple suivant (donné par PICARD pour illustrer son théorème sur les équations du second ordre), montre qu'il n'est pas toujours ainsi. La fonction $u = \sin x \sin y$ satisfait à l'équation $\triangle\triangle u + 4 \triangle u + 4u = 0$ et en tout point du contour du carré, formé par les droites $x = 0$, $x = \pi$, $y = 0$, $y = \pi$, on a $u = 0$ et $\triangle u = 0$. Nous trouvons un autre exemple, comme il suit. De $\triangle J_0(r) = -J_0(r)$ nous concluons, que $J_0(r)$ satisfait à l'équation $\triangle\triangle u + 2 \triangle u + u = 0$, et si λ est racine de l'équation $J_0(r) = 0$, sur la circonférence $r = \lambda$ on a $J_0(r) = 0$ et $\triangle J_0(r) = 0$.

Dans le cas des donnés $u = 0$ et $\frac{\partial u}{\partial n} = 0$ en tout point de C, il faut chercher une solution de $\triangle u + \frac{\beta}{\alpha} u = 0$ satisfaisant à ces deux conditions, (qui différemmant de $u = 0$ et $\triangle u = 0$ ne s'incluent pas). Dans ce cas il suit du théorème de CAUCHY-KOWALEWSKI que $u = 0$ est la seule solution, sans aucune restriction.

Troisième cas: $\alpha\gamma - \beta^2 < 0$.

Nous allons commencer dans ce cas par quelques exemples. Que le premier théorème, cù il est donné, que u et $\triangle u$ sont nulles sur le contour, ne vaut pas sans restriction, on le voit par l'exemple, analogue au précédent, $u = \sin x \sin y$; cette fonction satisfait à $\triangle\triangle u + 2\triangle u = 0$ et en tout point du contour du carré décrit ci dessus on a $u = 0$ et $\triangle u = 0$. De même on voit que $J_0(r)$ satisfait à $\triangle\triangle u + \triangle u = 0$ et aux points de la circonférence $r = \lambda$ on a $J_0(r) = 0$ et $\triangle J_0(r) = 0$.

Pour le théorème, où il est donné que u et $\frac{\partial u}{\partial n}$ sont nulles sur le contour, nous construirons de la même manière un exemple, où l'on voit que le théorème ne vaut pas sans restriction. La fonction $u = AJ_0(r) + BJ_0(2r)$ satisfait à l'équation $\triangle\triangle u + 5\triangle u + 4u = 0$, que l'on peut écrire $(\triangle + 4)(\triangle + 1) u = 0$. Nous déterminons R de manière que

$$A J_0(R) + B J_0(2R) = 0,$$

et

$$A J_0'(R) + 2B J_0'(2R) = 0$$

admettent une solution commune pour $\frac{A}{B}$. Ça donne

$$\frac{J_0'(R)}{J_0(R)} = \frac{2J_0'(2R)}{J_0(2R)}.$$

Cette équation a une suite infinie de racines réelles. Soit R_1 la racine positive la plus petite. Nous prenons $\frac{A}{B} = -\frac{J_0(2R_1)}{J_0(R_1)}$. Alors $u = AJ_0(r) + BJ_0(2r)$ satisfait à l'équation $\triangle\triangle u + 5\triangle u + 4u = 0$, tandis que sur la circonférence $r = R_1$ on a $u = 0$ et $\frac{\partial u}{\partial n} = 0$.

§ 2. Admettant la restriction que la courbe C est assez petite, la démonstration du théorème, que la fonction C satisfaisant à l'équation $\alpha\triangle\triangle u + \beta\triangle u + \gamma u = 0$ et aux conditions $u = 0$ et $\triangle u = 0$ en tout point de la courbe fermée C est zéro en tout point intérieur à C, est facile dans le cas spécial que α, β, γ sont constantes, satisfaisant à la relation $\alpha\gamma - \beta^2 < 0$. Alors on peut mettre l'équation sous la forme $(\triangle - \lambda)(\triangle - \mu)u = 0$. Posant $(\triangle - \mu) u = v$, nous trouvons $(\triangle - \lambda) v = 0$ et sur C $v = 0$, parce que $u = 0$ et $\triangle u = 0$. Alors le théorème de PICARD donne $v = 0$ en tout point intérieur à C, donc $(\triangle - \mu) u = 0$ et une nouvelle application du même théorème donne $u = 0$. La même démonstration vaut quand λ et μ sont fonctions de x, y. Il faut cependant remarquer qu'alors l'équation ne rentre pas dans le type (1). Nous allons donner la démonstration pour le cas général de l'équation (1) en modifiant les raisonnements sur le dernier cas.

Puisque

$$(\triangle-\lambda)(\triangle-\mu)u = \triangle\triangle u - (\lambda+\mu)\triangle u - 2\left(\frac{\partial\mu}{\partial x}\frac{\partial u}{\partial x} + \frac{\partial\mu}{\partial y}\frac{\partial u}{\partial y}\right) + (\lambda\mu - \triangle\mu)u = 0$$

nous pouvons mettre l'équation (1) sous la forme

$$\triangle\triangle u + 2\frac{\beta}{\alpha}\triangle u + \frac{\gamma}{\alpha}u \equiv (\triangle-\lambda)(\triangle-\mu)u + 2\left(\frac{\partial\mu}{\partial x}\frac{\partial u}{\partial x} + \frac{\partial\mu}{\partial y}\frac{\partial u}{\partial y}\right) + \left(\lambda\mu + \frac{\gamma}{\alpha} - \triangle\mu\right)u = 0,$$

posant $\frac{2\beta}{\alpha} = \lambda + \mu$. La fonction μ reste encore arbitraire, nous la choisirons d'une manière à définir bientôt.

Nous avons donc

$$(\triangle - \lambda)(\triangle - \mu)\, u + 2A\frac{\partial u}{\partial x} + 2B\frac{\partial u}{\partial y} + Cu = 0 \quad . \quad . \quad . \quad . \quad (4)$$

où

$$A = \frac{\partial \mu}{\partial x},\ B = \frac{\partial \mu}{\partial y},\ C = \lambda\mu - \triangle\mu + \frac{\gamma}{\alpha} = -\frac{2\beta}{\alpha}\mu - \mu^2 - \triangle\mu + \frac{\gamma}{\alpha}.$$

Posant

$$(\triangle - \mu)\, u = v, \quad \text{on a} \quad (\triangle - \lambda)\, v = -2A\frac{\partial u}{\partial x} - 2B\frac{\partial u}{\partial y} - Cu,$$

donc

$$\int u\left(\frac{\partial^2 u}{\partial x^2} + \frac{\partial^2 u}{\partial y^2} - \mu u - v\right) d\sigma = 0$$

et

$$\int v\left(\frac{\partial^2 v}{\partial x^2} + \frac{\partial^2 v}{\partial y^2} - \lambda v + 2A\frac{\partial u}{\partial x} + 2B\frac{\partial u}{\partial y} + Cu\right) d\sigma = 0,$$

nous étendrons les intégrations au domaine intérieur à la courbe C. Des donnés $u = 0$ et $\triangle u = 0$ sur C on conclut que aussi $v = 0$ sur C. L'intégration par parties donne alors

$$\int\left\{\left(\frac{\partial u}{\partial x}\right)^2 + \left(\frac{\partial u}{\partial y}\right)^2 + \mu v^2 + uv\right\} d\sigma = 0 \quad . \quad . \quad . \quad . \quad (5)$$

et

$$\int\left\{\left(\frac{\partial v}{\partial x}\right)^2 + \left(\frac{\partial v}{\partial y}\right)^2 + \lambda v^2 - 2Av\frac{\partial u}{\partial x} - 2Bv\frac{\partial u}{\partial y} - Cuv\right\} d\sigma = 0. \quad (6)$$

Soient maintenant M et N deux fonctions de x, y satisfaisant seulement à quelques conditions évidentes de continuité et de dérivabilité, on a

$$\int\left\{\frac{\partial Mu^2}{\partial x} + \frac{\partial Nu^2}{\partial y}\right\} d\sigma = 0,$$

donc

$$\int\left\{\left(\frac{\partial M}{\partial x} + \frac{\partial N}{\partial y}\right) u^2 + 2Mu\frac{\partial u}{\partial x} + 2Nu\frac{\partial u}{\partial y}\right\} d\sigma = 0 \quad . \quad . \quad (7)$$

et en additionnant (5), (6) et (7)

$$\int\left\{\left(\frac{\partial u}{\partial x}\right)^2 + \left(\frac{\partial u}{\partial y}\right)^2 + \left(\frac{\partial v}{\partial x}\right)^2 + \left(\frac{\partial v}{\partial y}\right)^2 + \lambda v^2 + \left(\mu + \frac{\partial M}{\partial x} + \frac{\partial N}{\partial y}\right) u^2 + \right.$$
$$\left. + 2(Mu - Av)\frac{\partial u}{\partial x} + 2(Nu - Bv)\frac{\partial u}{\partial y} + (1 - C)uv\right\} d\sigma = 0$$

ou

$$\int\left\{\left(\frac{\partial v}{\partial x}\right)^2 + \left(\frac{\partial v}{\partial y}\right)^2 + \left(\frac{\partial u}{\partial x} + Mu - Av\right)^2 + \left(\frac{\partial u}{\partial y} + Nu - Bv\right)^2 + \right.$$
$$\left.\left(\mu + \frac{\partial M}{\partial x} + \frac{\partial N}{\partial y} - M^2 - N^2\right) u^2 + (1 - C + 2AM + 2BN)\, uv + (\lambda - A^2 - B^2)\, v^2\right\} d\sigma = 0 \quad (8)$$

Nous pouvons tirer de cette équation les conclusions désirées, si nous choisissons les fonctions μ, M et N tels que

$$\left(\mu+\frac{\partial M}{\partial x}+\frac{\partial N}{\partial y}-M^2-N^2\right)u^2+(1-C+2AM+2BN)uv+(\lambda-A^2-B^2)v^2$$

soit une fonction de u, v définite positive. A cet effet nous choisissons d'abord μ tel que $\lambda-A^2-B^2>0$, c'est à dire

$$\frac{2\beta}{\alpha}-\mu-\left(\frac{\partial\mu}{\partial x}\right)^2-\left(\frac{\partial\mu}{\partial y}\right)^2>0,$$

nous pouvons toujours satisfaire à cette inégalité en ajoutant à besoin à μ une constante négative convenablement choisie. Puis il faut déterminer M et N tels, que

$$\mu+\frac{\partial M}{\partial x}+\frac{\partial N}{\partial y}-M^2-N^2>\frac{4(1-C+2AM+2BN)^2}{\lambda-A^2-B^2}.$$

Prenant $N=0$, il faut avoir

$$\frac{\partial M}{\partial x}-M^2\left\{1+\frac{16A^2}{\lambda-A^2-B^2}\right\}-\frac{16(1-C)A}{\lambda-A^2-B^2}M+\mu-\frac{4(1-C)^2}{\lambda-A^2-B^2}>0.$$

Dans cette relation nous regarderons y comme paramètre, nous poserons

$$M+\frac{8(1-C)A}{\lambda+15A^2-B^2}=M_1$$

et nous introduirons une nouvelle variable ξ en posant

$$\frac{\partial\xi}{\partial x}=1+\frac{16A^2}{\lambda-A^2-B^2}.$$

L'inégalité précédente s'écrit alors

$$\frac{\partial M_1}{\partial\xi}-M_1^2>\frac{8(\lambda-A^2-B^2)}{\lambda+15A^2-B^2}\frac{\partial}{\partial x}\left\{\frac{(1-C)A}{\lambda+15A^2-B^2}\right\}+$$
$$+\frac{4(1-C)^2}{\lambda+15A^2-B^2}-\frac{64(1-C)^2A^2}{(\lambda+15A^2-B^2)^2}-\frac{\lambda-A^2-B^2}{\lambda+15A^2-B^2}\mu.$$

Or $\lambda-A^2-B^2$ et par suite $\lambda+15A^2-B^2$ étant toujours positif, on peut déterminer une constante m^2 supérieure à la plus grande valeur du second membre, puis prendre pour M_1 une solution de l'équation différentielle

$$\frac{dM_1}{d\xi}-M_1^2=m_1^2,$$

$M_1=mtg\,(m\xi+c)$ où l'on peut prendre la constante c telle que M_1 soit continu et dérivable, quand ξ reste dans un certain intervalle autour de zéro. Dans ce cas M_1 et par suite M est fonction continue et dérivable de x et y dans le domaine considéré, si ce dernier est assez petit. Nous avons donc choisi les fonctions μ, M et N de manière que nous pouvons conclure de l'équation (8) que les quatre premiers termes sous le signe d'intégration et la somme des trois derniers soient toujours nulles. La conclusion $u=0$ est alors facile.

§ 3. Nous allons démontrer d'une manière semblable le théorème, que $u = 0$ dans tout l'intérieur, si $u = 0$ et $\frac{\partial u}{\partial n} = 0$ sur le contour. Dans ce cas le théorème de GREEN

$$\int v \triangle u \, d\sigma - \int u \triangle v \, d\sigma = \int v \frac{\partial u}{\partial n} \, ds - \int u \frac{\partial v}{\partial n} \, ds$$

donne

$$\int v \triangle u \, d\sigma - \int u \triangle v \, d\sigma = 0.$$

Si

$$(\triangle - \mu) u = v, (\triangle - \lambda) v = -2A \frac{\partial u}{\partial x} - 2B \frac{\partial u}{\partial y} - Cu,$$

on en déduit

$$\int \left\{ v^2 + \mu uv - \lambda uv + u \left(2A \frac{\partial u}{\partial x} + 2B \frac{\partial u}{\partial y} \right) + Cu^2 \right\} d\sigma = 0 . \quad . \quad (9)$$

D'autre part on a

$$\int u (\triangle u - \mu u - v) \, d\sigma = 0,$$

d'où, parce que

$$\int u \triangle u \, d\sigma = - \int \left\{ \left(\frac{\partial u}{\partial x} \right)^2 + \left(\frac{\partial u}{\partial x} \right)^2 \right\} d\sigma$$

quand au contour $u = 0$,

$$\int \left\{ \left(\frac{\partial u}{\partial x} \right)^2 + \left(\frac{\partial u}{\partial y} \right)^2 + \mu u^2 + uv \right\} d\sigma = 0 . \quad . \quad . \quad . \quad . \quad (10)$$

Puis, introduisant encore deux fonctions arbitraires M et N,

$$\int \left\{ \frac{\partial (Mu^2)}{\partial x} + \frac{\partial (Nu^2)}{\partial y} \right\} d\sigma = \int (Mu^2 \, dy + Nu^2 \, dx) = 0,$$

parce que au contour $u = 0$.

Donc

$$\int \left\{ u^2 \left(\frac{\partial M}{\partial x} + \frac{\partial N}{\partial y} \right) + 2 \left(Mu \frac{\partial u}{\partial x} + Nu \frac{\partial u}{\partial y} \right) \right\} d\sigma = 0. \quad . \quad . \quad (11)$$

Additionnant (9), (10) et (11) on trouve

$$\int \left[\left\{ v + \tfrac{1}{2} (\mu - \lambda + 1) u \right\}^2 + \left\{ \frac{\partial u}{\partial x} + (A + M) u \right\}^2 + \left\{ \frac{\partial u}{\partial y} + (B + N) u \right\}^2 + \right.$$

$$\left. + \left\{ C - \tfrac{1}{4} (\mu - \lambda + 1)^2 - (A + M)^2 - (B + N)^2 + \frac{\partial M}{\partial x} + \frac{\partial N}{\partial y} + \mu \right\} u^2 \right] d\sigma = 0.$$

De cette équation nous pouvons tirer le résultat voulu, $u = 0$ partout à l'intérieur de C, si nous démontrons, qu'on peut choisir M et N tels que

$$C - \tfrac{1}{4}(\mu - \lambda + 1)^2 - (A + M)^2 - (B + N)^2 + \frac{\partial M}{\partial x} + \frac{\partial N}{\partial y} + \mu > 0.$$

Or, prenant $N = -B$ et posant $A + M = M_1$, nous n'avons qu'à prendre pour M_1 une solution de

$$\frac{dM_1}{dx} - M_1^2 = m^2,$$

m^2 étant une constante supérieure à la plus grande valeur de la fonction donnée

$$-C + \tfrac{1}{4}(\mu - \lambda + 1)^2 + \frac{\partial A}{\partial x} + \frac{\partial B}{\partial y} - \mu.$$

Soit cette solution $M_1 = mtg(mx + C)$ on peut choisir la constante C telle que cette fonction soit continue et dérivable dans le domaine considéré, si ce dernier est assez petit.

Mathematics. — *Sur le théorème de déformation de* KOEBE. Par H. BOLDER. (Communicated by Prof. W. VAN DER WOUDE.)

(Communicated at the meeting of May 30, 1942.)

§ 1. Notations.

Ω: Un domaine simple et simplement connexe dans le plan de la variable complexe w, contenant dans son intérieur le point $w \neq 0$ et non le point $w = \infty$, et pour lequel la fonction de GREEN existe.

Σ: la frontière de Ω.

d: la plus petite distance de 0 à Σ.

$G(o, w)$: la fonction de GREEN de Ω avec pôle en 0.

$g(w)$: $G(0, w) - log\ |w|^{-1}$ pour $w \neq 0$, et continue pour $w = 0$.

$\Omega(G_1)$: la partie de Ω, dans laquelle $G(0, w) > G_1 \geqq 0$.

$\Sigma(G_1)$: la frontière de $\Omega(G_1)$, donc ligne de niveau de $G(0, w)$.

$n(w)$: la normale extérieure de $\Omega(G(w))$ en w ($|n| = 1$).

$\frac{\partial G(0,w)}{\partial n}$: la dérivée de $G(0, w)$ dans la direction $n(w)$.

$$\left(donc\ \frac{\partial G(0, w)}{\partial n} \leqslant 0 \right)$$

$\varrho^2(w)$: la densité d'une distribution de masse positive.

$M[D]$: la masse portée par l'ensemble D.

Indiquons enfin par $\Omega^*, \Sigma^*, d^*, G^*(0, w)$, etc. des entités analogues aux précédentes, qui sont soumises aux mêmes prémisses.

Domaine de KOEBE („Schlitzgebiet"): Un Ω, dont Σ est l'ensemble de points w pour lesquels $w = |w| e^{i\vartheta}$, où ϑ est constant, et $|w| \geqq d > 0$.

Le point $T = d e^{i\vartheta}$ s'appelle le sommet du domaine de KOEBE.

§ 2. Introduction.

M. MONNA a montré [1]), que le théorème de déformation de KOEBE s'exprime en termes de la théorie du potentiel par le

Théorème A. *Il existe une fonction $f(d)$ telle, que l'inégalité $g(0) \leqslant f(d)$ est valable pour tout Ω, dont la plus petite distance de 0 à Σ vaut d.*

Supposons le théorème valable pour une seule valeur d^* de d.

Soit Ω^* l'image de Ω dans le plan de w^* par la transformation $dw^* = d^* w$, nous avons

$$G_\Omega(0, w) = G_{\Omega^*}(0, w^*),\ log\ |w| - log\ d = log\ |w^*| - log\ d^*,$$

$$g_\Omega(w) - log\ d = G_\Omega(0, w) + log\ |w| - log\ d =$$

$$= G_{\Omega^*}(0, w^*) + log\ |w^*| - log\ d^* = g_{\Omega^*}(w^*) - log\ d^*,$$

et nous pouvons, en posant $f(d^*) - log\ d^* = log\ k$, préciser le théorème A par le

---

[1]) A. F. MONNA: Sur quelques inégalités de la théorie des fonctions et leurs généralisations spatiales, Proc. Ned. Akad. v. Wetensch., Amsterdam, **45**, p. 43 e.s., et p. 165 e.s. (1942).

Théorème B. *Il existe un nombre k tel, que l'inégalité* $g(0) \leqq \log k.d$ *est valable pour tout* Ω*,dont la plus petite distance de* 0 *à* Σ *vaut d.*

Dans la théorie de la représentation conforme il existe un théorème encore plus précis, qui s'exprime par le

Théorème C. *Soit* Ω^* *un domaine de* KOEBE, *l'inégalité* $g(0) \leqq g^*(0)$ *est valable pour tout* Ω *dont* $d = d^*$.

Le cas d'égalité ne se présente que si Ω *est aussi un domaine de* KOEBE. (Et par conséquent nous avons $f(d) = \log 4d$).

M. MONNA a posé le problème de démontrer ces théorèmes en s'appuyant exclusivement sur la théorie du potentiel, c.à.d. sans recourir aux notions et aux méthodes de la théorie de la représentation conforme.

L'article cité de M. MONNA contient une telle démonstration des théorèmes *A* et *B*. Dans la note présente je me propose d'établir une démonstration du caractère demandé du théorème *C*. On y reconnaîtra une démonstration connue de AHLFORS–NEVANLINNA [2]), dont une représentation conforme auxiliaire a été remplacée par l'introduction d'une distribution de masse positive telle, que la masse portée par chaque partie de Ω égale l'aire de son image. La fonction $\varrho(w)$ correspond à la dilatation linéaire de cette représentation; elle a une signification physique simple.

M. MONNA a déjà signalé, que dans l'espace il n'existe pas un théorème analogue à *A*. Cependant la généralisation spatiale des lemmes I—VI est immédiate, sans aucune restriction, et ils peuvent servir d'obtenir des limitations pour $g(0)$ dans certains cas particuliers, comme dans l'article de M. MONNA.

Par exemple on peut choisir pour Ω^* le sphère $x^2 + y^2 + z^2 = 1$, et prolonger le champ E^* correspondant par une inversion par rapport à Σ^* (d'où $\varrho(P) = r_p^{-2}$), ce qui fournit un théorème analogue au premier théorème de § 4.

On obtiendra une autre forme de ce théorème en choisissant pour Σ^* un plan (ne contenant par *O*), et en prolongeant le champ E^* correspondant par une réflexion par rapport a Σ^*. Nous n'insistons pas.

§ 3. **Lemmes.**

Lemme I. *Il existe à chaque* $\varepsilon > 0$ *un nombre* $N(\varepsilon)$ *tel, que*

$$G > N(\varepsilon) \text{ entraîne } \Omega^*(G + g^*(0) + \varepsilon) \subset \Omega(G + g(0) - \varepsilon).$$

Démonstration. A chaque $\varepsilon > 0$ correspond un voisinage A_ε de 0 tel, que dans A_ε

$$g(w) > g(0) - \varepsilon, \text{ et } g^*(w) < g^*(0) + \varepsilon,$$

d'où

$$g(w) - g(0) + \varepsilon > 0 > g^*(w) - g^*(0) - \varepsilon,$$

et

$$G(0, w) - g(0) + \varepsilon > G^*(0, w) - g^*(0) - \varepsilon.$$

Il existe un $N(\varepsilon)$ tel, que

$$\Omega^*(N(\varepsilon) + g^*(0) + \varepsilon) \subset A_\varepsilon, \text{ et } \Omega(N(\varepsilon) + g(0) - \varepsilon) \subset A_\varepsilon.$$

Pour

$$G > N(\varepsilon),\ G^*(0, w) - g^*(0) - \varepsilon > G \text{ entraîne } G(0, w) - g(0) + \varepsilon > G,$$

ce qui signifie

$$w \subset \Omega^*(G + g^*(0) + \varepsilon) \text{ entraîne } w \subset \Omega(G + g(0) - \varepsilon),$$

et le lemme est démontré.

---

[2]) R. NEVANLINNA: Eindeutige analytische Funktionen p. 92—94.

Introduisons maintenant une distribution de masse positive sur Ω. Pour les distributions considérées, chaque voisinage de 0 portera une quantité infinie, chaque partie excluante un voisinage de 0 portera une quantité finie.

Pour $w \neq 0$, la densité $\varrho^2(w)$ sera continue.

Lemme II.

$$2\pi M[\Omega(G_1)-\Omega(G_2)] \geqslant \int_{G_1}^{G_2} dG \cdot \left(\int_{\Sigma(G)} \varrho(w)\, ds \right)^2, \text{ si } 0 \leqslant G_1 < G_2.$$

Démonstration. Si $G_1 > 0$ nous avons

$$M[\Omega(G_1)-\Omega(G_2)] = \int_{G_1}^{G_2} dG \cdot \int_{\Sigma(G)} \varrho^2(w) \left(-\frac{\partial G(0,w)}{\partial n} \right)^{-1} ds \geqslant$$

$$\geqslant \int_{G_1}^{G_2} dG \left[\left(\int_{\Sigma(G)} \varrho\, ds \right)^2 \cdot \left(\int_{\Sigma(G)} \left(-\frac{\partial G(0,w)}{\partial n} \right) ds \right)^{-1} \right] =$$

$$= (2\pi)^{-1} \int_{G_2}^{G_3} dG \left[\int_{\Sigma(G)} \varrho\, ds \right]^2,$$

en vertu de l'inégalité de SCHWARZ, et de la formule

$$\int_{\Sigma(G)} \left(-\frac{\partial G(0,w)}{\partial n} \right) ds = 2\pi.$$

Si $G_1' > 0$ nous avons

$$M[\Omega(0)-\Omega(G_2)] > M[\Omega(G_1')-\Omega(G_2)],$$

d'où

$$M[\Omega(0)-\Omega(G_2)] \geqslant \lim_{G_1' \to 0} M[\Omega(G_1')-\Omega(G_2)] \geqslant$$

$$\geqslant \lim_{G_1' \to 0} (2\pi)^{-1} \int_{G_1'}^{G_2} dG \left[\int_{\Sigma(G)} \varrho\, ds \right]^2 = (2\pi)^{-1} \int_{0}^{G_2} dG \left[\int_{\Sigma(G)} \varrho\, ds \right]^2.$$

Il faut maintenant choisir la densité $\varrho^2(w)$.

Définissons, à un domaine Ω^* un champ vectoriel $E^*(w) = -\operatorname{grad} G^*(0,w)$, autrement dit

$$E^*(w) = \left| \frac{\partial G^*(0,w)}{\partial n^*} \right| \cdot n^*(w), \text{ et } \varrho(w) = |E^*(w)|.$$

Le potentiel $G^*(0,w)$, et le champ $E^*(w)$ peuvent être interprétés comme générés par une charge $+1$ en 0 et des charges négatives sur Σ^*, $\varrho^2(w)$ est proportionnel à la densité de l'énergie du champ $E^*(w)$.

Définition. *Soit D un domaine, contenant dans son intérieur le point 0, et soit Γ sa frontière. Soit $D+\Gamma \subset \Omega$. Soit, en un point w de Γ, $n'(w)$ la normale extérieure de D.*

Un champ vectoriel $F(w)$, défini dans Ω, sera dit être de la classe $U(\Omega)$, s'il possède les propriétés suivantes:

$F(w)$ est continu pour $w \neq 0$, et

$$\int_{\Gamma'} (F(w), n'(w))\, ds = 2\pi$$

pour tout D suffisant aux conditions précédentes.

Evidemment $E^*(w)$ est de la classe $U(\Omega^*)$.

Lemme III. *Soit $F(w)$ un champ vectoriel de la classe $U(\Omega(G))$, et $\varrho(w) = |F(w)|$, on a*

$$\int_{\Sigma(G')} \varrho(w)\, ds \geqq 2\pi \quad . \quad . \quad . \quad . \quad . \quad . \quad . \quad . \quad . \quad (1)$$

pour $G' > G$.

Le cas d'égalité ne se présente, que si en chaque point w de $\Sigma(G')$:

$$|F(w)| = (F(w), n(w)),$$

c.à.d. les directions de $F(w)$ et de $n(w)$ coïncident.

Lemme IV. *Soit $0 \leqq G_1 < G_2$. Si dans $\Omega(G_1) - \Omega(G_2)$ la fonction $\varrho(w)$ suffit à (1) pour tout G' de $G_1 < G' < G_2$ on a*

$$M[\Omega(G_1) - \Omega(G_2)] \geqq 2\pi (G_2 - G_1) \quad . \quad . \quad . \quad . \quad . \quad (2)$$

Le cas d'égalité ne se présente que si

$$\int_{\Sigma(G')} \varrho\, ds = 2\pi \text{ pour tout } G' \text{ de } G_1 < G' < G_2.$$

Démonstration. C'est une conséquence immédiate du lemme II.

Lemme V. *Pour $0 \leqq G_1 < G_2$, $\varrho(w) = |E^*(w)|$, on a*

$$M[\Omega^*(G_1) - \Omega^*(G_2)] = 2\pi (G_1 - G_2) \quad . \quad . \quad . \quad . \quad . \quad (3)$$

Démonstration. Si $G_1 > 0$ nous avons

$$M[\Omega^*(G_1) - \Omega^*(G_2)] = \int_{G_1}^{G_2} dG \int_{\Sigma^*(G)} \left(-\frac{\partial G^*(0,w)}{\partial n^*}\right)^2 \cdot \left(-\frac{\partial G^*(0,w)}{\partial n^*}\right)^{-1} ds =$$

$$= \int_{G_1}^{G_2} dG \int_{\Sigma^*(G)} \left(-\frac{\partial G^*(0,w)}{\partial n^*}\right) ds = 2\pi (G_2 - G_1)$$

Soit $G_1 = 0$.

$$\lim_{G_1' \to 0} (\Omega(G_1') - \Omega(G_2)) = \Omega(0) - \Omega(G_2),$$

par conséquent

$$M[\Omega(0) - \Omega(G_2)] = \lim_{G_1' \to 0} M[\Omega(G_1') - \Omega(G_2)] = \lim_{G_1' \to 0} 2\pi (G_2 - G_1') = 2\pi G_2.$$

Lemme VI. *Soit A un voisinage de 0, soit la fonction $\varrho(w)$ définie dans Ω et Ω^* tellement, que les relations (2) et (3) sont remplies pour tout G_1 et G_2 de $0 \leqq G_1 < G_2$; soient $a \geqq 0$ et $a^* \geqq 0$.*

Alors

$$M[\Omega(a)-A] \leqslant [\Omega^*(a^*)-A] \text{ entraîne } g(0)-a \leqslant g^*(0)-a^*.$$

Le cas d'égalité ne se présente que si dans (2) *l'égalité se présente pour tout* G_1 *et* G_2 *admis.*

Démonstration. Choisissons $\varepsilon > 0$. En vertu du lemme I nous avons

$$\Omega^*(G+g^*(0)+\varepsilon) \subset \Omega(G+g(0)-\varepsilon)$$

pour G assez grand. Nous avons donc

$$M[\Omega(a)-\Omega(G_1+g(0)-\varepsilon)] \leqslant M[\Omega^*(a^*)- \\ -\Omega(G+g(0)-\varepsilon)] \leqslant M[\Omega^*(a^*)-\Omega^*(G+g^*(0)+\varepsilon)],$$

et la démonstration se termine par l'application de (2) et (3).

§ 4. **Application des lemmes.**

L'application des lemmes précédents pour comparer $g(0)$ et $g^*(0)$ rencontre encore une difficulté. Si

$$\Omega \subset \Omega^* \text{ et } \varrho(w) = |E^*(w)|$$

les lemmes s'appliquent sans aucune restriction, et parce que, dans ce cas,

$$M[\Omega-A] \leqslant M[\Omega^*-A],$$

nous avons:

$$\Omega \subset \Omega^* \text{ entraîne } g(0) \leqslant g^*(0),$$

un résultat trivial (une conséquence immédiate du principe de CARLEMAN). Si une partie de Ω n'est pas contenue dans Ω^*, E^*, et par conséquent la fonction ϱ, ne sont pas définis dans tout Ω. Nous sommes conduits à chercher un prolongement du champ E^*.

Soit, par exemple, Ω^* le cercle $|w| < 1$, auquel correspondent:

$$G^*(0,w) = \log|w|^{-1},\ E^*(w) = w|w|^{-2},\ \varrho(w) = |w|^{-1}.$$

Prolongeons $E^*(w)$ par une inversion par rapport à Σ^*, nous obtenons un champ $E^*(w)$ de la classe U du plan complet.

$E^*(w)$ et $\varrho(w)$ s'expriment pour tout w par les mêmes formules

$$E^*(w) = w|w|^{-2},\ \varrho(w) = |w|^{-1}.$$

Nous en tirons le

Théorème: *Soit* Ω^* *le cercle* $|w| < 1$, *et* $\varrho(w) = |w|^{-1}$ *pour tout* w,

$$M[\Omega-A] \leqslant M[\Omega^*-A] \text{ entraîne } g(0) \leqslant g^*(0),$$

qui est un peu plus général que celui, par lequel s'exprime en termes du potentiel le théorème de KOEBE transformé, traité par M. NEVANLINNA (NEVANLINNA l.c. p. 81 e.s.).

Pour obtenir une démonstration directe du théorème C nous choisissons pour Ω^* un domaine de KOEBE, et $\varrho(w) = |E^*(w)|$.

Alors E^* est défini partout (sauf sur Σ^*), mais les lemmes ne s'appliquent pas encore. En effet, il y a peut-être des $\Sigma(G)$ incluantes des parties de Σ^*, où se trouvent des charges négatives, c.à.d. dans ce cas $E^*(w)$ n'est pas de la classe $U(\Omega)$.

Le lemme suivant éliminera cet obstacle.

Lemme VII. *Soit* Ω^* *un domaine de* KOEBE, *dont le sommet* T *est situé sur* Σ. *Il*

existe un champ vectoriel $E'(w)$ *de la classe* $U(\Omega)$, *tel que* $|E'(w)| = |E^*(w)|$ *pour tout* $w \subset \Omega$.

Démonstration. Formons un champ vectoriel bivalent $E_{1,2}$, en définissant $E_1(w) = E^*(w)$, et $E_2(w)$ son image réfléchie par rapport à Σ^*. Choisissons $E' = E_1$ dans le voisinage de 0, et prolongeons, *tout en restant dans l'intérieur de* Ω, par $E' = E_1$ ou $E' = E_2$, de sorte que E' est continu. Parce que Ω est simplement connexe, et ne contient pas dans son intérieur les deux points de ramification de $E_{1,2}$, T et ∞, nous obtenons un champ E' univalent.

Evidemment E' est de la classe $U(\Omega)$.

Passons enfin à la démonstration du théorème C.

Soit d la plus petite distance de 0 à Σ, il existe un point T de Σ, avec $|w_T| = d$. Choisissons pour Ω^* le domaine de KOEBE dont T est le sommet.

Formons le champ $E'(w)$ du lemme VII, et posons

$$\varrho(w) = |E^*(w)| = |E'(w)|.$$

Ω est simple, et Ω^* couvre le plan total, nous avons donc

$$M[\Omega - A] \leqslant M[\Omega^* - A].$$

Des lemmes III—VI nous déduisons immédiatement $g(0) \leqslant g^*(0)$.

Il faut encore considérer le cas d'égalité.

Nous avons dans ce cas

$$M[\Omega(G_1) - \Omega(G_2)] = 2\pi(G_2 - G_1)$$

pour tout $G_1 < G_2$ (lemme VI), d'où

$$\int_{\Sigma(G)} \varrho \, ds = \int_{\Sigma(G)} |E^*| \, ds = 2\pi$$

pour tout $G > 0$ (lemme IV). Par conséquent, en tout point w de $\Sigma(G(w))$ les directions de $E^*(w)$ et de $n(w)$ coïncident, c.à.d. $\Sigma(G)$ est une ligne équipotentielle du champ E^*,

$$\text{c. à. d. } \Sigma(G) \text{ coïncide avec } \Sigma^*(G^*).$$

Choisissant

$$A = \Omega(G) = \Omega^*(G^*)$$

nous avons

$$2\pi G = M[\Omega(0) - \Omega(G)] = M[\Omega^*(0) - \Omega^*(G^*)] = 2\pi G^*.$$

Nous avons donc obtenu:

$$\Omega(G) = \Omega^*(G) \text{ pour tout } G > 0,$$

d'où

$$G(0, w) = G^*(0, w) \text{ pour } w \subset \Omega^* \qquad (\text{ou } w \subset \Omega).$$

Parce que Ω est simplement connexe, il n'y a pas de points-frontières irréguliers, et $\Omega(G) = \Omega^*(G)$ subsiste pour $G = 0$.

Mathematics. — *Die Begründung der Trigonometrie in der hyperbolischen Ebene.* (Dritte Mitteilung.) Von J. C. H. GERRETSEN. (Communicated by Prof. J. G. VAN DER CORPUT.)

(Communicated at the meeting of May 30, 1942.)

§ 4. Die trigonometrischen Funktionen.

Ebenso wie die Strecken werden auch die Winkel in Klassen von mit einander kongruenten Winkeln eingeteilt, damit wir gegenüber Bewegungen invariante Begriffe erhalten. Wir können dann wieder in bekannter Weise die Summe $A_1 + A_2$ zweier Winkelklassen A_1 und A_2 definieren und eine Ordnungsbeziehung einführen. Für $A_1 > A_2$ ist auch immer die Differenz $A_1 - A_2$ sinnvoll. Wir bemerken aber, dasz die Addition nicht uneingeschränkt ausführbar ist und werden demgemäsz die Menge der Winkelklassen nicht zu einer additiven Gruppe zu erweitern versuchen. Für die geometrischen Anwendungen schadet das nicht.

Es wäre zu versuchen für die Winkelklassen eine Art Exponentialfunktion einzuführen um damit die trigonometrischen Funktionen zu definieren. Es stellt sich dabei heraus, dasz dann der Körper $\mathfrak{h}$ zu einem Körper mit imaginären Zahlen erweitert werden musz und das läszt sich vermeiden. Jedenfalls gibt es eine gewisse Übereinstimmung zwischen der Theorie der trigonometrischen Funktionen und der Theorie der hyperbolischen Funktionen.

Es sei irgend eine Winkelklasse A vorgegeben und es sei $\angle APB$ ein die Klasse A erzeugender Winkel. Die Enden der Geraden PA seien α und α', und die Enden der Geraden PB seinen β und β'. Dabei sei α bezw. β durch die Halbgerade PA bezw. PB bestimmt.

Wir bilden das Doppelverhältnis:

$$\delta^* = \begin{bmatrix} \alpha & \alpha' \\ \beta & \beta' \end{bmatrix} = \frac{\alpha - \beta}{\alpha' - \beta} \frac{\alpha' - \beta'}{\alpha - \beta'} \quad . \quad . \quad . \quad . \quad . \quad . \quad (4, 1)$$

Es hat offenbar für jeden Winkel der Klasse A denselben Wert und jeder Klasse A kann ein δ^* zugeordnet werden.

Wir wollen nun einen Winkel der Klasse A betrachten, dessen Schenkel die Halbgeraden $(O1)$ und $(O\alpha)$ sind; dabei liege α auf derselben Seite der Geraden $(-1, 1)$ wie das Ende ∞. Wir finden dann, da α und $-\frac{1}{\alpha}$ die Enden der Geraden $(O\alpha)$ sind:

$$\delta^* = \begin{bmatrix} \alpha & -\frac{1}{\alpha} \\ 1 & -1 \end{bmatrix} = -\left(\frac{\alpha - 1}{\alpha + 1}\right)^2 \quad . \quad . \quad . \quad . \quad . \quad . \quad (4, 2)$$

Daraus geht hervor, dasz δ^* stets negativ ist; auszerdem haben wir:

$$\frac{\alpha - 1}{\alpha + 1} = \sqrt{-\delta^*} \quad . \quad . \quad . \quad . \quad . \quad . \quad . \quad . \quad . \quad (4, 3)$$

da wegen der über α gemachten Voraussetzung die linke Seite von (4, 3) stets positiv ist.

Wenn wir auf (3, 16) achten, liegt die Vermutung nahe, dasz die Funktion $\sqrt{-\delta^*}$, als trigonometrische Tangente der Klasse $\frac{1}{2}A$ betrachtet werden kann. Demgemäsz setzen wir einstweilen:

$$\text{ts } A = \sqrt{-\delta^*} \quad . \quad . \quad . \quad . \quad . \quad . \quad . \quad . \quad . \quad (4, 4)$$

Wir erkennen sofort:

1. *Für jede Winkelklasse A ist* ts A *bestimmt und positiv.*

Umgekehrt gilt:

2. *Wenn irgend ein positives Ende ϑ vorgelegt ist, dann gibt es immer eine eindeutig bestimmte Winkelklasse A, wofür* ts $A = \vartheta$ *ist.*

Denn es gibt immer ein auf derselben Seite der Geraden (—1, 1) wie das Ende ∞ liegendes Ende α, das der Gleichung:

$$\frac{\alpha - 1}{\alpha + 1} = \vartheta \quad . \quad . \quad . \quad . \quad . \quad . \quad . \quad . \quad . \quad (4, 5)$$

genügt, und die Halbgeraden $(O1)$ und $(O\alpha)$ sind die Schenkel eines Winkels, der die gesuchte Klasse erzeugt.

Wir werden nun zeigen, dasz die Funktion ts das Additionstheorem der Tangensfunktion befolgt.

3. *Für die Funktion* ts *besteht das Additionstheorem:*

$$\text{ts}\,(A + B) = \frac{\text{ts}\,A + \text{ts}\,B}{1 - \text{ts}\,A\,\text{ts}\,B}, \quad . \quad . \quad . \quad . \quad . \quad . \quad (4, 6)$$

wenn $A + B$ einen Sinn hat.

Wir betrachten die Winkel der Klassen A und B mit gemeinsamem Schenkel $(O1)$ und die Schenkel $(O\alpha)$ und $(O\beta)$, wobei α und β wiederum auf derselben Seite der Geraden (—1,1) liegen wie das Ende ∞.

Wir legen den Betrachtungen nachfolgende Drehung um O zugrunde:

$$\bar{\xi} = \frac{\xi + \vartheta}{1 - \xi\vartheta}, \quad . \quad . \quad . \quad . \quad . \quad . \quad . \quad . \quad (4, 7)$$

und bestimmen ϑ derart, dasz das Ende 1 in das Ende β übergeführt wird. Dann ist:

$$\beta = \frac{1 + \vartheta}{1 - \vartheta} \quad . \quad . \quad . \quad . \quad . \quad . \quad . \quad . \quad . \quad (4. 8)$$

also:
$$\vartheta = \frac{\beta - 1}{\beta + 1} = \text{ts}\,B. \quad . \quad . \quad . \quad . \quad . \quad . \quad . \quad (4, 9)$$

Diese Drehung ordnet der Halbgeraden $(O\alpha)$ die Halbgerade $(O\gamma)$ zu, während der von den Halbgeraden $(O1)$ und $(O\gamma)$ gebildete Winkel eben die Klasse $A + B$ erzeugt. Wir haben dann:

$$\gamma = \frac{\alpha + \vartheta}{1 - \alpha\vartheta}$$

also:
$$\text{ts}\,(A + B) = \frac{\gamma - 1}{\gamma + 1} = \frac{\alpha + \vartheta + \alpha\vartheta - 1}{\alpha + \vartheta - \alpha\vartheta + 1}$$

$$= \frac{\dfrac{\alpha - 1}{\alpha + 1} + \vartheta}{1 - \dfrac{\alpha - 1}{\alpha + 1} \cdot \vartheta} = \frac{\text{ts}\,A + \text{ts}\,B}{1 - \text{ts}\,A\,\text{ts}\,B}, \text{ w.z.b.w.}$$

Weiter gilt:

4. *Ist die Winkelklasse A gröszer als die Winkelklasse B, dann besteht die Beziehung:*

$$\text{ts}\,(A - B) = \frac{\text{ts}\,A - \text{ts}\,B}{1 + \text{ts}\,A\,\text{ts}\,B}. \quad . \quad . \quad . \quad . \quad . \quad (4, 10)$$

Der Beweis wird fast ebenso geführt wie beim vorigen Satz; man musz jetzt aber die Drehung:

$$\bar{\xi} = \frac{\xi - \vartheta}{1 + \xi\vartheta}, \quad . \quad . \quad . \quad . \quad . \quad . \quad . \quad . \quad (4, 11)$$

mit $\vartheta =$ ts B anwenden.

Es liegt auf der Hand die trigonometrischen Funktionen folgendermaszen zu definieren:

$$\cos A = \frac{1 - \mathrm{ts}^2 A}{1 + \mathrm{ts}^2 A}, \quad . \quad . \quad . \quad . \quad . \quad . \quad . \quad (4, 12)$$

$$\sin A = \frac{2 \,\mathrm{ts}\, A}{1 + \mathrm{ts}^2 A}, \quad . \quad . \quad . \quad . \quad . \quad . \quad . \quad (4, 13)$$

$$\tan A = \frac{1}{\mathrm{ctg}\, A} = \frac{\sin A}{\cos A}. \quad . \quad . \quad . \quad . \quad . \quad (4, 14)$$

Wie ersehen daraus, dasz für jede Winkelklasse die trigonometrischen Funktionen Sinn haben (wenn man auch den Wert ∞ zuläszt) und es ist leicht den Wertverlauf dieser Funktionen zu überblicken.

5. *Es bestehen die Additionstheoreme:*

$$\cos (A + B) = \cos A \cos B - \sin A \sin B, \quad . \quad . \quad . \quad (4, 15)$$

$$\sin (A + B) = \sin A \cos B + \cos A \sin B, \quad . \quad . \quad . \quad (4, 16)$$

für irgend zwei Winkelklassen, für die $A + B$ einen Sinn hat.

Als Beispiel beweisen wir die Formel (4, 15). Zufolge Satz 3 haben wir:

$$\begin{aligned}\cos (A + B) &= \frac{1 - \mathrm{ts}^2 (A + B)}{1 + \mathrm{ts}^2 (A + B)} = \frac{(1 - \mathrm{ts}\, A\, \mathrm{ts}\, B)^2 - (\mathrm{ts}\, A + \mathrm{ts}\, B)^2}{(1 - \mathrm{ts}\, A\, \mathrm{ts}\, B)^2 + (\mathrm{ts}\, A + \mathrm{ts}\, B)^2} \\ &= \frac{(1 - \mathrm{ts}^2 A)(1 - \mathrm{ts}^2 B) - 4\, \mathrm{ts}\, A\, \mathrm{ts}\, B}{(1 + \mathrm{ts}^2 A)(1 + \mathrm{ts}^2 B)} \\ &= \frac{1 - \mathrm{ts}^2 A}{1 + \mathrm{ts}^2 A} \frac{1 - \mathrm{ts}^2 B}{1 + \mathrm{ts}^2 B} - \frac{2 \,\mathrm{ts}\, A}{1 + \mathrm{ts}^2 A} \frac{2 \,\mathrm{ts}\, B}{1 + \mathrm{ts}^2 B} \\ &= \cos A \cos B - \sin A \sin B.\end{aligned}$$

Weiter haben wir:

8. *Ist die Winkelklasse A gröszer als die Winkelklasse B, dann gilt:*

$$\cos (A - B) = \cos A \cos B + \sin A \sin B, \quad . \quad . \quad . \quad (4, 17)$$

$$\sin (A - B) = \sin A \cos B - \cos A \sin B. \quad . \quad . \quad . \quad (4, 18)$$

Der Beweis bietet keine Schwierigkeiten; man musz jetzt Satz 4 anwenden.

Die bekannten elementaren Formeln der trigonometrischen Funktionen können leicht hergeleitet werden. Insbesondere finden wir:

$$\tan \tfrac{1}{2} A = \frac{\sin A}{1 + \cos A} = \mathrm{ts}\, A, \quad . \quad . \quad . \quad . \quad . \quad (4, 19)$$

sodasz wir die Bezeichnung ts wegwerfen können.

Wir beschlieszen mit einer einfachen Begriffsbildung, die für die Anwendungen der trigonometrischen Funktionen auf Dreiecke wichtig ist. Zwei Klassen A und A' mögen *supplementär* genannt werden, wenn sie von Nebenwinkeln erzeugt werden. Ist $(O\alpha)$ eine Halbgerade auf derselben Seite der Geraden $(-1,1)$ wie das Ende ∞ und wird die Klasse A erzeugt von dem Winkel mit den Schenkeln $(O1)$ und $(O\alpha)$, dann wird A' von dem Winkel erzeugt, dessen Schenkel von O nach -1 und α ausgehen. Für das zu A' gehörige Doppelverhältnis finden wir:

$$\delta^{*\prime} = \begin{bmatrix} \alpha & -\frac{1}{\alpha} \\ -1 & 1 \end{bmatrix} = -\left(\frac{\alpha + 1}{\alpha - 1}\right)^2 = \frac{1}{\delta^*} \quad . \quad . \quad . \quad (4, 20)$$

wenn δ^* das zu A gehörige Doppelverhältnis ist. Daraus folgt:

9. *Für zwei supplementäre Winkelklassen A und A' bestehen die Relationen:*

$$\tan \tfrac{1}{2} A' = \operatorname{ctg} \tfrac{1}{2} A, \quad . \quad . \quad . \quad . \quad . \quad . \quad . \quad (4, 21)$$

$$\cos A' = -\cos A, \quad . \quad . \quad . \quad . \quad . \quad . \quad . \quad (4, 22)$$

$$\sin A' = \sin A. \quad . \quad . \quad . \quad . \quad . \quad . \quad . \quad (4, 23)$$

§ 5. Die trigonometrischen Formeln.

a. Die LOBATSCHEWSKIJsche Formel. Es sei AB irgend eine Strecke und a die von dieser Strecke erzeugte Klasse. Wir errichten in B auf der Geraden AB das Lot, dessen Enden ω und ω' sein mögen. Die beiden Winkel $BA\omega$ und $BA\omega'$ sind einander kongruent. Die von einem dieser Winkel erzeugte Winkelklasse werden wir mit $\Pi(a)$ bezeichnen. Aus den Kongruenzsätzen folgt, dasz die Streckenklasse a und die Winkelklasse $\Pi(a)$ einander umkehrbar eindeutig bestimmen. Man nennt jeden Winkel der Klasse $\Pi(a)$ einen *Parallelwinkel* zu irgend einer Strecke der Klasse a. Man kann $\Pi(x)$ auch für nicht-positive Klassen definieren, wenn man verabredet, dasz $\Pi(x)$ und $\Pi(-x)$ supplementär sein sollen. Insbesondere ist dann $\Pi(0)$ die Klasse der rechten Winkel.

Von N. I. LOBATSCHEWSKIJ ist eine berühmte Formel aufgestellt worden, welche die Beziehung zwischen $\Pi(x)$ und x mit Hilfe der in den beiden vorigen Paragraphen eingeführten Funktionen beschreibt. Es gilt der Satz:

1. *Zwischen irgend einer Streckenklasse x von $\mathfrak{S}$ und der dazu gehörigen Klasse $\Pi(x)$ besteht die Beziehung:*

$$\tan \tfrac{1}{2} \Pi(x) = \exp -x. \quad . \quad . \quad . \quad . \quad . \quad . \quad . \quad (5, 1)$$

Es sei OA eine Strecke der Klasse a, wobei A auf der von O nach ∞ ausgehenden Halbgeraden liegt. Die Enden der Senkrechten in A auf der Geraden (O, ∞) seien α und $-\alpha$, wobei α wiederum als positiv vorausgesetzt wird. Die Klasse $\Pi(a)$ wird von dem Winkel erzeugt, dessen Schenkel die Halbgeraden $(O\alpha)$ und $(O\infty)$ sind. Für das zu $\Pi(a)$ gehörige Doppelverhältnis gilt offenbar:

$$\delta^* = \begin{bmatrix} \alpha & -\dfrac{1}{\alpha} \\ \infty & 0 \end{bmatrix} = -\frac{1}{\alpha^2}, \quad . \quad . \quad . \quad . \quad . \quad . \quad (5, 2)$$

also ist:

$$\sqrt{-\delta^*} = \frac{1}{\alpha}.$$

Daraus folgt:

$$\tan \tfrac{1}{2} \Pi(a) = \exp -a,$$

womit die Richtigkeit der Formel (5, 1) für positive Streckenklassen schon gezeigt worden ist. Für nicht-positive Klassen folgt nun die Formel ohne Mühe.

Es ist möglich nur mit Hilfe der Formel (5, 1) die Formeln des rechtwinkligen Dreiecks herzuleiten, wie schon in der Einleitung hervorgehoben wurde. Wir werden aber ein anderes Verfahren zur Herleitung dieser Formeln anwenden, wobei die Endenrechnung mehr in den Vordergrund tritt.

b. Die Formeln des rechtwinkligen Dreiecks. Aus den Kongruenzsätzen geht hervor, dasz ein rechtwinkliges Dreieck durch zwei Elemente, welche vom rechten Winkel verschieden sind, bestimmt wird. Es sei das rechtwinklige Dreieck ABC vorgelegt mit rechtem Winkel BCA. Die von den Seiten BC, CA und AB erzeugten Streckenklassen werden hintereinander mit a, b und c bezeichnet, während die von den Winkeln BAC und ABC erzeugten Winkelklassen A und B genannt werden. Unser Ziel ist nun der Beweis des Satzes:

2. *Für jedes rechtwinklige Dreieck bestehen die Beziehungen:*

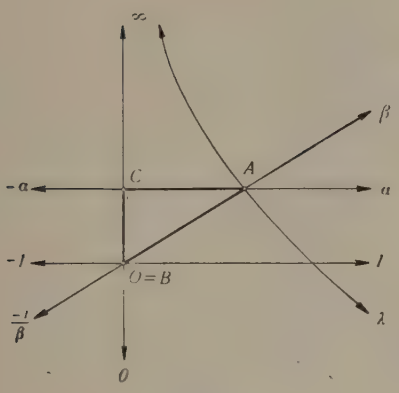

Fig. 1.

$$\tan B = \frac{\tanh b}{\sinh a}, \quad . \quad . \quad . \quad . \quad (5,3)$$

$$\tan A = \frac{\tanh a}{\sinh b}, \quad . \quad . \quad . \quad . \quad (5,3')$$

$$\operatorname{ctg} A \operatorname{ctg} B = \cosh c, \quad . \quad . \quad . \quad (5,4)$$

$$\cosh a \cosh b = \cosh c, \quad . \quad . \quad . \quad (5,5)$$

$$\sin A = \frac{\sinh a}{\sinh c}, \quad . \quad . \quad . \quad . \quad (5,6)$$

$$\sin B = \frac{\sinh b}{\sinh c}, \quad . \quad . \quad . \quad . \quad (5,6')$$

$$\cos A = \frac{\tanh b}{\tanh c}, \quad . \quad . \quad . \quad . \quad (5,7)$$

$$\cos B = \frac{\tanh a}{\tanh c} \quad . \quad . \quad . \quad . \quad (5,7')$$

$$\sin A \cosh b = \cos B, \quad . \quad . \quad . \quad (5,8)$$

$$\sin B \cosh a = \cos A. \quad . \quad . \quad . \quad (5,8')$$

1. Wir fangen an mit dem Beweis von (5, 3). Wir legen zunächst das Dreieck ABC in der Ebene derart, dasz B mit O zusammenfällt, C auf der Halbgeraden $(O\ \infty)$ liegt und A auf derselben Seite der Geraden (O, ∞) liegt wie das Ende 1, (Fig. 1). Die positiven Enden der Halbgeraden CA und BA mögen mit α bezw. β bezeichnet werden. Es sei λ das von ∞ verschiedene Ende der Geraden $(A\ \infty)$.

Die Bewegung $\mathfrak{S}_{-\frac{1}{2}\lambda}\,\mathfrak{S}_0$ führt A in einen Punkt der Geraden $(0, \infty)$ über. Die Enden β, $-\frac{1}{\beta}$, α und $-\alpha$ werden dabei in die Enden $\beta-\lambda$, $-\frac{1}{\beta}-\lambda$, $\alpha-\lambda$ und $-\alpha-\lambda$ übergeführt. Wenn wir uns Satz 4 des § 2 erinnern, sehen wir sofort die Richtigkeit ein von:

$$(\beta-\lambda)\left(-\frac{1}{\beta}-\lambda\right) = (\alpha-\lambda)(-\alpha-\lambda) \quad . \quad . \quad . \quad . \quad (5,9)$$

und daraus läszt sich folgern:

$$\frac{\lambda}{\alpha} = \frac{\alpha-\frac{1}{\alpha}}{\beta-\frac{1}{\beta}}. \quad . \quad . \quad . \quad . \quad . \quad . \quad . \quad . \quad (5,10)$$

Wenn wir erst die Bewegung $\mathfrak{P}_{\sqrt{-\frac{1}{\alpha}}}\mathfrak{P}_1$ anwenden und dann die positive Drehung mit einem rechten Winkel um O, dann wird schlieszlich C in den Punkt O übergeführt und auszerdem A in einen Punkt A' der Geraden $(0, \infty)$ zwischen O und ∞. Die durch Zusammensetzung der genannten Bewegungen erhaltene Bewegung induziert die Endentransformation:

$$\bar{\xi} = \frac{1+\xi/\alpha}{1-\xi/\alpha}. \quad . \quad . \quad . \quad . \quad . \quad . \quad . \quad . \quad (5,11)$$

Die Enden der Geraden (λ, ∞) werden dabei in

$$\bar{\lambda} = \frac{1+\lambda/\alpha}{1-\lambda/\alpha} \text{ bezw. } \bar{\lambda}' = -1$$

verwandelt. Nun sind die Enden der Senkrechten in A' auf der Geraden $(0, \infty)$ exp b und $-\exp b$, da die Strecken OA' und CA einander kongruent sind. Also gilt:

$$\bar{\lambda}\,\bar{\lambda}' = -\exp 2b,$$

wegen des Satzes 4 von § 2, und daher:

$$\frac{1+\lambda/a}{1-\lambda/a} = \exp 2b.$$

Daraus geht hervor:
$$\frac{\lambda}{a} = \frac{\exp 2b - 1}{\exp 2b + 1} = \tanh b. \quad \ldots\ldots \quad (5,12)$$

Weiter haben wir:
$$\frac{1}{2}\left(a - \frac{1}{a}\right) = \sinh a. \quad \ldots\ldots \quad (5,13)$$

Es bleibt also noch $\beta - \frac{1}{\beta}$ zu deuten.

Es ist:
$$\tan \tfrac{1}{2} B = \sqrt{-\begin{bmatrix} \beta & -\frac{1}{\beta} \\ \infty & 0 \end{bmatrix}} = \frac{1}{\beta},$$

also:

$$\tan B = \frac{1}{\frac{1}{2}\left(\beta - \frac{1}{\beta}\right)}. \quad \ldots\ldots \quad (5,14)$$

Wenn wir nun die in (5, 12), (5, 13) und (5, 14) dargestellten Resultate in (5, 10) eintragen, finden wir:

$$\tanh b = \tan B \sinh a.$$

Damit ist die Formel (5, 3) bewiesen. Natürlich folgt daraus sofort (5, 3′) durch Buchstabenvertauschung.

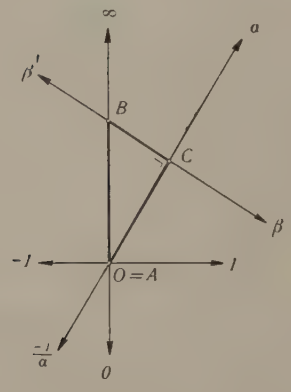

Fig. 2.

2. Um die Formel (5, 4) zu beweisen, verfahren wir folgendermaszen. Wir legen das Dreieck ABC in der Ebene derart, dasz A mit O zusammenfällt, B auf der Halbgeraden $(O\ \infty)$ liegt und C auf derselben Seite der Geraden $(0, \infty)$ liegt wie das Ende 1, (Fig. 2). Die Enden der Geraden AC seien a und $-a$, $(a > 0)$ und die Enden der Geraden BC seien β und β', $(\beta > 0)$.

Da die Geraden AC und BC senkrecht auf einander stehen haben wir:

$$\begin{bmatrix} \beta & \beta' \\ a & -\frac{1}{a} \end{bmatrix} = -1 \quad \ldots \quad (5,15)$$

wie z.B. mit Hilfe der Formel (2, 7) eingesehen werden kann. Nach leichtem Rechnen folgt aus (5, 15):

$$\beta\beta' - 1 = \tfrac{1}{2}(\beta + \beta')\left(a - \frac{1}{a}\right). \quad \ldots\ldots \quad (5,16)$$

Nun ist, wie wir soeben sahen:
$$\tan A = \frac{2}{a - \frac{1}{a}} \quad \ldots\ldots \quad (5,17)$$

während:
$$\tan \tfrac{1}{2} B = \sqrt{\frac{-\beta}{\beta'}} = -\frac{1}{\beta'}\sqrt{-\beta\beta'}, \quad \ldots\ldots \quad (5,18)$$

wobei man beachte, dasz β' negativ ist. Also:

$$\tan B = \frac{-2\sqrt{-\beta\,\beta'}}{\beta+\beta'}. \quad . \quad . \quad . \quad . \quad . \quad . \quad . \quad (5,19)$$

Wenn wir (5, 17) und (5, 19) in (5, 16) eintragen, erhalten wir:

$$\frac{1}{2}\left(\sqrt{-\beta\,\beta'}+\frac{1}{\sqrt{-\beta\,\beta'}}\right)=\operatorname{ctg} A \operatorname{ctg} B. \quad . \quad . \quad . \quad (5,20)$$

Wir wissen, dasz $$-\beta\,\beta' = \exp 2c,$$

also: $$\frac{1}{2}\left(\sqrt{-\beta\,\beta'}+\frac{1}{\sqrt{-\beta\,\beta'}}\right)=\cosh c. \quad . \quad . \quad . \quad . \quad (5,21)$$

Aus (5, 20) und (5, 21) folgt aber (5, 4).

3. Die anderen Formeln können nun durch ganz einfache Rechnungen hergeleitet werden. Zunächst findet man die Formel (5, 5) sofort mittels der Formeln (5, 3), (5, 3′) und (5, 4). Weiter haben wir:

$$\frac{1}{\sin^2 A}=1+\operatorname{ctg}^2 A=\frac{\tanh^2 a+\sinh^2 b}{\tanh^2 a}=\frac{\sinh^2 a+\sinh^2 b\cosh^2 a}{\sinh^2 a}$$

$$=\frac{\cosh^2 a\cosh^2 b-1}{\sinh^2 a}=\frac{\cosh^2 c-1}{\sinh^2 a}=\frac{\sinh^2 c}{\sinh^2 a},$$

woraus (5, 6) hervorgeht. Damit ist natürlich auch (5, 6′) als richtig erwiesen. Die übrigen Formeln erfolgen durch fast triviale Rechnungen aus den schon bewiesenen. Damit ist der Beweis des Satzes beendet.

c. Die Formeln des allgemeinen Dreiecks. Mit der von den Formeln des rechtwinkligen Dreiecks geschaffenen Grundlage ist es nicht schwer, die Formeln eines beliebigen Dreiecks herzuleiten. Das kann nach den bekannten Methoden geschehen. Wenn ein Dreieck ABC vorgelegt ist, können wir die von den Seiten BC, CA und AB erzeugten Streckenklassen mit a, b und c bezeichnen, sowie die von den Winkeln CAB, ABC und BCA erzeugten Winkelklassen bezw. mit A, B und Γ. Behufs einer Anwendung im nächsten Paragraphen erwähnen wir den *Seitenkosinussatz*, welche folgendermaszen lautet:

$$\cosh c=\cosh a\cosh b-\sinh a\sinh b\cos\Gamma, \quad . \quad . \quad . \quad (5,22)$$

und die daraus durch zyklische Buchstabenvertauschung hervorgehenden Relationen.

Damit betrachten wir die Aufgabe der Begründung der Trigonometrie in der hyperbolischen Ebene als erledigt.

§ 6. Zwei Sätze über den Kreis.

Als Anwendung der trigonometrischen Formeln werden wir zwei Sätze beweisen:

1. *Eine Gerade, die einen Punkt innerhalb eines Kreises enthält, trifft den Kreis in zwei Punkten.*

Bekanntlich genügt es, die Existenz eines gemeinsamen Punktes zu beweisen. Offenbar ist unter der gemachten Voraussetzung der Abstand des Kreismittelpunktes von der Geraden kleiner als der Halbmesser des Kreises. Wir sind fertig, wenn wir gezeigt haben, dasz es ein beim Punkte C rechtwinkliges Dreieck gibt, dessen Seiten AB und AC zu vorgegebenen Streckenklassen c, bezw. b gehören, insofern $c > b$ ist.

Setzen wir $$\gamma=\frac{\cosh c}{\cosh b}, \quad . \quad . \quad . \quad . \quad . \quad . \quad . \quad . \quad (6,1)$$

dann gibt es wegen $\gamma > 1$ eine Streckenklasse a mit $\cosh a = \gamma$. Denn dazu braucht man

nur zu beweisen, dasz es eine Streckenklasse a gibt mit $\exp a = \xi_1$, wobei $\xi_1 > 1$ und eine Lösung ist der Gleichung:

$$\frac{1}{2}\left(\xi + \frac{1}{\xi}\right) = \gamma$$

oder

$$\xi^2 - 2\gamma\xi + 1 = 0. \quad . \quad . \quad . \quad . \quad . \quad . \quad . \quad . \quad (6, 2)$$

Die Gleichung (6, 2) ist gewisz lösbar, denn ihre Diskriminante ist positiv. Weiter sieht man sofort, dasz es eine Wurzel $\xi_1 > 1$ gibt. Auf Grund des Satzes 2 von § 3 gehört dazu eine Streckenklasse a mit $\exp a = \xi_1$, also $\cosh a = \gamma$.

Es existiert ein Dreieck mit Seiten CA und CB, welche zu den Klassen b, bezw. a gehören, während der Winkel ACB ein rechter ist. Auf Grund der Formel (5, 5) gehört die Seite AB zu der Klasse c', welche der Relation:

$$\cosh c' = \cosh a \cosh b$$

genügt. Wegen (6, 1) und $\cosh a = \gamma$ folgt also:

$$\cosh c' = \cosh c,$$

und wegen der Monotonie der cosh-Funktion haben wir $c = c'$, w.z.b.w.

2. *Enthält ein Kreis einen inneren und einen äuszeren Punkt eines zweiten Kreises, dann schneiden sich die beiden Kreise, und zwar in zwei Punkten.*

Auch jetzt brauchen wir nur die Existenz eines gemeinsamen Punktes zu zeigen. Wir bemerken zunächst, dasz die Voraussetzungen des Satzes gleichwertig sind mit der Bedingung, dasz die Entfernung der beiden Mittelpunkte gröszer ist als der Absolutwert der Differenz, aber kleiner als die Summe der Halbmesser der beiden Kreise.

Offenbar sind wir fertig, wenn wir dartun können, dasz ein Dreieck ABC existiert, dessen Seiten bezw. zu den Streckenklassen a, b und c gehören, wobei die Ungleichungen:

$$|a - b| < c < a + b \quad . \quad . \quad . \quad . \quad . \quad . \quad . \quad (6, 3)$$

erfüllt sind. Aus diesen Ungleichungen folgt:

$$\cosh a \cosh b - \sinh a \sinh b < \cosh c < \cosh a \cosh b + \sinh a \sinh b.$$

Darum gilt, wenn wir

$$\frac{\cosh a \cosh b - \cosh c}{\sinh a \sinh b} = \gamma \quad . \quad . \quad . \quad . \quad . \quad . \quad (6, 4)$$

setzen:

$$-1 < \gamma < 1. \quad . \quad . \quad . \quad . \quad . \quad . \quad . \quad . \quad (6, 5)$$

Aus (6, 5) folgt aber, dasz $\frac{1-\gamma}{1+\gamma}$ positiv ist und auf Grund des Satzes 2 von § 4 gibt es eine Winkelklasse Γ, welche die Beziehung

$$\tan \tfrac{1}{2}\Gamma = \sqrt{\frac{1-\gamma}{1+\gamma}}$$

erfüllt. Dann ist aber:

$$\cos \Gamma = \gamma. \quad . \quad . \quad . \quad . \quad . \quad . \quad . \quad . \quad . \quad (6, 6)$$

Es existiert gewisz ein Dreieck ABC, dessen Seiten CA und CB zu den Streckenklassen b, bezw. a gehören und dessen Winkel BCA zu der Winkelklasse Γ gehört. Die dritte Seite AB gehört zu der Klasse c' und es gilt auf Grund des Kosinussatzes:

$$\cosh c' = \cosh a \cosh b - \sinh a \sinh b \cos \Gamma. \quad . \quad . \quad . \quad (6, 7)$$

Aus (6, 4) und (6, 6) erfolgt dann:

$$\cosh c' = \cosh c,$$

also $c' = c$, w.z.b.w.

Berichtigung: In Satz 18 des § 1 lese man $\mathfrak{S}_\alpha \mathfrak{S}_0$ statt $\mathfrak{S}_\alpha \mathfrak{S}$ und in Satz 25 des § 1 lese man $\mathfrak{P}_\alpha \mathfrak{P}_1$ statt $\mathfrak{P}_\alpha \mathfrak{S}_1$.

Mathematics. — *Zur hyperbolischen Geometrie.* Von J. C. H. GERRETSEN. (Communicated by Prof. J. G. VAN DER CORPUT.)

(Communicated at the meeting of May 30, 1942.)

Einleitung.

Behufs der Begründung der Bolyai-Lobatschewskijschen Geometrie hat HILBERT die Endenrechnung erfunden und hat damit gezeigt, dasz man den Geraden der hyperbolischen Ebene derart Koordinaten zuordnen kann, welche der Menge der Enden entnommen sind, dasz die Gleichung eines Punktes eine lineare ist [1]). Damit ist die Möglichkeit gegeben die hyperbolische Geometrie in die projektive Geometrie einzuordnen.

Vor kurzem hat DE KERÉKJÁRTÓ eine Begründungsmethode [2]) gegeben, die wesentlich von der von HILBERT gegebenen verschieden ist und sich vielmehr an ein Verfahren anlehnt, das HESSENBERG für die Begründung der elliptischen Geometrie verwendet hat [3]). In der von DE KERÉKJÁRTÓ gegebenen Darstellung wird eine Pseudogeometrie konstruiert, welche sich als Euklidisch erweist, wodurch die hyperbolische Geometrie in der bekannten von POINCARÉ herrührenden Gestalt erscheint. Zwar wird das Ziel mit ganz elementaren Mitteln erreicht, aber das Vorgehen ist ziemlich weitschweifig. Zudem hat die Arbeit DE KERÉKJÁRTÓS eine Lücke, denn für die Möglichkeit des Aufbaus des Poincaréschen Modells in einer Euklidischen Ebene musz auszerdem noch ein Satz gelten, den ich das „Axiom des Kreises" nennen möchte und folgendermaszen lautet: *Jede Gerade, von der ein Punkt innerhalb eines Kreises liegt, trifft den Kreis in zwei Punkten* [4]). Dieser Satz fehlt in der De Kerékjártóschen Arbeit und läszt sich auch nicht aus den da verifizierten Axiomen der Euklidischen Geometrie herleiten. Jedoch gilt er in der konstruierten Pseudogeometrie, aber für seinen Beweis musz man bei der Entwicklung der hyperbolischen Geometrie weiter ausholen als DE KERÉKJÁRTÓ und HILBERT getan haben.

Ich möchte darauf hinweisen, dasz man mit Hilfe der Hilbertschen Endenrechnung sehr leicht das Poincarésche Modell aufbauen kann. Zu diesem Zwecke bediene ich mich ebenfalls einer Pseudogeometrie, welche unter Zugrundelegung des Endenkörpers $\mathfrak{h}$, den ich in einer vorigen Arbeit [5]) gebraucht habe, konstruiert wird. Es stellt sich dabei heraus, dasz die Axiome der absoluten ebenen Geometrie [6]) ebenso wie das Euklidische Parallelenaxiom in dieser Geometrie erfüllt sind. Dasz auch das oben genannte Axiom des Kreises gilt, ist eine fast triviale Folge der Tatsache, dasz im Körper $\mathfrak{h}$ jedes positive Element eine Quadratwurzel hat [7]). Damit ist dann dargetan: *Alle Sätze, die man auf dem Wege der*

---

[1]) D. HILBERT, Grundlagen der Geometrie, 7 Aufl. (Leipzig und Berlin 1930), Anhang III, § 4.

[2]) B. DE KERÉKJÁRTÓ, Nouvelle méthode d'édifier la géometrie plane de Bolyai et de Lobatchefski, Comm. Math. Helv. **13** (1940—1941), 11—48.

[3]) G. HESSENBERG, Begründung der elliptischen Geometrie, Math. Ann. **61** (1905), 173—184.

[4]) In der Euklidischen Geometrie folgt dann leicht, dasz zwei Kreise einander treffen, wenn der eine Kreis einen Punkt innerhalb und einen Punkt auszerhalb des anderen Kreises enthält. Die gemeinsamen Punkte sind dann die Schnittpunkte eines der Kreise und der Potenzlinie.

[5]) J. C. H. GERRETSEN, Die Begründung der Trigonometrie in der hyperbolischen Ebene, Diese Proceedings **45** (1942), 360—366, 479—483 und 559—566, § 1. Im folgenden werde ich diese Arbeit mit „Trig." zitieren.

[6]) Trig., Einleitung.

[7]) Trig., § 1, Satz 26.

Poincaréschen Deutung findet, gehören zum Bestande der hyperbolischen Geometrie (im Hilbertschen Sinne), *insofern man sich für die in dieser Deutung zur Anwendung kommenden Sätze der Euklidischen Geometrie nur auf die Axiome der absoluten ebenen Geometrie, das Euklidische Parallelelenaxiom und das Axiom des Kreises beruft.*

§ 1. Die Poincaréschen Koordinaten.

Es sei P irgendein Punkt der hyperbolischen Ebene. Das von dem Ende ∞ verschiedene Ende der Geraden (P ∞) sei ξ. Die Bewegung $\mathfrak{S}_{-\frac{1}{2}\xi}\,\mathfrak{S}_0$ führt P in einen Punkt P' der Geraden $(0, \infty)$ über [8]). Das positive Ende des Lotes in P' auf dieser Geraden sei η. Wir werden nun dem Punkte P das Elementepaar $\{\xi, \eta\}$ zuordnen und ξ, η die *Poincaréschen Koordinaten* (kurz Koordinaten) des Punktes P nennen, aus einem Grunde, der nachher ersichtlich ist. Umgekehrt läszt sich zu jedem Paar $\{\xi, \eta\}$, wobei ξ und $\eta > 0$ Elemente des Körpers $\mathfrak{h}$ sind, ein Punkt P finden, dessen Kordinaten eben ξ und η sind. Denn P ist der Punkt, in den der Fuszpunkt P' des Lotes aus dem Ende ξ auf der Geraden $(0, \infty)$ durch die Bewegung $\mathfrak{S}_{-\frac{1}{2}\xi}\,\mathfrak{S}_0$ übergeführt wird. Es wird sich weiterhin als nützlich erweisen auch den von ∞ verschiedenen Enden Koordinaten zu erteilen und zwar ordnen wir dem Ende ξ die Koordinaten $\{\xi, 0\}$ zu.

Vor allem ist es wichtig zu untersuchen, welche Transformationen die Koordinaten durch die hyperbolischen Bewegungen erleiden. Um das Ergebnis bequem abfassen zu können, werden wir dem Körper $\mathfrak{h}$ die imaginäre Einheit i adjungieren. Es gilt nun folgender Satz:

Die hyperbolischen Bewegungen werden gegeben durch die Formeln:

$$\xi \pm i\eta = \frac{\lambda(\xi + i\eta) + \mu}{\lambda'(\xi + i\eta) + \mu'}. \quad \ldots\ldots \quad (1,1)$$

Dabei sind $\{\bar{\xi}, \bar{\eta}\}$ die Koordinaten des Punktes, bezw. des Endes, der dem Punkt, bezw. das dem Ende mit Koordinaten $\{\xi, \eta\}$ zugeordnet wird vermöge einer Bewegung [9]). *In* (1,1) *gilt das obere oder das untere Zeichen, je nachdem die Transformationsdeterminante $\lambda\mu' - \lambda'\mu$ positiv oder negativ ist.*

Wir werden den Beweis des Satzes in einigen Schritten führen.

a. Zunächst betrachten wir die Bewegung $\mathfrak{S}_0$, die Spiegeling an der Geraden $(0, \infty)$. Es sei P ein Punkt und P' der daraus durch die Bewegung $\mathfrak{S}_{-\frac{1}{2}\xi}\,\mathfrak{S}_0$ hervorgehende Punkt. Aus der Tatsache, dasz P' bei der Bewegung $\mathfrak{S}_0$ ungeändert bleibt, während dem Punkt P der Spiegelpunkt $\bar{P}$ von P inbezug auf die Gerade $(0, \infty)$ zugeordnet wird, folgt:

$$\bar{\xi} = -\xi$$
$$\eta = \eta$$

also:

$$\bar{\xi} - i\bar{\eta} = -(\xi + i\eta) \quad \ldots\ldots \quad (1,2)$$

b. Etwas mehr Schwierigkeiten bietet uns die Untersuchung der Bewegung $\mathfrak{P}_1$. Es seien γ und $-\gamma$ die Enden des Lotes aus P auf der Geraden $(0, \infty)$. Die Bewegung $\mathfrak{S}_{-\frac{1}{2}\xi}\,\mathfrak{S}_0$ führt dieses Lot in die Gerade durch P' mit den Enden $-\xi + \gamma$ und $-\xi - \gamma$ über. Daraus folgt auf Grund eines bekannten Satzes [10]):

$$(-\xi + \gamma)(-\xi - \gamma) = -\eta^2,$$

---

[8]) Trig., § 1, Satz 18.

[9]) Offenbar liegt hier eine naturgemäsze Erweiterung der Sätze 1 und 2 des § 2 von Trig. vor, denn die Spezialisierung $\eta = \bar{\eta} = 0$ ergibt eben die dort erwähnte Formel (2, 1).

[10]) Trig., § 2, Satz 4.

also:

$$\xi^2 + \eta^2 = \gamma^2. \quad \ldots\ldots\ldots \quad (1,3)$$

Die Bewegung $\mathfrak{P}_1$ ordnet der Geraden $(-\gamma, \gamma)$ die Gerade $(-\frac{1}{\gamma}, \frac{1}{\gamma})$ zu. Wir können nun auch den vorgegebenen Punkt P durch die Bewegung $\mathfrak{P}_{\sqrt{\frac{1}{\gamma^2}}}\mathfrak{P}_1$ in $\bar{P}$ überführen [11]); mithin

$$\bar{\xi} = \frac{\xi}{\gamma^2} = \frac{\xi}{\xi^2 + \eta^2},$$

$$\bar{\eta} = \frac{\eta}{\gamma^2} = \frac{\eta}{\xi^2 + \eta^2},$$

und daraus finden wir:

$$\bar{\xi} - i\bar{\eta} = \frac{\xi - i\eta}{\xi^2 + \eta^2} = \frac{1}{\xi + i\eta}, \quad \ldots\ldots \quad (1,4)$$

c. Es sei nun die Bewegung $\mathfrak{S}_{\frac{1}{2}\nu}\mathfrak{S}_0$ vorgelegt. Da dabei das Ende ∞ ungeändert bleibt und die Punkte $\bar{P}'$ und P' zusammenfallen, wenn wir mit $\bar{P}'$ den durch die Bewegung $\mathfrak{S}_{-\frac{1}{2}\bar{\xi}}\mathfrak{S}_0$ aus $\bar{P}$ hervorgehenden Punkt bezeichnen, so haben wir:

$$\bar{\xi} = \xi + \nu,$$

$$\bar{\eta} = \eta,$$

also:

$$\bar{\xi} + i\bar{\eta} = (\xi + i\eta) + \nu. \quad \ldots\ldots\ldots \quad (1,5)$$

d. Schlieszlich betrachten wir die Bewegung $\mathfrak{P}_{\sqrt{\varkappa}}\mathfrak{P}_1$, $(\varkappa > 0)$. Zunächst haben wir:

$$\bar{\xi} = \varkappa\xi,$$

da auch jetzt das Ende ∞ ungeändert bleibt. Ferner wird $\bar{P}$ aus P' erhalten durch die Bewegung $\mathfrak{S}_{-\frac{1}{2}\xi}\mathfrak{S}_0\mathfrak{P}_{\sqrt{\varkappa}}\mathfrak{P}_1\mathfrak{S}_{\frac{1}{2}\xi}\mathfrak{S}_0$. Der Koordinate η wird also die Koordinate

$$\eta = -\bar{\xi} + \varkappa(\xi + \eta) = \varkappa\eta$$

zugeordnet. Damit haben wir gefunden:

$$\bar{\xi} + i\bar{\eta} = \varkappa(\xi + i\eta). \quad \ldots\ldots\ldots \quad (1,6)$$

Jede Bewegung wird durch Zusammensetzung der Bewegungen $\mathfrak{S}_0, \mathfrak{P}_1, \mathfrak{S}_{\frac{1}{2}\nu}\mathfrak{S}_0, \mathfrak{P}_{\sqrt{\varkappa}}\mathfrak{P}_1$ gefunden; daraus ersehen wir, dasz dadurch die Koordinaten eine Transformation (1, 1) erleiden. Die dabei auftretenden Koeffizienten sind bis auf einen gemeinsamen Faktor bestimmt. Ist umgekehrt eine Transformation (1, 1) vorgelegt, dann können wir diese aus den soeben betrachteten Transformationen (1, 2), (1, 4), (1, 5) und (1, 6) zusammensetzen. Dazu gehören gewisse Bewegungen, die eben die Transformationen induzieren und die Zusammensetzung dieser Bewegungen ergibt eine Bewegung, welche die vorgelegte Transformation hervorruft. Es kostet wenig Mühe darzutun, dasz diese Bewegung durch die Transformation eindeutig bestimmt ist [12]).

---

[11]) Trig., § 1, Satz 25.

[12]) Man vergleiche die Betrachtungen von Trig., § 2.

Wir bemerken noch, dasz man die Koordinatentransformation sofort hinschreiben kann, wenn man die zur Bewegung gehörige Endentransformation kennt, denn die Koeffizienten in beiden Transformationen sind die nämlichen.

§ 2. Die Gleichungen der Geraden und des Kreises.

Aus der Definition der Poincaréschen Koordinaten ergibt sich ohne weiteres:

1. *Die Gleichung einer durch das Ende ∞ gehenden Geraden lautet:*

$$\xi = a_0. \quad . \quad . \quad . \quad . \quad . \quad . \quad . \quad . \quad . \quad . \quad (2, 1)$$

Dabei ist a_0 das von ∞ verschiedene Ende der Geraden.

Wir wollen nun eine Gerade betrachten, die nicht durch das Ende ∞ geht. Dafür gilt:

2. *Die Gleichung einer nicht durch das Ende ∞ gehenden Geraden lautet:*

$$(\xi - a_0)^2 + \eta^2 = \beta_0^2. \quad . \quad . \quad . \quad . \quad . \quad . \quad . \quad . \quad (2, 2)$$

Dabei sind $\{a_0, \beta_0\}$ die Koordinaten des Fuszpunktes des Lotes aus dem Ende ∞ auf der Geraden.

Wir können die gegebene Gerade durch die Bewegung $\mathfrak{P}\frac{1}{i\beta_0}\mathfrak{P}_1\mathfrak{S}_{-\frac{1}{2}a_0}\mathfrak{S}_0$ in die Gerade $(-1, +1)$ überführen. Irgendeinem Punkt $P\{\xi, \eta\}$ der gegebenen Geraden wird der Punkt $\bar{P}\{\bar{\xi}, \bar{\eta}\}$ der Geraden $(-1, +1)$ zugeordnet, während:

$$\bar{\xi} + i\bar{\eta} = \frac{1}{\beta_0}(\xi + i\eta - a_0), \quad . \quad . \quad . \quad . \quad . \quad . \quad (2, 3)$$

wie auf Grund der am Schlusse des vorigen Paragraphen gemachten Bemerkung ohne Mühe ersichtlich ist. Die Multiplikation mit dem konjugiert komplexen Ausdruck ergibt:

$$\bar{\xi}^2 + \bar{\eta}^2 = \frac{1}{\beta_0^2}((\xi - a_0)^2 + \eta^2).$$

Wir sahen aber beim Beweise des Satzes des vorigen Paragraphen, dasz

$$\bar{\xi}^2 + \bar{\eta}^2 = 1$$

ist (Formel (1, 3)), also:

$$(\xi - a_0)^2 + \eta^2 = \beta_0^2, \quad \text{w. z. w. b.}$$

Wir werden nun die Gleichung eines Kreises mit Halbmesser r herleiten, dessen Mittelpunkt der Punkt O ist. Es sei $\varrho = \exp r$ gesetzt. Dann hat offenbar der auf der Halbgeraden $(O\ \infty)$ liegende Punkt des Kreises die Koordinaten $\{0, \varrho\}$ [13]). Ist nun $\{\xi, \eta\}$ irgendein Punkt des Kreises, dann kann der soebengenannte Punkt durch eine Drehung um O in den letztgenannten Punkt übergeführt werden. Wenn wir den Drehungsparameter mit ϑ bezeichnen [14]), so gilt mit Rücksicht auf die Bemerkung am Schlusse des vorigen Paragraphen:

$$\xi + i\eta = \frac{i\varrho + \vartheta}{1 - i\varrho\vartheta}. \quad . \quad . \quad . \quad . \quad . \quad . \quad . \quad (2, 2)$$

Die Multiplikation mit dem konjugiert komplexen Ausdruck ergibt:

$$\xi^2 + \eta^2 = \frac{\varrho^2 + \vartheta^2}{1 + \varrho^2\vartheta^2},$$

---

[13]) Trig., § 3.

[14]) Trig., § 2, Satz 5.

und daraus geht hervor:

$$\xi^2 + \eta^2 + 1 = \frac{(1+\varrho^2)(1+\vartheta^2)}{1+\varrho^2\vartheta^2}. \quad . \quad . \quad . \quad . \quad . \quad . \quad (2,3)$$

Anderseits ergibt sich nach leichter Rechnung aus (2, 2):

$$\eta = \frac{\varrho(1+\vartheta^2)}{1+\varrho^2\vartheta^2}. \quad . \quad . \quad . \quad . \quad . \quad . \quad . \quad (2,4)$$

Daraus folgt in Verbindung mit (2, 3):

$$\xi^2 + \eta^2 + 1 = (\varrho + \varrho^{-1})\eta = 2\eta \cosh r,$$

oder:

$$\xi^2 + (\eta - 1)^2 = 4\eta \sinh^2 \tfrac{1}{2} r. \quad . \quad . \quad . \quad . \quad . \quad . \quad (2,5)$$

Wir sind nun imstande folgenden Satz zu beweisen:

2. *Die Gleichung eines Kreises mit Halbmesser r und Mittelpunkt* $\{\alpha_0, \beta_0\}$ *lautet:*

$$(\xi - \alpha_0)^2 + (\eta - \beta_0)^2 = 4\eta\beta_0 \sinh^2 \tfrac{1}{2} r. \quad . \quad . \quad . \quad . \quad . \quad (2,6)$$

Die Bewegung $\mathfrak{P}_{\sqrt{\frac{1}{\beta_0}}} \mathfrak{P}_1 \mathfrak{S}_{-\frac{1}{\beta_0}\alpha_0} \mathfrak{S}_0$ ordnet nämlich einem beliebigen Punkt $\{\xi, \eta\}$ dieses Kreises den Punkt des Kreises um O mit dem Halbmesser r zu, dessen Koordinaten $\bar{\xi} = \frac{1}{\beta_0}(\xi - \alpha_0)$, $\bar{\eta} = \frac{1}{\beta_0}\eta$ sind. Aus (2, 5) folgt nun leicht die Richtigkeit der Behauptung.

§ 3. Die Entfernungsformeln.

Es seien $P_1\{\xi_1, \eta_1\}$ und $P_2\{\xi_2, \eta_2\}$ zwei nicht zusammenfallende Punkte. Unter der *Entfernung* dieser Punkte verstehen wir die von der Strecke P_1P_2 erzeugte Streckenklasse[15]). Es gilt der Satz:

1. *Die Entfernung d der Punkte* $P_1\{\xi_1, \eta_1\}$ *und* $P_2\{\xi_2, \eta_2\}$ *wird gegeben durch die Formel:*

$$4 \sinh^2 \tfrac{1}{2} d = \frac{(\xi_1 - \xi_2)^2 + (\eta_1 - \eta_2)^2}{\eta_1 \eta_2}. \quad . \quad . \quad . \quad . \quad (3,1)$$

Der Beweis geht sofort aus dem Satz 2 des vorigen Paragraphen hervor, wenn wir beachten, dasz $\{\xi_1, \eta_1\}$ ein Punkt des Kreises um den Punkt $\{\xi_2, \eta_2\}$ mit dem Halbmesser d ist.

Wir wollen nun noch einen anderen Ausdruck für die Entfernung herleiten. Zu dem Zweck beweisen wir:

2. *Es seien* α *und* β *die beiden Enden der durch die Punkte* $P_1\{\xi_1, \eta_1\}$ *und* $P_2\{\xi_2, \eta_2\}$ *bestimmten Geraden, und zwar sei* α *das von der von* P_1 *ausgehenden und den Punkt* P_2 *enthaltenden Halbgeraden bestimmte Ende. Dann ist das Doppelverhältnis.*

$$\begin{bmatrix} \xi_1 + i\eta_1 & \xi_2 + i\eta_2 \\ \alpha & \beta \end{bmatrix}. \quad . \quad . \quad . \quad . \quad . \quad . \quad (3,2)$$

reell (d.h. zum Körper $\mathfrak{h}$ gehörig) *und gleich* $\exp d$.

Beim Beweise hat man darauf zu achten, dasz das Doppelverhältnis (3, 2) gegenüber

---

[15]) Trig., § 3.

Bewegungen invariant ist, sowie die Klasse d. Wir können somit P_1 mit O zusammenfallen lassen und P_2 in den Punkt $\{0, \exp d\}$ legen. Dann wird das Doppelverhältnis (3, 2):

$$\begin{bmatrix} i & i \exp d \\ \infty & 0 \end{bmatrix} = \frac{i-\infty}{i-0} \cdot \frac{i \exp d - 0}{i \exp d - \infty} = \exp d,$$

womit der Beweis schon erbracht ist.

Man könnte natürlich auch

$$\mathfrak{a} = \ln \alpha$$

statt

$$\alpha = \exp \mathfrak{a}$$

schreiben. Dann findet man den bekannten Ausdruck:

$$d = \ln \begin{bmatrix} \xi_1 + i\eta_1 & \xi_2 + i\eta_2 \\ \alpha & \beta \end{bmatrix}. \quad . \quad . \quad . \quad . \quad . \quad . \quad (3, 3)$$

Allerdings darf man nicht übersehen, dasz die formal eingeführte Funktion ln zwar der Funktionalbeziehung

$$\ln \xi\eta = \ln \xi + \ln \eta$$

genügt, aber keine Basis besitzt, denn in der Menge der Streckenklassen ist keine Klasse als die Einheit ausgezeichnet.

§ 4. Die Pseudogeometrie.

Den folgenden Betrachtungen wird der Körper $\mathfrak{h}$ zugrunde gelegt. Unter Punkt der *Pseudoebene* verstehen wir ein Elementepaar $\{\xi, \eta\}$ und unter Gerade der Pseudoebene verstehen wir das Verhältnis dreier Elemente $\{\alpha, \beta, \gamma\}$, wobei α, β nicht beide Null sind, während der Punkt zu der Geraden gehört, wenn die Gleichung

$$\alpha\xi + \beta\eta + \gamma = 0. \quad . \quad . \quad . \quad . \quad . \quad . \quad . \quad . \quad (4, 1)$$

besteht.

Die Reihenfolge der Punkte $\{\xi_1, \eta_1\}$, $\{\xi_2, \eta_2\}$, $\{\xi_3, \eta_3\}$, ... auf einer Geraden, wovon keine zwei zusammenfallen, wird bestimmt durch die Reihenfolge der Elemente $\xi_1, \xi_2, \xi_3, \ldots$. oder $\eta_1, \eta_2, \eta_3, \ldots$. Von den Punkten für die $\alpha\xi + \beta\eta + \gamma$ dasselbe Vorzeichen hat, sagen wir, dasz sie auf derselben Seite der Geraden $\{\alpha, \beta, \gamma\}$ liegen.

Die Bewegungen in der Pseudoebene werden gegeben durch die Formeln:

$$\bar{\xi} \pm i\bar{\eta} = (\varkappa + i\sigma)(\xi + i\eta) + \xi_0 + i\eta_0. \quad . \quad . \quad . \quad . \quad (4, 2)$$

Dabei sind $\varkappa, \sigma, \xi_0, \eta_0$ gegebene Elemente mit $\varkappa^2 + \sigma^2 = 1$.

In bekannter Weise kann man verifizieren, dasz in der Pseudogeometrie die Axiome der absoluten ebenen Geometrie und das Euklidische Parallelenaxiom erfüllt sind. Auszerdem läszt sich leicht nachprüfen, dasz auch das Axiom des Kreises erfüllt ist, da im Körper $\mathfrak{h}$ die Quadratwurzelziehung aus positiven Elementen möglich ist.

Aus den vorhergehenden Betrachtungen erweist sich, dasz die Punkte der hyperbolischen Ebene umkehrbar eindeutig auf den Punkten der Pseudohalbebene $\eta > 0$ abgebildet werden können. Das Bild einer hyperbolischen Geraden ist entweder eine Halbgerade, senkrecht auf der Geraden $\eta = 0$ und mit dem Endpunkt auf dieser Geraden, oder ein Halbkreis, dessen Endpunkte zu dieser Geraden gehören. Den hyperbolischen Bewegungen ent-

sprechen bestimmte Transformationen der Pseudoebene, die aus den folgenden zusammengesetzt werden können:

a. die Spiegelung an der Geraden $\xi = 0$;

b. die Inversion inbezug auf den Einheitskreis um den Punkt $\{0, 0\}$;

c. Translationen längs der Geraden $\eta = 0$;

d. Homothetien, deren Faktor positiv ist und als Zentrum den Punkt $\{0, 0\}$ haben.

Den Kreisen der hyperbolischen Ebene entsprechen Kreise der Pseudohalbebene und konzentrischen Kreisen der hyperbolischen Ebene sind Kreise zugeordnet, welche einem Büschel mit Potenzlinie $\eta = 0$ angehören.

Die von ∞ verschiedenen Enden korrespondieren umkehrbar eindeutig mit den Punkten der Geraden $\eta = 0$. Man kann sich nun leicht klar machen, durch welche elementargeometrischen Operationen die Hilbertsche Endenrechnung sich veranschaulichen läszt.

Mathematics. — *Deux théorèmes sur la dérivée d'une fonction holomorphe univalente et bornée dans un demi-plan au voisinage de la frontière.* Par Prof. J. WOLFF. (Communicated by Prof. J. G. VAN DER CORPUT.)

(Communicated at the meeting of May 30, 1942.)

Soit $f(z)=f(x+iy)$ holomorphe, univalente et bornée dans le demi-plan $D(x>0)$. Envisageons dans D une suite S_0 de points $z_n=x_n+iy_n$, $n=1,2,\ldots$ telle que $x_{n+1}<c\,x_n$, c étant une constante positive plus petite que l'unité.

Pour toute valeur réelle de t soit S_t la suite des points z_n+it, obtenue en appliquant à tous les points de S_0 une même translation parallèle à l'axe imaginaire.

Nous savons que $x\,f'(z)$ tend vers zéro quelle que soit la manière dont x tend vers zéro [1]). Par conséquent sur S_t le produit $x_n f'(z_n+it)$ tend vers zéro pour n infini, quelle que soit la valeur réelle de t. Nous aurons un résultat plus précis en nous bornant à une certaine plénitude de valeurs de t (ensemble dont l'ensemble complémentaire est de mesure nulle). Nous démontrerons le

THÉORÈME I. L'axe imaginaire contient une plénitude de points it tels que sur les suites S_t le produit $f'(z_n+it).\sqrt{x_n}$ tend vers zéro pour n infini.

Démonstration. Soit t' une valeur de t n'ayant pas cette propriété. Il existe alors un nombre positif ε et une suite d'indices $n_k\to\infty$ tels que

$$\left.\begin{aligned} x_{n_k}\,.\,|f'(z_{n_k}+it')|^2&>\varepsilon\\ x_{n_{k+1}}&<c\,x_{n_k}\end{aligned}\right\}\quad k=1,2,\ldots \quad . \quad . \quad . \quad . \quad (1)$$

Considérons les segments σ_k définis par

$$y=y_{n_k}+t',\quad c\,x_{n_k}\leqq x\leqq x_{n_k},\quad k=1,2,\ldots \quad . \quad . \quad . \quad (2)$$

La fonction $f(z)$ étant holomorphe et univalente dans les cercles de centres $z_{n_k}+it'$ et de rayons x_{n_k}, le théorème de KOEBE assure l'existence d'une constante positive K telle que sur les σ_k

$$|f'(z)|>K\,.\,|f'(z_{n_k}+it')|. \quad . \quad . \quad . \quad . \quad . \quad . \quad (3)$$

D'après (3), (1), (2) nous aurons

$$\int_{\sigma_k}|f'|^2\,dx>K^2\,.\,\frac{\varepsilon}{x_{n_k}}\,.\,(1-c)\,x_{n_k}=(1-c)\,K^2\,\varepsilon,\qquad k=1,2,\ldots,$$

d'où

$$\sum_{k=1}^{\infty}\int_{\sigma_k}|f'|^2\,dx=\sum_{k=1}^{\infty}\int_{c\,x_{n_k}}^{x_{n_k}}|f'(x+iy_{n_k}+it')|^2\,dx=+\infty. \quad . \quad (4)$$

---

[1]) A. DENJOY (Comptes Rendus de l'Ac. des Sc., Paris, 23 Juin 1941, p. 1072) J. WOLFF (Proceedings Ned. Ak. v. Wetensch., Amsterdam, vol. 44, No. 8, 1941, p. 956).

D'autre part dans la représentation conforme réalisée par $f(z)$ l'aire A de l'image de la bande $B\,(0<x<x_1)$ s'exprime par l'intégrale double

$$A=\int_{-\infty}^{\infty}\left\{\sum_{n=1}^{\infty}\int_{x_{n+1}}^{x_n}|f'(x+iy_n+it)|^2\,dx\right\}dt. \quad . \; . \; . \quad (5)$$

L'équation (5) et les inégalités $x_{n+1}<c\,x_n$ entraînent l'inégalité

$$\int_{-\infty}^{\infty}\left\{\sum_{n=1}^{\infty}\int_{c\,x_n}^{x_n}|f'(x+iy_n+it)|^2\,dx\right\}dt<A \quad . \; . \; . \; . \quad (6)$$

Parce que $f(z)$ est bornée, A est finie. De (6) résulte que (4) ne se produit que pour des valeurs de t d'un ensemble de mesure nulle, ce qui démontre le théorème.

Avant de passer au second théorème considérons dans D le système des courbes Γ_t d'équations

$$y=x^p+t, \quad -\infty<t<\infty \; . \; . \; . \; . \; . \; . \; . \quad (7)$$

où p est une constante positive. Pour $p>1$ les Γ_t sont tangentes à l'axe imaginaire aux différents points $i\,t$, tandis que pour $p\geqq 1$ elles y font un angle positif avec cet axe. Dans ce dernier cas nous savons qu'il existe une plénitude de valeurs de t telles que sur Γ_t

$$\lim_{z\to it} f'(z)\,.\,\sqrt{x}=0\ ^{2}). \quad . \; . \; . \; . \; . \; . \; . \quad (8)$$

Quel que soit p, le théorème I nous assure que toute suite S_0 sur Γ_0 de l'espèce considérée donne naissance à une plénitude de valeurs de t telles que sur Γ_t le produit $f'(z).\sqrt{x}$ tend vers zéro quand z parcourt la suite S_t. Cela n'implique pas l'existence d'une plénitude de valeurs de t telles que ce produit tendrait vers zéro quand z parcourt sur Γ_t une suite *quelconque* de la dite espèce, ce qui reviendrait à (8). Car l'ensemble de ces suites S_0 sur Γ_0 étant non-dénombrable, l'ensemble des plénitudes correspondantes est de même non-dénombrable et leur ensemble commun n'est pas nécessairement une plénitude ; il peut même être vide. Nous donnerons un exemple de fonction $f(z)$ holomorphe, univalente et bornée dans D, telle que pour $p<\frac{1}{2}$ *aucune* Γ_t ne satisfait à (8), en démontrant le

THÉORÈME II. A tout nombre p entre 0 et $\frac{1}{2}$ correspondent des fonctions $f(z)$ holomorphes, univalentes et bornées dans D, telles que sur chaque courbe $y=x^p+t$, $-\infty<t<\infty$,

$$\limsup_{z\to it}|f'(z)|\,.\,\sqrt{x}=\infty. \; . \; . \; . \; . \; . \; . \; . \quad (9)$$

Démonstration. Construisons une suite de points α_k, $k=1,2,\ldots$ partout dense sur l'intervalle $I\,(x=0,\,0<y<1)$ de l'axe imaginaire et telle que pour une infinité de valeurs de n les points $\alpha_1,\alpha_2,\ldots\alpha_n$ divisent I en $n+1$ parties égales. On voit sur le

---

2) A. DENJOY (l.c. p. 1071),
J. WOLFF (l.c. p. 960, le théorème VI appliqué au cas $\psi(x)=x^p$, $0<p\leqq 1$).

champ que tout point it de l'intervalle $\bar{I}(x=0, 0 \leqq y < 1)$ jouit de la propriété que la suite des a_k contient une suite partielle de points a_{k_ν}, $\nu = 1, 2, \ldots$ tels que

$$\left.\begin{aligned} k_\nu \,.\, |a_{k_\nu} - it| &\leqq 1 \\ \frac{a_{k_\nu}}{i} &> t \end{aligned}\right\} \quad \nu = 1, 2, \ldots \quad . \quad . \quad . \quad . \quad . \quad (10)$$

Parce que $p < \frac{1}{2}$ nous pouvons fixer deux nombres positifs ϱ et ϑ tels que

$$\vartheta + p(1+\varrho) < \tfrac{1}{2} \,. \quad . \quad . \quad . \quad . \quad . \quad . \quad . \quad . \quad (11)$$

Considérons la série

$$\psi(z) = \sum_{k=1}^{\infty} k^{-1-\varrho} (z - a_k)^{\vartheta}, \qquad z \text{ dans } D. \quad . \quad . \quad . \quad (12)$$

où $(z - a_k)^{\vartheta}$ est positif quand $z - a_k$ est positif. Chaque terme de la série a sa partie réelle positive parce que $\vartheta < 1$ en vertu de (11), et ϱ étant positif la série converge uniformément dans tout domaine borné. Par suite $\psi(z)$ est holomorphe dans D et sa partie réelle est positive. En outre $\psi(z)$ est continue sur $\bar{D}(x \geqq 0)$, donc elle est bornée au voisinage de tout point de l'axe imaginaire. Remarquons encore que pour tout point de D l'inégalité

$$|\psi(z)| < M(|z| + 1)^{\vartheta} \quad . \quad . \quad . \quad . \quad . \quad . \quad . \quad (13)$$

est valable, M étant indépendant de z.

La dérivée

$$\psi'(z) = \vartheta \sum_{k=1}^{\infty} k^{-1-\varrho} (z - a_k)^{\vartheta-1} \quad . \quad . \quad . \quad . \quad . \quad . \quad (14)$$

est à partie réelle positive, car chaque terme de la série (14) l'est parce que $0 < \vartheta < 1$. Donc $\psi(z)$ est univalente dans D.

Soit maintenant it un point quelconque de l'intervalle $\bar{I}$. Sur Γ_t considérons la suite des points z_ν situés avec les a_{k_ν} sur des droites parallèles à l'axe réel, donc

$$z_\nu - a_{k_\nu} = x_\nu = |a_{k_\nu} - it|^{\frac{1}{p}}, \qquad \nu = 1, 2, \ldots \quad . \quad . \quad . \quad (15)$$

En vertu de (14), la partie réelle de chaque terme étant positive,

$$|\psi'(z_\nu)| \geqq \Re\{\psi'(z_\nu)\} > \vartheta \; k_\nu^{-1-\varrho} \, x_\nu^{\vartheta-1},$$

d'où, en appliquant successivement (10), (15), (11),

$$\left.\begin{aligned} |\psi'(z_\nu)| \geqq \Re\{\psi'(z_\nu)\} &> \vartheta \,.\, |a_{k_\nu} - it|^{1+\varrho} \, x_\nu^{\vartheta-1} = \\ &= \vartheta \, x_\nu^{p(1+\varrho)+\vartheta-1} = \vartheta \, x_\nu^{-\frac{1}{2}-q}, \quad \nu = 1, 2, \ldots \end{aligned}\right\} \quad (16)$$

où q est une constante positive. Donc $\psi(z)$ satisfait à (9) *quel que soit it sur $\bar{I}$*. Posons

$$\Phi(z) = \sum_{n=-\infty}^{\infty} n^{-2} \psi(z + in). \quad . \quad . \quad . \quad . \quad . \quad . \quad (17)$$

L'inégalité (13) entraîne que dans tout domaine borné la série (17) a pour majorante une série de terme générale $K n^{-2+\vartheta}$, K constant. Donc, puisque $\vartheta < 1$, $\Phi(z)$ est holomorphe

dans D, continue sur $\overline{D}\,(x \geqq 0)$, par conséquent bornée au voisinage de tout point de l'axe imaginaire, comme $\psi(z)$. De plus $\phi(z)$ est univalente. En effet, la partie réelle de $\phi'(z)$ est positive parce que la partie réelle de la dérivée de chaque terme de la série (17) est positive.

Soit it un point quelconque de l'axe imaginaire. Il existe un entier m tel que $it - im$ est sur $\bar{I}$. En appliquant (16) aux z_ν qui correspondent à $t-m$ nous aurons sur Γ_{t-m}

$$\Re\{\psi'(z_\nu)\} > \delta x_\nu^{-\frac{1}{2}-q}, \qquad \nu = 1, 2, \ldots$$

De (17) on tire, en prenant le terme d'indice $-m$,

$$|\Phi'(z_\nu + im)| \geqq \Re\{\Phi'(z_\nu + im)\} > m^{-2}\,\Re\{\psi'(z_\nu)\} > \delta m^{-2} x^{-\frac{1}{2}-q},$$

les parties réelles des dérivées des autres termes étant positives. Or la suite $z_\nu + im$ est sur Γ_t et $z_\nu + im$ tend vers it pour ν infini. Donc $\phi(z)$ satisfait à (9) en tout point it de l'axe imaginaire.

Il s'agit encore d'en déduire une fonction holomorphe, univalente *et bornée dans* D qui montre la même conduite. Posons

$$f(z) = \frac{1}{\Phi(z) + 1}.$$

$f(z)$ est holomorphe et bornée dans D parce que $\phi(z)$ est holomorphe et à partie réelle positive. $f(z)$ est univalente parce que $\phi(z)$ l'est. Soit it un point quelconque de l'axe imaginaire. $\phi(z)$ étant bornée au voisinage de it, les z_ν sur Γ_t satisfont à

$$|f'(z_\nu)| = \frac{|\Phi'(z_\nu)|}{|\Phi(z_\nu) + 1|^2} > H(t) \cdot |\Phi'(z_\nu)| > h(t)\, x_\nu^{-\frac{1}{2}-p} \qquad \nu = 1, 2, \ldots$$

où $H(t)$ et $h(t)$ sont positifs et indépendants de ν. Donc $f(z)$ satisfait à (9) quel que soit it sur l'axe imaginaire. *C. Q. F. D.*

Mathematics. — *Sur le théorème de* MINKOWSKI, *concernant un système de formes linéaires réelles.* IV. *Quatrième communication: Démonstration du lemme 1 (fin), Remarque sur le Théorème 1.* Par J. F. KOKSMA et B. MEULENBELD. (Communicated by Prof. J. G. VAN DER CORPUT.)

(Communicated at the meeting of May 30, 1942.)

§ 1. Dans § 1 de cette dernière communication du mémoire présent nous terminons la démonstration du lemme 1; les formules (6)—(15), citées ici sont celles de § 4 de la troisième communication.

Nous choisissons le nombre arbitraire et positif δ; sans nuire à la généralité nous supposons $\delta \leqq \frac{1}{2}$, et enfin nous choisissons un nombre positif ε', tel que

$$\varepsilon' < \tfrac{1}{100}\,\delta, \quad \text{et donc} \quad 1 < \frac{1+\varepsilon'}{1-\varepsilon'} < 1+3\varepsilon'. \quad . \quad . \quad . \quad . \quad (16)$$

Alors le lemme 4 nous apprend, qu'en prenant le nombre $\varepsilon = \varepsilon(\varepsilon')$ suffisamment petit, on aura

$$\sum_{\nu=r+1}^{n+1} |u'_\nu| < \frac{1+\varepsilon'}{t}, \quad \sum_{\nu=r+1}^{n+1} |u''_\nu| < \frac{1+\varepsilon'}{t}, \quad . \quad . \quad . \quad . \quad (17)$$

et en outre

$$\sum_{\nu=1}^{r} \frac{|u'_\nu|}{a} + \frac{2^{\overline{n+1-r}}\, r^{\overline{n+1-r}}\,(n+1-r) \sum_{\nu=r+1}^{n+1} |u'_\nu|\, t}{(n+1)^{\overline{n+1-r}}} < 1+\varepsilon', \text{ avec } \sum_{\nu=r+1}^{n+1} |u'_\nu|\, t < \left(\frac{n+1}{2r}\right)^{\overline{n+1-r}} (1+\varepsilon')$$

ou

$$\sum_{\nu=r+1}^{n+1} |u'_\nu|\, t \left\{ \sum_{\nu=1}^{r} \frac{|u'_\nu|}{a} + 1 \right\}^{\overline{n+1-r}} < 1+\varepsilon', \text{ avec } \left(\frac{n+1}{2r}\right)^{\overline{n+1-r}} (1-\varepsilon') < \sum_{\nu=r+1}^{n+1} |u'_\nu|\, t < 1+\varepsilon',$$

et

$$\sum_{\nu=1}^{r} \frac{|u''_\nu|}{a} + \frac{2^{\overline{n+1-r}}\, r^{\overline{n+1-r}}\,(n+1-r) \sum_{\nu=r+1}^{n+1} |u''_\nu|\, t}{(n+1)^{\overline{n+1-r}}} < 1+\varepsilon', \text{ avec } \sum_{\nu=r+1}^{n+1} |u''_\nu|\, t < \left(\frac{n+1}{2r}\right)^{\overline{n+1-r}} (1+\varepsilon')$$

ou

$$\sum_{\nu=r+1}^{n+1} |u''_\nu|\, t \left\{ \sum_{\nu=1}^{r} \frac{|u''_\nu|}{a} + 1 \right\}^{\overline{n+1-r}} < 1+\varepsilon', \text{ avec } \left(\frac{n+1}{2r}\right)^{\overline{n+1-r}} (1-\varepsilon') < \sum_{\nu=r+1}^{n+1} |u''_\nu|\, t < 1+\varepsilon'.$$

Nous remarquons que l'égalité: $x'_\nu = x''_\nu$ n'est pas valable pour tous les $\nu = 1, \ldots, n+1$. Car alors d'après (6) on aurait aussi $z'_\nu = z''_\nu$ pour tous les $\nu = 1, \ldots, n+1$, et les points spéciaux $(z'_1, \ldots, z'_{n+1})$ et $(z''_1, \ldots, z''_{n+1})$ ne seraient pas différents. Il y a donc au moins une valeur de ν $(1 \leqq \nu \leqq n+1)$, qui vérifie l'inégalité:

$$x'_\nu \neq x''_\nu. \quad . \quad . \quad . \quad . \quad . \quad . \quad . \quad . \quad . \quad (22)$$

Si nous posons

$$X_\nu = x_\nu' - x_\nu'', \quad L_\nu = L_\nu' - L_\nu'' \qquad (\nu = 1, \ldots, n+1),$$

nous avons d'après (6) et (22):

$$L_\nu = u_\nu' - u_\nu'' \qquad (\nu = 1, \ldots, n+1), \quad . \quad . \quad . \quad . \quad . \quad . \quad (23)$$

$$X = max.\,(|X_1|, \ldots, |X_{n+1}|) \geqq 1.$$

Maintenant nous déduisons les inégalités:

$$\sum_{\nu=1}^{r} |L_\nu| < (2+\delta)\,a, \quad . \quad . \quad . \quad . \quad . \quad . \quad . \quad . \quad (24)$$

$$\sum_{\nu=r+1}^{n+1} |L_\nu| < \frac{2+\delta}{t}, \quad . \quad . \quad . \quad . \quad . \quad . \quad . \quad . \quad (25)$$

$$\left(\sum_{\nu=1}^{r} |L_\nu|\right)^r \cdot \left(\sum_{\nu=r+1}^{n+1} |L_\nu|\right)^{n+1-r} < \frac{(1+\delta)^{n+1}\,a^r}{t^{n+1-r}}. \quad . \quad . \quad (26)$$

En vertu de (23) l'inégalité (25) suit de (17) immédiatement, puisque d'après (16) $2\,\varepsilon'$ est inférieur à δ.

Pour la démonstration de (24) et 26 nous distinguons trois cas différents.

1. Supposons que les inégalités (18) et (20) valent. Alors on obtient par soustraction:

$$\sum_{\nu=1}^{r} \frac{|L_\nu|}{a} + \frac{2^{\frac{n+1}{n+1-r}}\, r^{\frac{r}{n+1-r}}\,(n+1-r)\sum_{\nu=r+1}^{n+1} |L_\nu|\,t}{(n+1)^{\frac{n+1}{n+1-r}}} < 2 + 2\varepsilon' < 2 + \delta$$

d'après (16), et de cette inégalité il suit d'abord (24).

Selon le théorème de la moyenne géométrique et la moyenne arithmétique on en déduit en outre:

$$\left(\sum_{\nu=1}^{r} \frac{|L_\nu|}{a}\right)^r \left(\frac{r\,2^{\frac{n+1}{n+1-r}}\, r^{\frac{r}{n+1-r}} \sum_{\nu=r+1}^{n+1} |L_\nu|\,t}{(n+1)^{\frac{n+1}{n+1-r}}}\right)^{n+1-r} < \left(\frac{r\,(2+2\varepsilon')}{n+1}\right)^{n+1},$$

d'où

$$\left(\sum_{\nu=1}^{r} \frac{|L_\nu|}{a}\right)^r \left(\sum_{\nu=r+1}^{n+1} |L_\nu|\,t\right)^{n+1-r} < (1+\varepsilon')^{n+1} < (1+\delta)^{n+1}$$

d'après (16); ainsi (26) est démontré.

2. Supposons que les inégalités (18) et (21) valent [11]). On a donc

$$\sum_{\nu=1}^{r} \frac{|u_\nu'|}{a} < 1 - \frac{2^{\frac{n+1}{n+1-r}}\, r^{\frac{r}{n+1-r}}\,(n+1-r)\sum_{\nu=r+1}^{n+1} |u_\nu'|\,t}{(n+1)^{\frac{n+1}{n+1-r}}} + \varepsilon',$$

$$\sum_{\nu=1}^{r} \frac{|u_\nu''|}{a} < \left(\frac{1+\varepsilon'}{\sum_{\nu=r+1}^{n+1} |u_\nu''|\,t}\right)^{\frac{n+1-r}{r}} - 1,$$

[11]) Le cas où (19) et (20) valent se rend facilement à celui-ci.

et alors d'après (23):

$$\sum_{\nu=1}^{r} \frac{|L_\nu|}{a} < \left(\frac{1+\varepsilon'}{\sum_{\nu=r+1}^{n+1} |u_\nu''|\, t} \right)^{\frac{n+1-r}{r}} - \frac{2^{\frac{n+1}{n+1-r}} r^{\frac{r}{n+1-r}} (n+1-r) \sum_{\nu=r+1}^{n+1} |u_\nu'|\, t}{(n+1)^{\frac{n+1}{n+1-r}}} + \varepsilon'. \quad (27)$$

En vertu de (21) il suit de (27) immédiatement:

$$\sum_{\nu=1}^{r} \frac{|L_\nu|}{a} < \left(\frac{2r}{n+1} \right) \left(\frac{1+\varepsilon'}{1-\varepsilon'} \right)^{\frac{n+1-r}{r}} + \varepsilon' < 2 + 7\varepsilon' < 2 + \delta$$

d'après (16); ainsi (24) est démontré. Nous posons

$$\sum_{\nu=r+1}^{n+1} |u_\nu'|\, t = p \left(\frac{n+1}{2r} \right)^{\frac{r}{n+1-r}} (1+\varepsilon'); \quad \sum_{\nu=r+1}^{n+1} |u_\nu''|\, t = q \left(\frac{n+1}{2r} \right)^{\frac{r}{n+1-r}} (1-\varepsilon').$$

Alors nous avons d'après (18) et (21):

$$0 \leqq p < 1, \quad 1 < q < \frac{1+\varepsilon'}{1-\varepsilon'} \left(\frac{2r}{n+1} \right)^{\frac{r}{n+1-r}} < 2^{\frac{n+1}{n+1-r}} \quad . \quad . \quad (28)$$

et d'après (23):

$$\sum_{\nu=r+1}^{n+1} |L_\nu|\, t \leqq (p+q) \left(\frac{n+1}{2r} \right)^{\frac{r}{n+1-r}} (1+\varepsilon'). \quad . \quad . \quad . \quad (29)$$

Alors nous pouvons écrire pour (27):

$$\sum_{\nu=1}^{r} \frac{|L_\nu|}{a} < \frac{2r}{n+1} \cdot \frac{1}{q^{\frac{n+1-r}{r}}} \cdot \left(\frac{1+\varepsilon'}{1-\varepsilon'} \right)^{\frac{n+1-r}{r}} - \frac{2p(n+1-r)}{n+1} (1+\varepsilon') + \varepsilon'$$

ou

$$\sum_{\nu=1}^{r} \frac{|L_\nu|}{a} < \frac{2r}{(n+1)\, q^{\frac{n+1-r}{r}}} - \frac{2p(n+1-r)}{n+1} + 7\varepsilon'. \quad . \quad . \quad (30)$$

d'après $q > 1$ et (16). En vertu de

$$\frac{1}{q^{\frac{n+1-r}{r}}} - \frac{1}{(p+q)^{\frac{n+1-r}{r}}} \leqq \frac{(n+1-r)\, p}{r\, q^{\frac{n+1}{r}}},$$

on obtient

$$\frac{2r}{(n+1)\, q^{\frac{n+1-r}{r}}} < \frac{2(n+1-r)\, p}{n+1} + \frac{2r}{(n+1)(p+q)^{\frac{n+1-r}{r}}}$$

d'après $q > 1$, donc

$$\frac{2r}{(n+1)\, q^{\frac{n+1-r}{r}}} - \frac{2p(n+1-r)}{n+1} < \frac{2r}{(n+1)(p+q)^{\frac{n+1-r}{r}}}.$$

Il suit de (30):

$$\sum_{\nu=1}^{r} \frac{|L_\nu|}{a} < \frac{2r}{(n+1)(p+q)^{\frac{n+1-r}{r}}} + 7\varepsilon',$$

et donc en vertu de (29)

$$\sum_{\nu=1}^{r} \frac{|L_\nu|}{a} < \frac{(1+\varepsilon')^{\frac{n+1-r}{r}}}{\left(\sum_{\nu=r+1}^{n+1} |L_\nu|\, t\right)^{\frac{n+1-r}{r}}} + 7\varepsilon',$$

ou (d'après (28) et (16)):

$$\left(\sum_{\nu=1}^{r} \frac{|L_\nu|}{a}\right)\left(\sum_{\nu=r+1}^{n+1} |L_\nu|\, t\right)^{\frac{n+1-r}{r}} < (1+\varepsilon')^{\frac{n+1-r}{r}} + 7\varepsilon'(p+q)^{\frac{n+1-r}{r}}\left(\frac{n+1}{2r}\right)(1+\varepsilon')^{\frac{n+1-r}{r}}$$

$$< (1+\varepsilon')^{\frac{n+1-r}{r}}\left\{1 + 7\varepsilon'\left(2 \cdot 2^{n+1-r}\right)^{\frac{n+1-r}{r}}\right\} < (1+\delta)^{\frac{n+1-r}{r}}(1+\delta) = (1+\delta)^{\frac{n+1}{r}}$$

et par cela (26) est démontré.

3. Supposons que les inégalités (19) et (21) valent. On a donc:

$$\sum_{\nu=1}^{r} \frac{|u'_\nu|}{a} < -1 + \left(\frac{1+\varepsilon'}{\sum_{\nu=r+1}^{n+1} |u'_\nu|\, t}\right)^{\frac{n+1-r}{r}} \text{ et } \sum_{\nu+1}^{r} \frac{|u''_\nu|}{a} < -1 + \left(\frac{1+\varepsilon'}{\sum_{\nu=r+1}^{n+1} |u''_\nu|\, t}\right)^{\frac{n+1-r}{r}};$$

donc d'après (23):

$$\sum_{\nu=1}^{r} \frac{|L_\nu|}{a} < \left(\frac{1+\varepsilon'}{\sum_{\nu=r+1}^{n+1} |u'_\nu|\, t}\right)^{\frac{n+1-r}{r}} + \left(\frac{1+\varepsilon'}{\sum_{\nu=r+1}^{n+1} |u''_\nu|\, t}\right)^{\frac{n+1-r}{r}} - 2. \quad (31)$$

En vertu de (19) et (21) il suit de (31) immédiatement:

$$\sum_{\nu=1}^{r} \frac{|L_\nu|}{a} < \left(\frac{4r}{n+1}\right)\left(\frac{1+\varepsilon'}{1-\varepsilon'}\right)^{\frac{n+1-r}{r}} - 2 < 2 + 12\varepsilon' < 2 + \delta$$

d'après (16); ainsi (24) est démontré. Posons maintenant

$$\sum_{\nu=r+1}^{n+1} |u'_\nu|\, t = p_1\left(\frac{n+1}{2r}\right)^{\frac{r}{n+1-r}}(1-\varepsilon'); \sum_{\nu=r+1}^{n+1} |u''_\nu|\, t = q_1\left(\frac{n+1}{2r}\right)^{\frac{r}{n+1-r}}(1-\varepsilon'), \quad (32)$$

avec $p_1 > 1$, $q_1 > 1$, $p_1 \geqq q_1$ (on peut supposer la dernière inégalité sans nuire à la généralité). Il suit de (23) et (32):

$$0 < \sum_{\nu=r+1}^{n+1} |L_\nu|\, t \leqq (p_1 + q_1)\left(\frac{n+1}{2r}\right)^{\frac{r}{n+1-r}}(1-\varepsilon'), \quad (33)$$

et de (31) et (32):

$$\sum_{\nu=1}^{r} \frac{|L_\nu|}{a} < \left(\frac{1}{p_1^{\frac{n+1-r}{r}}} + \frac{1}{q_1^{\frac{n+1-r}{r}}} \right) \frac{2r}{n+1} \left(\frac{1+\varepsilon'}{1-\varepsilon'} \right)^{\frac{n+1-r}{r}} - 2. \quad . \quad (34)$$

En vertu de (17) et (23) il suit encore:

$$0 < \sum_{\nu=r+1}^{n+1} |L_\nu| t < 2(1+\varepsilon'). \quad . \quad . \quad . \quad . \quad . \quad . \quad (35)$$

Parce que

$$\frac{1}{p_1^{\frac{n+1-r}{r}}} - \frac{1}{(p_1+q_1)^{\frac{n+1-r}{r}}} \leqq \frac{(n+1-r)\,q_1}{r\,p_1^{\frac{n+1}{r}}} \leqq \frac{n+1-r}{r\,q_1^{\frac{n+1-r}{r}}}$$

(d'après $p_1 \geqq q_1$), on a en vertu de $q_1 > 1$ et (33):

$$\frac{1}{p_1^{\frac{n+1-r}{r}}} + \frac{1}{q_1^{\frac{n+1-r}{r}}} \leqq \frac{1}{(p_1+q_1)^{\frac{n+1-r}{r}}} + \frac{n+1}{r\,q_1^{\frac{n+1-r}{r}}}$$

$$< \frac{1}{\left(\sum_{\nu=r+1}^{n+1} |L_\nu| t \right)^{\frac{n+1-r}{r}}} \cdot \frac{n+1}{2r} (1-\varepsilon')^{\frac{n+1-r}{r}} + \frac{n+1}{r},$$

et d'après (34) et (16):

$$\sum_{\nu=1}^{r} \frac{|L_\nu|}{a} < \frac{1}{\left(\sum_{\nu=r+1}^{n+1} |L_\nu| t \right)^{\frac{n+1-r}{r}}} (1+\varepsilon')^{\frac{n+1-r}{r}}$$

$$+ 2 \left(\frac{1+\varepsilon'}{1-\varepsilon'} \right)^{\frac{n+1-r}{r}} - 2 < \frac{(1+\varepsilon')^{\frac{n+1-r}{r}}}{\left(\sum_{\nu=r+1}^{n+1} |L_\nu| t \right)^{\frac{n+1-r}{r}}} + 6\varepsilon',$$

donc:

$$\left(\sum_{\nu=1}^{r} \frac{|L_\nu|}{a} \right) \left(\sum_{\nu=r+1}^{n+1} |L_\nu| t \right)^{\frac{n+1-r}{r}} < (1+\varepsilon')^{\frac{n+1-r}{r}} + 6\varepsilon' \left(\sum_{\nu=r+1}^{n+1} |L_\nu| t \right)^{\frac{n+1-r}{r}}$$

$$< (1+\varepsilon')^{\frac{n+1-r}{r}} \left(1 + 6\varepsilon' \cdot 2^{\frac{n+1-r}{r}} \right) < (1+\delta)^{\frac{n+1-r}{r}} (1+\delta) = (1+\delta)^{\frac{n+1}{r}},$$

en vertu de (34) et (16). Ainsi, dans ce cas l'inégalité (26) est démontrée. Nous avons donc démontré qu'à tout nombre δ positif, arbitraire au moins un système de nombres entiers $(X_1, \ldots X_{n+1})$ avec $X \geqq 1$, (24), (25) et (26) correspond; ainsi en vertu de (12) et de la définition de $\varrho_{r,n}$ les inégalités (1a), (2a), et (3a) de la deuxième communication sont démontrées dans le cas A, c'à.d. pour $\frac{n+1}{2} \leqq r \leqq n+1$.

B. Supposons maintenant $1 \leqq r < \frac{n+1}{2}$. Alors nous considérons dans l'espace R'_{n+1} l'ensemble S'', défini par les inégalités:

$$\sum_{\nu=1}^{r} |u_\nu| < b$$

$$\sum_{\nu=r+1}^{n+1} |u_\nu|\, t + \frac{2^{\frac{n+1}{r}} (n+1-r)^{\frac{n+1-r}{r}} r \sum_{\nu=1}^{r} \frac{|u_\nu|}{b}}{(n+1)^{\frac{n+1}{r}}} < 1, \text{ si } \sum_{\nu=1}^{r} \frac{|u_\nu|}{b} \leqq \left(\frac{n+1}{2(n+1-r)}\right)^{\frac{n+1-r}{r}},$$

$$\sum_{\nu=1}^{r} \frac{|u_\nu|}{b} \left\{ \sum_{\nu=r+1}^{n+1} |u_\nu|\, t + 1 \right\}^{\frac{n+1-r}{r}} < 1, \text{ si } \left(\frac{n+1}{2(n+1-r)}\right)^{\frac{n+1-r}{r}} < \sum_{\nu=1}^{r} \frac{|u_\nu|}{b} < 1,$$

avec

$$b = \sqrt[r]{\frac{t^{n+1-r}\,\triangle}{\varrho_{n,\,n+1-r}}}. \quad \ldots\ldots\ldots \quad (36)$$

Soit le volume de S'' désigné par V''. Par la transformation

$$u_\nu = b\,t\; u^*_{\nu+n+1-r} \quad (\nu = 1, \ldots, r), \quad u_\nu = \frac{1}{b\,t}\, u^*_{\nu-r} \quad (\nu = r+1, \ldots, n+1),$$

l'ensemble S'' est transformé en l'ensemble S^*, défini par:

$$\sum_{\nu=n+2-r}^{n+1} |u^*_\nu|\, t < 1$$

$$\sum_{\nu=1}^{n+1-r} \frac{|u^*_\nu|}{b} + \frac{2^{\frac{n+1}{r}} (n+1-r)^{\frac{n+1-r}{r}} r \sum_{\nu=n+2-r}^{n+1} |u^*_\nu|\, t}{(n+1)^{\frac{n+1}{r}}} < 1, \text{ si } \sum_{\nu=n+2-r}^{n+1} |u^*_\nu|\, t \leqq \left(\frac{n+1}{2(n+1-r)}\right)^{\frac{n+1-r}{r}}$$

$$\sum_{\nu=n+2-r}^{n+1} |u^*_\nu|\, t \left\{ \sum_{\nu=1}^{n+1-r} \frac{|u^*_\nu|}{b} + 1 \right\}^{\frac{n+1-r}{r}} < 1, \text{ si } \left(\frac{n+1}{2(n+1-r)}\right)^{\frac{n+1-r}{r}} < \sum_{\nu=n+2-r}^{n+1} |u^*_\nu|\, t < 1.$$

Appliquant le lemme 6 avec $n+1-r$ au lieu de $r\left(n+1-r > \frac{n+1}{2}\right)$ et b au lieu de a, nous trouvons que l'ensemble S^* possède le volume

$$V^* = \frac{b^{n+1-r}\,\varrho_{n,\,n+1-r}}{t^r}.$$

Comme le déterminant D de la transformation est égal à $\frac{1}{b^{n+1-2r}\,t^{n+1-2r}}$, on trouve (d'après (36)):

$$V'' = D\,V^* = \frac{b^r\,\varrho_{n,\,n+1-r}}{t^{n+1-r}} = \triangle.$$

De la même manière de laquelle nous avons appliqué le lemme 4 à l'ensemble S', nous l'appliquons à S'', et nous utiliserons les mêmes désignations pour la translation (14), les points $(z'_1, \ldots, z'_{n+1})$, $(z''_1, \ldots, z''_{n+1})$; $(u'_1, \ldots, u'_{n+1})$, $(u''_1, \ldots, u''_{n+1})$; $(x'_1, \ldots, x'_{n+1})$, $(x''_1, \ldots, x''_{n+1})$ et les formes $L'_1, \ldots, L'_{n+1}$ et $L''_1, \ldots, L''_{n+1}$. En outre nous choisissons ε' avec (16). L'application du lemme 4 nous donne

$$\sum_{\nu=1}^{r} |u'_\nu| < (1+\varepsilon')\,b. \quad \sum_{\nu=1}^{r} |u''_\nu| < (1+\varepsilon')\,b,$$

et en outre

$$\sum_{\nu=r+1}^{n+1} |u'_\nu|\, t + \frac{2^{\frac{n+1}{r}} (n+1-r)^{\frac{n+1-r}{r}}\, r \sum_{\nu=1}^{r} \frac{|u'_\nu|}{b}}{(n+1)^{\frac{n+1}{r}}} < 1+\varepsilon', \text{ avec } \sum_{\nu=1}^{r} \frac{|u'_\nu|}{b} < \left(\frac{n+1}{2(n+1-r)}\right)^{\frac{n+1-r}{r}} (1+$$

ou

$$\sum_{\nu=1}^{r} \frac{|u'_\nu|}{b} \left\{ \sum_{\nu=r+1}^{n+1} |u'_\nu|\, t+1 \right\}^{\frac{n+1-r}{r}} < 1+\varepsilon', \text{ avec } \left(\frac{n+1}{2(n+1-r)}\right)^{\frac{n+1-r}{r}} (1-\varepsilon') < \sum_{\nu=1}^{r} \frac{|u'_\nu|}{b} < 1+\varepsilon',$$

et

$$\sum_{\nu=r+1}^{n+1} |u''_\nu|\, t + \frac{2^{\frac{n+1}{r}} (n+1-r)^{\frac{n+1-r}{r}}\, r \sum_{\nu=1}^{r} \frac{|u''_\nu|}{b}}{(n+1)^{\frac{n+1}{r}}} < 1+\varepsilon', \text{ avec } \sum_{\nu=1}^{r} \frac{|u''_\nu|}{b} < \left(\frac{n+1}{2(n+1-r)}\right)^{\frac{n+1-r}{r}} (1+\varepsilon$$

ou

$$\sum_{\nu=1}^{r} \frac{|u''_\nu|}{b} \left\{ \sum_{\nu=r+1}^{n+1} |u''_\nu|\, t+1 \right\}^{\frac{n+1-r}{r}} < (1+\varepsilon'), \text{ avec } \left(\frac{n+1}{2(n+1-r)}\right)^{\frac{n+1-r}{r}} (1-\varepsilon') < \sum_{\nu=1}^{r} \frac{|u''_\nu|}{b} < 1+\varepsilon'$$

Il est clair que c'est impossible que $x'_\nu = x''_\nu$ pour toutes les valeurs de $\nu = 1, .., n+1$. Posons $X_\nu = x'_\nu - x''_\nu$, $L_\nu = L'_\nu - L''_\nu$ $(\nu = 1, .., n+1)$; nous avons donc

$$L_\nu = u'_\nu - u''_\nu \quad (\nu = 1, \ldots, n+1), \quad X = max.(|X_1|, \ldots, |X_{n+1}|) \geqq 1.$$

Toute de la même manière de laquelle nous avons démontré (24), (25) et (26), nous pouvons démontrer les inégalités:

$$\sum_{\nu=1}^{r} |L_\nu| < (2+\delta)\, b, \qquad \sum_{\nu=r+1}^{n+1} |L_\nu| < \frac{2+\delta}{t},$$

$$\left(\sum_{\nu=1}^{r} |L_\nu|\right)^r \left(\sum_{\nu=r+1}^{n+1} |L_\nu|\right)^{n+1-r} < \frac{(1+\delta)^{n+1}\, b^r}{t^{n+1-r}}.$$

Nous nous en reposons sur le lecteur de démontrer ces inégalités. En vertu de (36) et de la définition de $\varrho^*_{n,r}$ par ceci les inégalités (1a), (2a) et (3a) de la deuxième communication sont démontrées pour $1 \leqq r < \frac{n+1}{2}$. D'après la remarque chez le lemme 1. ce lemme est donc démontré complètement.

§ 2. *Remarque sur la rédaction du Théorème 1.*

Nous remarquons que l'évaluation de l'intégrale P_{ll} à l'aide des changements successives de l'ordre d'intégration mène à une expression pour le nombre $\varrho_{n,r}$, défini dans le théorème 1, un peu moins compliquée que celle donnée dans la première communication. Nous trouvons

$$\varrho_{n,r} = \frac{2^{n+1}}{(n+1)!} \left\{ \frac{1}{r^r} \sum_{\mu=0}^{r} \binom{n+1}{\mu} \left(r - \frac{n+1}{2}\right)^\mu (n+1-r)^{r-\mu} + \right.$$

$$\left. + \frac{r(n+1)}{n+1-r} \binom{n}{r} \sum_{\mu=r+1}^{\infty} \frac{1}{\mu\, r^\mu} \left(r - \frac{n+1}{2}\right)^\mu \right\} \qquad \left(\frac{n+1}{2} \leqq r \leqq n\right).$$

Biochemistry. — *Complexcoacervation in the presence of buffers and of non-electrolytes, preventing gelatination.* By H. G. BUNGENBERG DE JONG and E. G. HOSKAM. (Communicated by Prof. H. R. KRUYT.)

(Communicated at the meeting of March 28, 1942.)

1. *Introduction.*

The complex coacervation of purified gelatine and gum arabic was previously studied in detail at 40°, the pH desired of the two isohydric sols being brought about by the addition of HCl, (resp. acetic acid) [1]).

So for the preparation of isohydric sols the determination of pH titration curves of the two stock sols should precede. The purpose of the following investigation is to see whether the characteristic properties of the complex coacervation (a.o. intensity of the coacervation as a function of the mixing proportion of the two isohydric sols, and the occurrence of the double valence rule on neutralization of the complex coacervation with neutral salts) are retained:

A. When buffers are used to regulate the pH,

B. When the investigation is carried out at room temperature in the presence of well-chosen non-electrolytes which prevent gelatination.

2. *Complex coacervation with buffered sols.*

In choosing a buffer we must bear in mind that the buffer salt, like any other salt, has a neutralizing effect on the complex coacervation. As the intensity of the neutralizing effect depends on the valence of the two ions — increasing with equal concentration (in m. aeq. p. L.) as the valence is higher — a buffer will preferably be selected in which there are only monovalent ions. For that reason acetate buffers were used in what follows. But since the neutralizing effect of a salt increases with the concentration of the salt, we shall have to arrange the buffers in such a way that for the variation of the pH the acetic acid concentration only is varied, that of the Na-acetate remaining constant. As the complex coacervation gelatine + gum arabic is already neutralized at 30 to 40 m. aeq. NaCl, we must choose the Na-acetate final concentration considerably lower. In what follows we choose 10 m. aeq. p. L. which is achieved by adding to 10 cc stock sol 5 cc buffer in which the Na-acetate conc. is 30 m. aeq. p. L.

The following tables give the pH of some sols buffered in this way (measurements with the H electrode at 40° C.).

The stock sols were prepared by dissolving 5 gr. airdry colloid preparation in 250 cc dist. water (further indicated as "2 % stock sol"). Next a series of buffer mixtures was prepared, consisting of 30 cc Na-acetate 0.1 N + a cc acetic acid 2 N + (70—a) dist. water.. Besides the mixtures of 10 cc stock sol + 5 cc buffer we measured mixtures of the composition of 10 cc dist. water + 5 cc buffer. The upper half of the table refers to purified colloid preparations, the lower half to unpurified preparations [2]). The results of the first series are pictured in Fig. 1.

---

[1]) H. G. BUNGENBERG DE JONG and W. A. L. DEKKER. Kolloid Beihefte **43**, 143 (1935); **43**, 213 (1936).

[2]) Gelatine F00 extra of the "Lijm- en Gelatinefabriek 'Delft' " at Delft. Gum arabic: Gomme Senegal petite boule blanche I of ALLAND et ROBERT Paris: Na-nucleinicum e faece of E. MERCK. For the purification of these preparations see for isoelectric gelatine Kolloid Beihefte, **43**, 256 (1936); for Na-Arabinate and Na-Nucleinate Kolloid Beihefte **47**, 260 resp. 257 (1938).

a	pH				△ pH		
	Blank	Na Arabinate	Isoelectr. gelatine	Na Nucleinate	Na Arabinate	Isoelectr. gelatine	Na Nucleinate
2.5	4.43	4.47	4.53	4.71	+0.04	+0.10	+0.28
4	4.24*	4.28	4.35	4.50	+0.04	+0.11	+0.26
10	3.86	3.93	4.00	4.13	+0.07	+0.14	+0.27
25	3.49*	3.57	3.65*	3.76	+0.08	+0.16	+0.27
60	3.13	3.24	3.31	3.40	+0.09	+0.18	+0.27
	Blank	Gum Arabic	Gelatine	Na Nucleinicum	Gum Arabic	Gelatine	Na Nucleinicum
2.5	4.42	4.42	4.52	4.66	0	0.10	+0.24
4	4.23*	4.22	4.34	4.46	−0.01	+0.11	+0.23
10	3.86	3.87	4.00	4.11	+0.01	+0.14	+0.25
25	3.49*	3.53	3.65	3.74	+0.04	+0.16	+0.25
60	3.12	3.19	3.30	3.38	+0.07	+0.18	+0.26

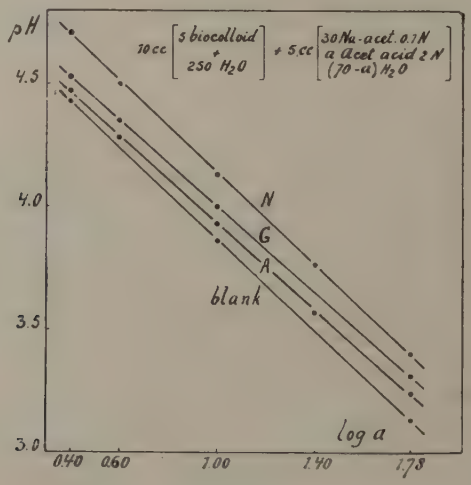

Fig. 1.

In the last three columns of the table are indicated the pH differences between the buffered sols and the buffer by itself (blank), showing that with the colloid concentration chosen here and the concentrations of the buffer components the pH of the nucleinate sols deviates most, that of the gelatine deviates less and that of the arabinate sols less again. With the relatively small final concentration of the Na-acetate these deviations are not surprising, but as has been said above it is not very well possible to increase them more, since then (at least in the gelatine-arabinate combination) the complex coacervation is too much neutralized. Better buffering can of course be obtained by choosing lower colloid concentrations.

When for instance the concentration of the stock sols is chosen 10 × smaller, the △ pH of the arabinate sols in the entire pH section will be less than 0.01 and the △ pH of the gelatine sols will also remain below 0.02. With such diluted sols it is also very well possible to demonstrate the characteristic features of the complex coacervation (e.g. with turbidity measurements), but this is not suitable for the method we have in mind

(measurement of the coacervate volume). The coacervate volume which is then separated from, for instance, 15 cc total system, becomes then very small, and for accurate measuring we should have to make use of sedimentation tubes of unpractical sizes (e.g. 150 cc).

For the purpose of investigation therefore, we have to compromise, viz. that with the simple method of experimentation the sols prepared with 10 m. aeq. acetate buffer are not exactly isohydric, but that the pH of the gelatine sol is ca. 0.1 higher than that of the arabinate sol.

Here then we can start from the two buffered sols, mixing them in different mixing proportions, or the watery sols are mixed in different mixing proportions and the buffer is added later. The first method is applied in § 4. Fig. 2 shows the results obtained by the second method (coacervate volumes noted after one night in the thermostat at 40°): a cc 2 % A (or N) + (10—a) cc 2 % G + 5 cc buffer, in which A, N and G represent the purified gelatine, Na-arabinate and Na-nucleinate preparations, the buffer consisting of 30 cc Na-acetate 0.1 N + 25 cc acetic acid 2 N added in a 100 cc measuring flask adding dist. water up to the mark.

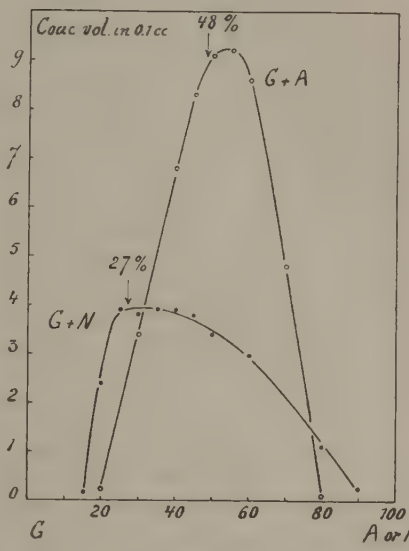

Fig. 2.

From Fig. 1 we find graphically for the pH of the corresponding unmixed sols: arabinate = 3.57, gelatine = 3.65, Na-nucleinate = 3.76. Arrows in the figure indicate the location of the electrophortically determined points of reversal of charge (48 % A in the combination G + A resp. 27 % N in the combination G + N).

As appears from Fig. 2 the points of reversal of charge do not lie exactly at, but to the left of the maximum, the coacervates on the left ascending curve branches are therefore charged positively, on the right descending branches the charge is negative.

The two curves in Fig. 2 differ in two ways, namely:

1. There is much less nucleinate (27 % N) than arabinate (48 % A) needed for the charge compensation of the gelatine.

2. The maximal coacervate volume in the G + N combination is much smaller than in the G + A combination (the waterpercentage of the G + N coacervate is much lower).

These differences are caused by the fact that the nucleinate is a colloid of much denser charge (smaller equivalent weight) than the arabinate.

In what follows we shall restrict ourselves to the complex coacervation gelatine-arabinate. The analogous combination gelatine-nucleinate is less suitable for demonstrating purposes, as here the waterpercentage of the coacervate is much lower and the coalescence of the drops to a perfectly clear layer of liquid takes place with some difficulty. Moreover there is in this combination the complication that with pH reduction of the nucleinate sol nucleine acid may form. Hence the buffered sols are clear only above ca. pH 3.7, below it they are slightly or more pronouncedly opalescent to very turbid as the pH is taken lower.

3. *Prevention of gelatination at room temperature.*

It is also possible to realize the complex coacervation at room temperature, when we see to it that there is a sufficient concentration of suitable non-electrolytes which prevent gelatination. This is a.o. possible with urea, the final concentration of which must then

be over ca. 16 %. In the presence of this it is possible to demonstrate the typical features of the complex coacervation at room temperature.

Urea however, has the following drawbacks:

1. The coacervate drops coalesce very slowly, so that a cohering coacervate layer is formed very slowly;

2. Urea has a marked "swelling" effect on the coacervate in consequence of which on the one hand the section of mixing proportions in which coacervation occurs is relatively small, on the other hand the complex coacervate is neutralized at much smaller salt concentrations than without urea. The great sensitiveness to salt therefore prevents the application here of diluted buffers to regulate the pH.

For our purposes we should dispose of a non-electrolyte which exclusively prevents gelatination and has neither a swelling, nor a condensing effect on the complex coacervate. We do not know such a substance, but we can make shift with a suitably chosen mixture of two gelatination-preventing substances, the one of which (urea) having a swelling, the other a condensing effect. The phenols generally belong to the latter category.

With a pH which is sufficiently removed from the i.e.p. of the gelatine the purpose is achieved with e.g. 10 % urea + 4 % resorcinol, in which the condensing effect of the resorcinol entirely destroys the swelling effect of the urea, so that with respect to the blank experiment (i.e. without urea + resorcinol; at 40°) the coacervates are even in a slightly condensed condition. Hence the coacervate drops rapidly coalesce and the layer is soon formed, the coacervation extends over a broad section of mixing proportions and the coacervates are evidently more resistent to neutral salts than at 40° without urea + resorcinol. Owing to the fact that the resorcinol effect becomes stronger as we approach the i.e.p. of the gelatine, resorcinol + urea are not suitable for a study of the complex coacervation in which we vary the pH systematically.

Here follow some experiments demonstrating the "opening" effect of urea and the "condensing", effect of phenols. In both cases we used stock sols of the following composition: 5 g gelatine + 6 g gum arabic + 190 cc dist. water.

In Fig. 3 A and B the composition of the mixtures for the series at 40° was a cc HCl 0.1 N + (7.5—a) cc H_2O + 5 cc stock sol. For the series at room temperature we used a stock sol prepared from the original one by adding 50 cc stock sol to 25 g urea placed in a 100 cc measuring flask, adding dist. water up to the mark. With this new stock sol mixtures were made as follows:

a cc HCl 0.1 N + (2.5—a) cc H_2O + 10 cc stock sol,

so that the final volume (12.5) cc and the colloid final concentrations were as great as in the series without urea at 40°. Fig. 3 gives the coacervate volumes after 1 night as functions of the added quantity of HCl, Fig. 3 B giving these volumes as functions of the pH measured with the H electrode.

The increase of the maximal coacervate volume and the little viscous character of the coacervate (demonstrated by tilting the sedimentation tubes) point to an "opening" effect of the urea (i.e. to a decrease of the colloid concentration in the coacervate). As additional effect there is shifting of the peak from pH 3.7 to ca. 4.0. Possibly this additional effect is to be ascribed to the HCl binding to urea which increases as the pH values become lower. Although urea is only a very weak base ($K = 1.5 \times 10^{-14}$), we can yet in our final concentration (20 % urea) reckon with the presence of some tenths of m. aeq. p. L. of urea hydrochlorid at pH 4, at pH 3 this is even some m. aeq. p. L. If in this case, as with any salts we assume a neutralizing effect, this effect increases in the direction of lower pH's and this may be one of the causes of the peak of the coacervate volume curve shifting to a higher pH.

Fig. 3 C gives the effect of some phenols on the coacervate volume at 40° C. Here we used a buffer:

(100 cc Na-acetate 0.1 N + 100 cc acetic acid 1 N + 800 cc H_2O),

the composition of the mixtures being:

a cc 0.5 mol "phenol" dissolved in buffer + (10—a) cc buffer + 5 cc stock sol (5 g + 6 A + 190 H_2O).

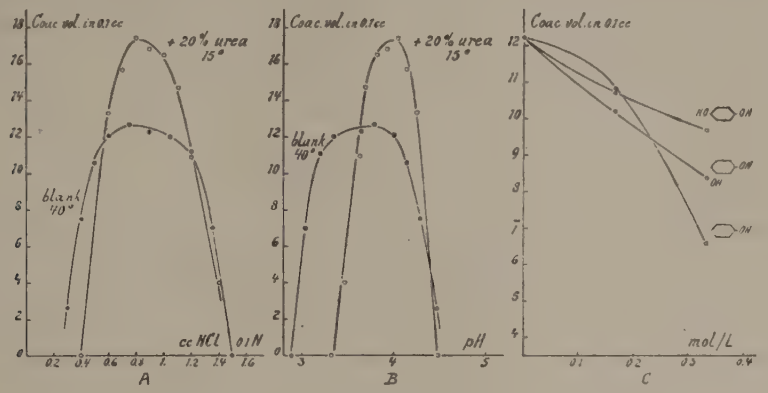

Fig. 3.

Fig. 3 C gives the results for phenol, hydrochinon and resorcinol. Also with the other phenols investigated (the effect of pyrocatechol is ca. that of resorcinol, of pyrogallol and phloroglucinol it is a little stronger, at least when the final concentration is smaller) we find: decrease of the coacervate volume and more difficult coalescibility of the coacervate drops to a clear coacervate layer. The two effects are attributable to "condensation" of the coacervate (i.e. "increase" of the colloid concentration in the coacervate). In agreement with this is also the increasing viscosity of the coacervate layer (seen when the sedimentation tubes are tilted).

4. *Simple experiments concerning complex coacervation at 40° with buffers.*

A. *Complex coacervation in an approximately isohydric mixing series.*

We first prepare a buffer by placing 200 cc Na-acetate 0.1 N + 100 cc acetic acid 2 N in a measuring flask, adding water to 1000 cc. Next we prepare separately a 4% gelatine sol (G) and a 4% gum arabic sol (A).

Now the two "isohydric" sols are prepared, by mixing:

1 vol. 4% G + 1 vol. buffer
resp. 1 vol. 4% A + 1 vol. buffer.

The two buffered sols are now filled in burettes (the one containing gelatine in a burette surrounded by a wider glass tube, filled with water of 40° C.). 4, 6, 8, 9, 10, 11, 12, 14 and 16 cc of the buffered gum arabic sol are then placed in a number of sedimentation tubes, which are then placed in a stand in the thermostat of 40° in order to heat them to the right temperature, after which 16, 14, 12, 11, 10, 9, 8, 6 and 4 cc of the buffered gelatine sol is added to them. After mixing we again place the tubes in the thermostat and after 5 minutes they are again well shaken. After some time coacervate layers begin to form in the central section and after 3 hours the coacervate volumes can already be noted. See Table and Fig. 4 A.

Electrophoretic measurements (last column of the table) show that on the left ascending branch of the curve the coacervates are positively and on the right descending branch negatively charged. The reversal of charge is here again at a mixing proportion of 50% A, while by constructing a bisecting line the maximum of the coacervate volume curve is found to be at 51.5% A. So here we find the same as in § 2 with purified

colloids: The reversal of charge is not exactly at but slightly to the left of the maximum of the coacervate volume curve.

cc A	cc G	% A	Coac. vol. in 0.1 cc (after 3 hrs.)	pH Measured (40°)	U (40°) (arbitrary units)
—	—	0 (100 % G)	—	3.70	—
4	16	20	0.3	—	—
6	14	30	7.0	—	—
8	12	40	13.6	3.75	+ 90
9	11	45	15.8	—	+ 56
10	10	50	17.4	3.76	+ 0
11	9	55	16.0	—	— 83
12	8	60	15.1	3.75	—122
14	6	70	9.0	—	—
16	4	80	1.2	—	—
—	—	100	—	3.82	—

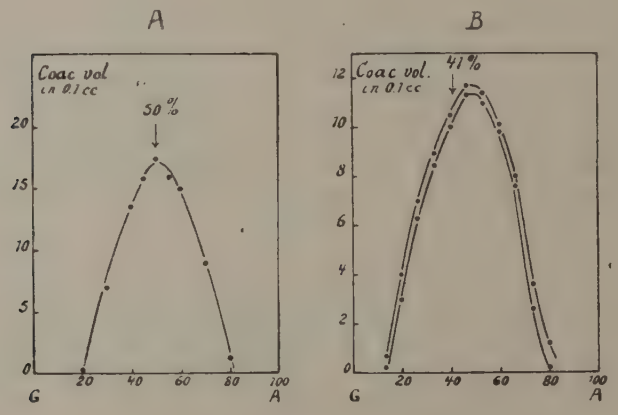

Fig. 4.

B. *Double valence rule on the neutralization of the complex coacervation with neutral salts.*

We shall here restrict ourselves to the neutralization of the coacervation with neutral salts at the optimal mixing proportion. When again we choose the final concentration of the colloids as 2 % and the Na-acetate final concentration 10 m. aeq. p. L., this is the mixing proportion of 50 % as is seen from A. In order to have sufficient space for the neutral salts added we proceed as follows: we prepare a buffer by placing 300 cc Na-acetate 0.1 N + 150 cc acetic acid 2 N in a measuring flask, distilled water is added till 1000 cc ("30 m. aeq. acetate buffer"). Then we make a mixed sol by dissolving 3 g gum arabic together with 3 g gelatine in 100 cc dist. water ("6 % A + G sol").

In sedimentation tubes we now place each time 5 cc salt solution of varying strength, then 5 cc "30 m. aeq. acetate buffer" and then 5 cc "6 % A + G sol". In these final mixtures, as in A, the Na-acetate concentration is then 10 m. aeq. p. L. and the colloid final concentration is 2 %, the mixing proportion of the two colloids being 50 %. Fig. 5 A shows the result after 1½ hours at 40°.

It is true that the sedimentation is then not yet complete, the layers growing ca. 0,03 cc

after one night, but the general character of the curve bundles does not undergo a change [1]).

So we see that the double valence rule applies to the neutralization of the complex coacervation: i.e. the salt concentrations necessary for achieving the coacervate volume = 0 (complete neutralization) are the smaller as with equal valence of the anion (monovalent) the valence of the cation increases, similar, with equal valence of the cation (monovalent) the valence of the anion increases. So the neutralizing effect decreases from left to right in following series:

$$\begin{matrix} 3-1 > 2-1 > 1-1 \\ 1-3 > 1-2 > 1-1 \end{matrix} \quad \text{"double valence rule"}$$

5. *Simple experiments concerning complex coacervation at room temperature.*

A. *Complex coacervation in an approximately isohydric mixing series.*

In each of two measuring glasses of 250 cc we put 25 g urea + 10 g resorcinol. As described in 4. we now prepare buffered gum arabic and buffered gelatine sols, adding the first to one measuring glass and the second to the other until 250 cc. We mix and leave them to cool to room temperature. The two sols are now filled in burettes and a mixing series is begun with them. Fig. 4 B gives the result after 1½ hours and after 22 hours at room temperature. The arrow indicates the location of the point of reversal of charge, determined electrophoretically. Here again we see what we noted in 3 and 4: the reversal (here at 41 % A) is near but before the maximum (here 48.5 % A) of the coacervate volume curve. As regards 3 and 4 the reversal and the maximum of the curve have both shifted to lower values of the mixing proportion. This is partly accounted for by the higher pH (compare § 2 in which we saw that in the presence of urea the pH is 0.3 higher). We could not measure any constant potential differences with the H electrode (presence of resorcinol?) so that the glass electrode had to be used. With this we found: 100 % G = 4.07; 25 % A = 4.04; 50 % A = 4.01; 75 % A = 3.96; 100 % A = 3.92.

Hence the pH difference of the two approximately isohydric sols (= 0.15) was found to be of the order expected.

Remark.

The peak of the coacervate volume curve was 11.3 after 1½ hours, after 5 hours it was 11.6 and after 22 hours 11.7. In 4 A on the other hand we found 17.4. This difference is partly due to the different final volumes of the mixtures (in 4 A = 20 cc, here 15 cc) and to the fact that in preparing the buffered sols containing urea + resorcinol the colloid concentration had fallen below 2 %.

The decrease of the concentration we can calculate approximately from the s.g. of urea (= 1.335) and resorcinol (1.283). 25 g urea and 10 g resorcinol occupy a volume of (25 : 1.335) + (10 : 1.283) = 19 + 7.8 = 26.8 cc. This makes the colloid concentration (250—26.8) : 250 = 0.89 × the original one. When the two causes are taken into account the colloid final concentration is here 0.75 × 0.89 = 0.67 of the one in 4 A, so that the maximal coacervate volume must be 0.67 × 17.3 = 11.6, which is very near the values found. From this general agreement it is seen that with the concentration chosen of urea and resorcinol the volume diminishing effect of the resorcinol and the volume-

---

[1]) The mixtures and coacervates with $K_3Fe(CN)_6$ are bluish green after one night, but this colour is not so pronounced after 1½ hours. Here we have an additional effect (oxidizing effect of $K_3Fe(CN)_6$ on the gelatine). This complication may be avoided by using $K_3CH(SO_3)_3$, the K salt of methane trisulfonic acid, which however is not so strongly neutralizing as $K_3Fe(CN)_6$, but still stronger than K_2SO_4.

increasing effect of the urea (see § 3) with the pH chosen, do indeed approximately compensate each other.

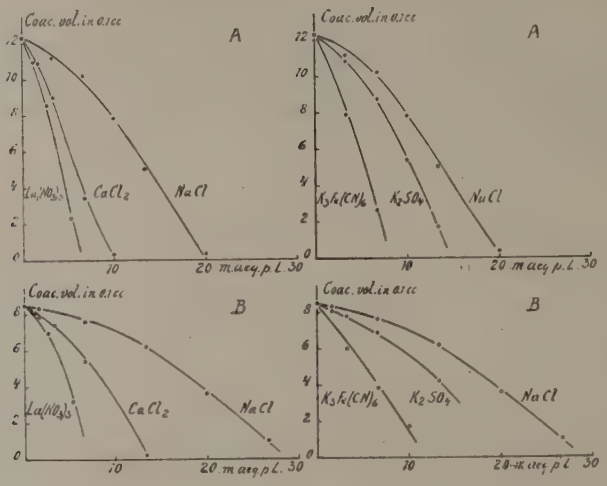

Fig. 5.

B. *Double valence rule on the neutralization of the complex coacervation with neutral salts.*

In a measuring glass of 200 cc we place 60 g urea + 24 g resorcinol, adding "6% A + G sol" (of § 4 B) until 200 cc. Further we proceed in the same way as in 4 B, namely we again make mixtures: 5 cc salt solution + 5 cc buffer + 5 cc solmixture (containing urea + resorcinol). The results after 3 hours are pictured in Fig. 5 B. Here again we see the typical occurrence of the double valence rule:

$$3-1 > 2-1 > 1-1$$
$$1-3 > 1-2 > 1-1$$

After one night the coacervate volumes have only become a little greater, but the general character of the curve bundles remains unchanged. When we compare this experimental series with the on in 5 A we see that the neutralization by neutral salts takes place here at greater concentrations than at 40° without urea + resorcinol. At any rate the condensing resorcinol has compensated or possibly overcompensated the swelling effect of urea (which heightens the sensitiveness to salts when urea only is present). The question in how far the difference in temperature (40°—18°) affects the sensitiveness to salts remains, of course, unanswered.

Summary.

1. When studying complex coacervation it is possible to make use of diluted acetate buffers. When the effect of the pH is to be studied buffers are indicated with constant Na-acetate concentration (e.g. 10 m. aeq. p. L.) and varied acetic acid concentration.

2. Urea and resorcinol in sufficiently high concentrations neutralize the gelatination of gelatine sols. With them the complex coacervation of gelatine + gum arabic is also possible at room temperature. The strong additional effects of urea ("opening") and resorcinol (strongly condensing) however prevent their application.

3. The opening effect of 10% urea is practically compensated by the condensing effect of 4% resorcinol.

4. Simple experiments at 40° with buffers, and at room temperature with buffers + urea + resorcinol are indicated for the purpose of demonstrating some properties of the complex coacervation.

Leiden, Laboratory for Medical Chemistry.

Biochemistry. — *On flocculation and reversal of charge of negative biocolloids through alkaloid salts and basic stains.* III. By H. G. BUNGENBERG DE JONG and C. V. D. MEER. (Communicated by Prof. H. R. KRUYT.)

(Communicated at the meeting of May 30, 1942.)

1. *Introduction.*

In previous communications we discussed the reversal of charge of a number of biocolloids through four alkaloid salts [1]).

The order of decreasing affinity (increasing reversal of charge concentration) in which these four organic cations arrange themselves:

chinine > strychnine > novocaine > guanidine

appeared to be independent of the composition of the ionogenic group of the biocolloids (phosphate-, sulphate-, carboxylcolloids).

In this investigation we have occupied ourselves with flocculations of biocolloids whether or not occurring with alkaloids and we shall show in how far statistics concerning flocculation can give us a preliminary impression of the order of decreasing affinity for a much greater number of organic cations. The order obtained will be checked in a few instances by electrophoretic measurements. It will be further seen that such statistics also allow of conclusions as regards different tendencies of the biocolloids to flocculation in dependence of the composition of the ionogenic group of the biocolloid.

2. *The autocomplex nature of the flocculation negative biocolloid + alkaloid cation.*

In the first named publication we discussed the fact that the flocculation of negative biocolloids with alkaloid cations is of an autocomplex nature. Analogously with the autocomplex flocculation with anorganic cations [2]) it is to be expected that the change that a given alkaloid causes flocculation will increase: *A.* as the reversal of charge takes place at smaller concentration, *B.* as the colloid possesses a greater charge density.

This is as a matter of fact, indicated by the behaviour of the biocolloids studied in the

TABLE 1. Flocculability of negative biocolloids with 4 alkaloid salts.

Alkaloid salt	Na-Carraghene	K-Chondroitine sulphate	Na-Yeast nucleinate	Soybean phosphatide alcohol insoluble	Na-Pectinate	Na-Arabinate	Soybean phosphatide alcohol soluble	Egg. lecithin
Chinine Cl	+	+	+	+	−	−	−	−
Strychnine Cl	+	+	+	−	−	−	−	−
Novocaine Cl	+	−	−	−	−	−	−	−
Guanidine Cl	−	−	−	−	−	−	−	−
$\frac{10^3}{\text{R.H.N.}}$ of the Colloid anion	4.65	3.92	3.62	1.28	0.98	0.95	0.25	0.05

previous communication towards the four alkaloids used there: see table I, in which + means that the sol will flocculate, — that the soll will remain clear.

---

[1]) H. G. BUNGENBERG DE JONG and J. G. WAKKIE, I Biochem. Z. **297**, 70 (1938); II Biochem. Z. **297**, 221 (1938).

[2]) H. G. BUNGENBERG DE JONG and P. H. THEUNISSEN, I Kolloid Beihefte **47**, 254 (1938), II **48**, 33 (1938).

In the table the alkaloid chlorides are placed below each other in the order of increasing reversal of charge concentration (decreasing affinity) the biocolloids in the order of the charge density decreasing from left to right. So the regularity mentioned under A and B finds expression in Table I in the fact that the combinations in which there is flocculation are found in a triangular field of the table.

3. *Statistics concerning the flocculation of a greater number of biocolloids through a greater number of alkaloid chlorides.*

When we have at our disposal more extensive statistics concerning the flocculation of a greater number of biocolloids through a greater number of alkaloid chlorides, we can collect the results in a table analogous to Table I. We must then see to it that the alkaloids are placed below each other in such a way that the number of times that flocculation occurs in a horizontal row decreases from top to bottom (in Table I chinine-chloride 4 ×; strychnine chloride 3 ×; novocaine-chloride 1 ×; guanidine chloride 0 ×).

In this way we must then find the series of decreasing affinity of the alkaloid cations for the negative biocolloids.

Table II gives the results of such an investigation of the flocculation power. In two points it differs from Table I: A.) we have not exclusively arranged the biocolloids according to charge density decreasing from left to right, but we have combined this arrangement with the one according to the composition of the ionogenic groups. B.) We have used a greater number of qualifications than only flocculation power (+) or absence of flocculation power (—).

Ad A. The reason why in the table we have divided the biocolloids into 3 groups will be discussed in § 5.

Ad. B. Although it seems an easy matter to determine through qualitative experiments whether a biocolloid will flocculate with an alkaloid chloride, it is not simple, because besides the very evident cases of flocculation and perfect clearness, all transitional stages possible were observed (slight turbidity, weak and very weak opalescence).

The following signs are used in the table:

++	evident flocculation or marked turbidity
+	slight turbidity [1])
?	slight opalescence
??	very slight opalescence
—	perfect clearness of the sol.

On arranging the alkaloids in the order of Table II we have taken this into account. Therefore we gave marks to each of these notations and these were added in each horizontal row. We counted ++ as 4; + (+) = 3; + = 2; ? = 1 and ?? and — = 0. The "flocculation power" (fl.p.) thus obtained for each alkaloid is given directly after the name in Table II. From top to bottom the alkaloids in this table are arranged according to decreasing flocculation power. As a few combinations, namely those marked with an asterisk in the table, have not been tested, the order may have slightly changed. As we shall see, the absence of some data does not affect our final conclusion.

Here follow some details about the method applied in determining the qualifications mentioned (++, +, ?, ??). In so far as the sols used in the experiments are formed by simple solution in cold, resp. boiling (agar) water, they were prepared from the purified colloid preparations described previously [2]).

We used 1 % sols of Na-yeast nucleinate, Na-arabinate and Na-pectinate; 0.5)% sols of Na-agar and chondroitine sulphate: A 0.25 % sol of Na-pectate; A 0.2 % sol of Na-semen-line-mucilage and A 0.1 % sol of Na-carraghene. The phosphatide sols used

---

[1]) In a few cases we have used +(+) as a qualification, signifying a case between ++ and +.

[2]) H. G. BUNGENBERG DE JONG and P. H. THEUNISSEN, Koll. Beihefte, loc. cit. I.

TABLE II.

Alkaloid-chloride	Fl. P.	Phosphate colloids: Na-Yeast nucleinate	Soybean phosphatide alcohol non-soluble	Soybean phosphatide alcohol soluble	Egg-lecithin	Fl. P.	Sulphate colloids: Na-Carraghene	K-Chondroitine sulphate	Na-agar	Fl. P.	Carboxyl colloids: Na-Pectate	Na-Semen Lini mucilage	Na-pectinate	Na-Arabinate	Fl.P.
Aeth.hydrocupr.	26	++	++	—	?	9	+(+)	++	+	9	++	+	+	—	8
Papaverine	26	++	++	—	—	8	++	++	+	10	+	++	+	—	8
Chinine	23	++	++	—	?	9	++	++	+	10	++	—	—	—	4
Narcotine	23	++	?	—	+	7	++	++	—	8	++	+	+	—	8
Apomorphine	22	++	++	—	—	8	+	++	—	6	++	++	—	—	8
Hydrastine	18	++	*	?	?	6	++	++	*	8	++	—	—	—	4
Thebaine	20	++	++	—	—	8	++	++	—	8	+	+	—	—	4
Brucine	18	++	*	—	—	4	++	++	—	8	++	+	—	—	6
Pantocaine	16	++	*	—	—	4	+	++	*	6	++	+	—	—	6
Emetine	14	++	++	—	—	8	??	++	—	4	+	—	—	—	2
Strychnine	14	++	??	—	—	4	++	++	—	8	+	—	—	—	2
Tropacocaine	10	++	+	??	—	6	++	—	—	4	—	—	—	—	0
Heroine	8	++	*	—	—	4	+	+	—	4	—	—	—	—	0
Aethylmorphine	7	+(+)	—	—	—	3	++	—	—	4	—	—	—	—	0
$N(CH_3)_4$	6	++	*	+	—	6	—	—	*	0	—	—	—	—	0
Tutocaine	6	+	??	—	—	2	++	—	—	4	—	—	—	—	0
Morphine	6	++	—	—	—	4	+	—	—	2	—	—	—	—	0
Eucaine	5	+	—	—	—	2	(+(+)	—	—	3	—	—	—	—	0
Cocaine	4	??	—	—	—	0	++	—	—	4	—	—	—	—	0
Cotarnine	4	+	—	—	—	2	+	—	*	2	—	—	—	—	0
Alypine	4	—	??	—	—	0	++	—	—	4	—	—	—	—	0
Novocaine	4	—	—	—	—	0	++	—	—	4	—	—	—	—	0
Stovaine	3	?	??	—	—	1	+	—	—	2	—	—	—	—	0
Codeine	2	??	—	—	—	0	+	—	—	2	—	—	—	—	0
Scopolamine (Br)	1	—	—	—	—	0	?	—	—	1	—	—	—	—	0
Homotropine (Br)	1	—	—	—	—	0	?	—	—	1	—	—	—	—	0
Ephedrine	0	—	*	—	—	0	—	—	—	0	—	—	—	—	0
Hydrastinine	0	??	*	—	—	0	—	—	*	0	—	—	—	—	0
Guanidine	0	—	—	—	—	0	—	—	*	0	—	—	—	—	0
Pilocarpine	0	—	—	—	—	0	—	—	—	0	—	—	—	—	0
Acetylcholine	0	—	—	—	—	0	—	—	—	0	—	—	—	—	0
$\frac{10^3}{\text{R. H. N.}}$ of the colloid anion		3.62	1.28	0.25	0.05		4.65	3.92	0.45		5.46	1.84	0.98	0.95	
Flocculability of biocolloids with alkaloid salts		70	27	3	5		74	46	6		36	18	6	0	

were the same as in communications I (soybean phosphatide alcohol soluble) and II (soybean phosphatide alcohol non-soluble and egg-lecithin).

In judging the flocculation power we used three methods:

A. A drop of sol and a drop of cold-saturated solution of the alkaloid chloride were placed side by side on an objectglass and a covering glass was carefully placed on it. The contact zone of the two drops was then examined microscopically. When floccules, fibrils or coacervate drops are observed we mark this biocolloid-alkaloid chloride combination ++.

For with a positive result of the microscopic examination the experiments described sub B and C are also markedly positive. In the table the qualification+(+) occurs three times, namely where with A a slightly positive result was obtained while by B and C the result was markedly positive.

In some cases one can also place crystals of the alkaloid-chlorides in the undiluted sol and in their vicinity look for the occurrence of floccules, fibrils or coacervate drops.

B. Sol and saturated alkaloid chloride solution are mixed in test tubes in different proportions and the occurrence of flocculation, turbidity resp. opalescence is noted with transmitted light. When there was slight but evident turbidity, as with method C, while a negative result was obtained by method A, we marked the combination+. When with method B there is a slight or very slight opalescence we marked the combination ? resp. ??.

C. We proceed as in B with this difference that crystals of the alkaloid chloride are added to the undiluted sol. Usually C gives the same result as B, so that method C need only be applied when with B the result was ? resp. ??.

Finally we remark that the experiments with agar were made at a higher temperature (over 40°), in order to prevent disturbances in consequence of gelatination. In the experiment by A we used an electrically heated microscope table, by B and C a thermostat of 50°.

4. *Electrophoretic measurements for control of the alkaloid order of Table II.*

Table II is drawn up in analogy with Table I. The flocculation power as regards the 11 biocolloids examined decreases from top to bottom in the table. So we may expect that the order of the alkaloids thus found will also be the one in which the reversal of charge concentration of the average biocolloid will increase. For the sake of control we determined with a number of alkaloids the reversal of charge concentrations for a sol of alcohol-soluble soybean phosphatide (Table III), while we also measured the reversal of charge concentrations for SiO_2 powder (Table IV). In these tables are also given the values taken from Table II for the flocculation power as regards all 11 biocolloids and as regards the group of the biocolloids belonging to the object examined electrophoretically (phosphate colloids in the case of Table III) or which from an electrochemical point of view may be considered related (sulphate colloids in the case of Table IV) [1].

In both tables the alkaloids have been arranged according to increasing reversal of charge concentrations, i.e. according to decreasing affinity of the alkaloid cation for the negatively charged ionized group. So we must expect this also to be the order in which they are found in Table II. In how far this is true may at once be seen from the figures in Tables III and IV of the flocculation power, which must decrease from top to bottom. We see then that on the whole this expectation has become true. The slight deviations do not disappear when we view the flocculation power as regards the group of bio-

---

1) The reversal of charge "spectre" of SiO_2 shows the characteristics of the sulphate colloids. The analogous spectre of TiO_2 shows similarity with that of the carboxyl-colloids) (see H. G. BUNGENBERG DE JONG and P. H. THEUNISSEN, loc. cit. II, p. 88—90). We also tried to measure the reversal of charge of TiO_2 with alkaloid salts, but the results were very irregular. (Rapid change of the electrophoretic velocity in course of time), so that we had to abandon this plan.

colloids which one would in the first place consider in this respect, and not as regards all 11 biocolloids.

But naturally there are so many possible sources of errors, e.g. in consequence of the scale of appreciation used, that in spite of the deviations we may be satisfied. Hence we

TABLE III.

Reversal of charge with soybean phosphatide soluble in alcohol with different alkaloid salts.

Alkaloid-chloride	log C (C=reversal of charge conc.)	Flocculation power	
		all colloids	phosphate colloids
Aethylhydro-cupreine	0.05—3	26	9
Apomorphine	0.21—3	25	8
Chinine	0.39—3 0.22—3 [1]	23	9
Papeverine	0.73—3	26	8
Thebaine	0.96—3	20	8
Narcotine	0.07—2	22	7
Strychnine	0.24—2 0.22—2 [1]	14	4
Brucine	0.46—2	18	4
Heroine	0.63—2	8	4
Aethyl-morphine	0.87—2	7	3
Morphine	0.02—1	6	4
Codeine	0.18—1	2	0
Novocaine [1]	0.36—1	4	0
Guanidine [1]	0.74—1	0	0

[1] Value taken from Communication I.

TABLE IV.

Reversal of charge of SiO_2 particles with different alkaloid salts.

Alkaloid-chloride	log C (C=reversal of charge conc.)	Flocculation power	
		all colloids	sulphate coll.
Apomorphine	0.03—3	25	8
Papaverine	0.41—3	26	10
Aethylhydro-cupreine	0.72—3	26	9
Chinine	0.76—3	23	10
Thebaine	0.87—3	20	8
Brucine	0.89—3	18	8
Narcotine	0.04—2	22	8
Strychnine	0.31—2	14	8
Heroine	0.44—2	8	4
Cotarnine	0.54—2? [1]	4	2
Tropacocaine	0.73—2? [2]	10	4
Aethyl-morphine	0.84—2	7	4
Morphine	0.91—2	6	2
Novocaine	0.89—2 [3]	4	4
Codeine	0.94—2	2	2
Scopolamine (Br)	0.15—1	1	1
Pilocarpine	0.26—1	0	0
Guanidine	0.01 [3]	0	0

[1] The electrophoresis velocity here changed fairly rapidly in course of time, hence the value log C = 0.54 — 2 is very uncertain.

[2] Owing to changes of the electrophoresis velocity in course of time, the value log C = 0.73 — 2 is uncertain.

[3] Value taken from Communication II.

conclude that the order of decreasing affinity following from the flocculation statistics is on the whole confirmed by electrophoretic measurements.

5. *Connection between flocculation power of the biocolloids, their charge density and the composition of their ionogenic groups.*

Table I clearly shows the connection between flocculability and charge density of the biocolloid. As the density is greater there is flocculation with alkaloid cations which are further to the right in the affinity order of the alkaloids chinine > strychnine > novocaine > guanidine.

With the analogous autocomplex flocculation with anorganic cations it seems that with less extensive statistic material the charge density of the biocolloids is the predominant factor. But with more extensive statistic material it appears that the composition of the ionogenic groups of the biocolloid is also an important factor [1]).

Of the alkaloids it can also be said that if with the more extensive statistic material of Table II we had arranged the biocolloids exclusively according to charge density decreasing from left to right, there would be nothing left of the connection between charge density and flocculability, which seems so evident in Table I. For then we should get the following values for the flocculability with charge density decreasing from left to right:

36 — 74 — 46 — 80 — 18 — 27 — 6 — 0 — 6 — 3 — 5.

The connection between charge density and flocculability, however, is evident in Table II, where we have divided the biocolloids into three groups according to the composition of the ionized groups.

Within each division the connection between charge density and flocculability is very evident.

When we set out graphically the values of the "flocculability" (indicated in Fig. 1 as Fl and mentioned at the bottom of the columns in Table II) as function of the charge density and then connect with each other the points belonging to the phosphate colloids, likewise of the sulphate colloids and again those of the carboxyl colloids, we get Fig. 1, which shows what we have discussed above:

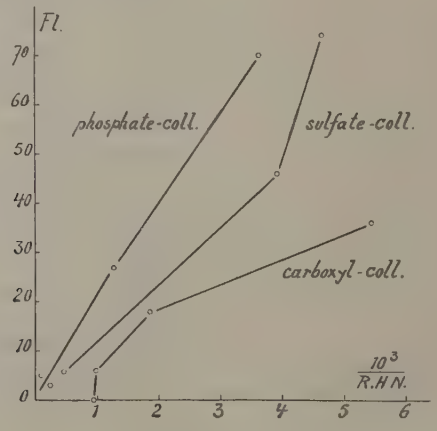

Fig. 1.

A. of each of the three groups of biocolloids it may be said that the flocculability increases with increasing charge density;

B. with equal charge density a phosphate colloid has greater flocculability than a sulphate colloid, and the latter than a carboxylcolloid.

The order: phosphate colloid > sulphate colloid > carboxylcolloid is different from the order found with the inorganic cations. This difference is possibly owing to the fact that with inorganic cations the polarizability of the ionized groups of the biocolloid plays a part, with the great organic cations (see Communication II) there is no question of polarization of the ionized groups of the biocolloid. The order phosphate colloid > carboxylcolloid > sulphate colloid found for the inorganic cations is therefore the one of decreasing polarizability power of the ionized groups. The cause of the order found here with the great organic cations cannot yet be indicated.

---

[1]) H. G. BUNGENBERG DE JONG and P. T. THEUNISSEN, loc. cit. I, p. 307.

6. *Connection between structure of the alkaloid cations and place in the affinity series.*

In Tables III and IV we have included a number of nearly related alkaloids, which are important for the problem of the connection between structure of the alkaloid cation and place in the affinity series. It is the following:

apomorphine > thebaine > heroine > aethylmorphine > morphine > codeine

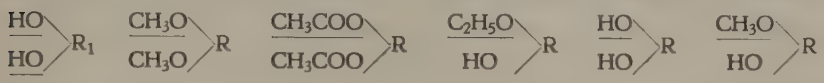

The order of which is the same for reversal of charge of the phosphatide and of SiO_2.

In the schematic structure formulae given we have underlined the phenolhydroxyl of morphine and the CH_3O—, C_2H_5O—, resp. CH_3COO groups each time taking its place, the alcoholic hydroxyl in morphine resp. the groups corresponding with it, on the other hand, have not been underlined.

With apomorphine, where the ring skeleton is slightly different (hence R_1 instead of R) there are two phenolhydroxyles in the molecule.

For the explanation of the order found it seems plausible to start from the assumption that the introduction of a hydroxyl group will decrease the affinity. On substitution of these hydrophile groups by the much less hydrophile CH_3O—, C_2H_5O—resp. CH_3COO groups the affinity must increase again. On the ground of this assumption the order thebaine > heroine > aethylmorphine > morphine can be accounted for, but it is not explained why the reversal of charge of codeine takes place with higher concentrations than of morphine, nor why apomorphine is found entirely on the left side of the affinity series. The facts allow of explanation however, when it is assumed that exclusively *an alcoholic hydroxyl has a weakening effect on the affinity, whereas the effect of a phenol hydroxyl is strengthening.*

We shall further use the results of a previous systematic investigation of L. THEUNISSEN VAN ZIJP [1]) from which it was seen that when a carbon chain is lengthened the affinity increases. This is evident for instance in the series aethylmorphine > codeine.

On methylating morphine to codeine the affinity decreases, which we explain as follows: the introduction of CH_3 has two effects: increase of the affinity owing to the introduction of the CH_3 group itself and decrease of the affinity owing to the elimination of the phenolhydroxyl, the latter effect preponderating.

In morphine, codeine and aethylmorphine there is still the greatly weakening alcoholic hydroxylgroup. Elimination of the latter by methylation, resp. acetylation causes a strong increase of the affinity.

All this explains to us the order:

thebaine resp. heroine > aethylmorphine > morphine > codeine,

but we cannot answer the question why methylation has a greater effect than acetylation [2]).

Finally the distinction we have made between alcoholic and phenolhydroxyls also accounts for the position on the extreme left in the affinity series of apomorphine. For both hydroxyl groups are here phenolhydroxyls.

7. *Significance of charge density and chemical composition of the ionized groups of negative biocolloids for their flocculation with stain cations.*

With the same 11 biocolloids we made an analogous investigation of the flocculation power with 14 basic stains (preparations of Messrs. Dr. G. GRÜBLER). The stains examined (with the number of their flocculation power in brackets) were: nile blue (40), toluidinblue (40), trypaflavin (40), indulin scharlach rot (36), neutral red (36), methy-

---

1) L. THEUNISSEN VAN ZIJP, Dissertation, Leiden 1939.

2) Possibly the acetylgroup is more hydrophile than the methoxylgroup.

lene blue (35), crystal violet (33), pyronine (30), auramin (28), chrysoidine (28), fuchsine (28), methylgreen (20), brilliant green (20), malachite green (20).

The same regularities discussed in detail in Table II are also expressed in this statistic material.

We shall first consider the values for the flocculability of the biocolloids:

Phosphate colloids: yeast nucleinate (56) soybean phosphatide, alcohol nonsoluble (56) soybean phosphatide alcohol soluble (44) egglecithin (9).

Sulphate colloids: Na-carraghene (56), K chondtroitin sulphate (56) Na-agar (4).

Carboxyl colloids: Na-pectate (54), Na-semen lini mucilage (42), Na-arabinate (34), Na-pectinate (23).

It is true that here too we see the connection — so clear in Table II — between decreasing flocculability and decreasing charge density, but this can no longer find expression between the two phosphate colloids mentioned first and between the two sulphate colloids mentioned first which all four are marked 56. This is owing to the much greater affinity of the stain cations than the alkaloid cations for the biocolloids. As these four biocolloids flocculate strongly with all the stains examined (= 4), they obtain the maximal value of 56 (= 14 × 4).

When the values of the flocculability are set out against the charge density of the biocolloids in the same way in Fig. 1, we again obtain the order: phosphate colloid > sulphate colloid > corboxyl colloid.

Summary.

1. The flocculation (coacervation resp.) of negatively charged biocolloids with alkaloid cations, resp. stain cations is of an autocomplex nature. It is to be expected that from more extensive statistic material concerning the flocculability of a number of biocolloids by a number of alkaloids, resp. stains, conclusions can be drawn in a general way as to the affinity order of these cations.

2. The statistic material necessary is given (flocculability of 11 biocolloids with 31 alkaloids and 14 basic stains).

3. The resulting affinity order is checked by some electrophoretic measurements and is on the whole found correct.

4. The tendency to flocculation of the biocolloids with alkaloids, resp. stains increases with increasing charge density of the colloid anion, it is moreover dependent on the chemical composition of the ionized groups of the biocolloid:

phosphate group > sulphate group > carboxyl group.

5. It would seem that from the affinity order:

apomorphine > thebaine > heroine > aethylmorphine > morphine > codeine

it follows that the affinity of the alkaloid cation for the biocolloid anion is diminished by an alcoholic hydroxyl group, but is increased by a phenolhydroxyl.

Leiden, Laboratory for Medical Chemistry.

Biochemistry. — *Lipophile protein-oleate coacervates and the effect on them of alcohols.* By H. G. BUNGENBERG DE JONG and C. H. BOOY–VAN STAVEREN. (Communicated by Prof. H. R. KRUYT.)

(Communicated at the meeting of May 30, 1942.)

1. *Introduction, lipophile protein-oleate coacervates.*

Oleate and phosphatide coacervates are very sensitive to various organic compounds[1]). They cause either "condensation" (increase of the colloid percentage) or "opening" (decrease of the colloid percentage). When we restrict ourselves to the homologous series of the n-primary alcohols, it is seen that the first terms (methyl-, aethyl-, propylalcohol) have an "opening" ("swelling") effect, whereas the higher terms (butyl, amylalcohol) have a "condensing" effect (which at a great excess may pass into a swelling effect). As the carbon chain is longer these effects become evident at smaller concentrations. To the question what sort of colloid systems can take part in the protoplasm membrane, the physiological fact is significant that here again applies that as the carbon chain is longer, the effect (e.g. increase of the permeability) with successive terms of a homologous series (e.g. alcohols, ketones, urethanes) occurs with ever smaller concentrations. In contradistinction to the above lipophile coacervates, however, there is no change in the character of the effects on progression in the homologous series.

In the following pages a new sort of lipophile coacervates is discussed with which the effect of the alcohols also occurs with ever smaller concentration as we choose a higher term of the homologous series, but with which there is no change in the quality of the effect (swelling).

This sort of coacervates is formed when K salts are added to a suitably chosen mixture of gelatine and oleatesol. The K concentration necessary is much slighter than is necessary for the coacervation of each of the sols separately, which points to a strong mutual effect of the two colloids. The separating coacervates contain oleate as well as gelatine. The former is indicated by the marked lipophily, the latter by the power to gelatinize on cooling.

For this coacervation it is necessary that the pH is not too low (with pH $<$ ca. 8.7 it does not take place). In what follows we use one salt (K tetraborate) in order to bring about the pH required (e.g. ac. 9.2), as well as the K-ion concentration necessary.

The mechanism and the properties of the gelatine-oleate coacervates we mean to discuss in due time.

2. *Effect of n-primary alcohols on the coacervation.*

In order more carefully to observe the effect of alcohols, briefly mentioned in the above, we measured the coacervate volume at 40°, starting from a stock sol, obtained by mixing equal volumes of a 6% isoelectric gelatine sol[2]) and a 6% Na-oleate sol[3]). Further we kept a stock-solution of $\frac{1}{2}$ mol K biborate p. L. (19.5 g to 100 cc) and solutions of a certain percentage of methyl-, aethyl- and propylalcohol. In sedimentation tubes we made mixtures of the following composition:

---

[1]) H. G. BUNGENBERG DE JONG and coöperators, Protoplasma **28**, 329, 498, 543 (1937) **29**, 481, 536 (1938) **30**, 1, 53, 206 (1938); S. ROSENTHAL, Dissertation, Leiden 1939.

[2]) Obtained by purifying (Kolloid Beihefte **43**, 213 (1936) (see footnote on page 256) of gelatine F00 extra of the Lijm- en Gelatinefabriek "Delft" at Delft.

[3]) Na-oleinicum medicinale pur. pulv. of E. MERCK, Darmstadt.

5 cc K biborate 0.5 mol + a cc alcoholsolution + (5—a) cc dist. water + 5 cc stock sol.

With the higher homologues of the alcohols we followed another method, after we had ascertained that it yielded reproducible results. The difficulty is that soon the solubility in water becomes so slight that the quantity of alcohol required can no longer be introduced into the system by this way. We prepare mixtures of 5 cc K biborate 0.5 mol + 5 cc dist. water + 5 cc stock sol, adding a certain number of the alcohol drops from a slowly dripping microburette. We then also determined the volume in cc of 40—60 alcohol drops, so that from this and from the s.g. we can calculate the weight of one drop of the alcohol.

With this method of dosage we practically work no longer with constant final volume, but the volume of the quantity of alcohol added maximally (ca. 0.25 cc) is slight in proportion to the total volume of the mixture, so that we may neglect this increase.

After having added the fixed number of alcohol drops we must repeatedly vigorously shake the mixture until the alcohol added has completely dissolved. We close the sedimentation tube with a rubber stop, shake a few minutes vigorously, place the tube a few moments in the thermostat, shake again and repeat this process several times. Especially with the highest terms: heptyl and actylalcohol the solution is a fairly slow process. The coacervated mixtures are left during the night in the thermostat and the next morning the coacervate layers are read with a pocket lens through the window of the thermostat. Usually the coacervate layer is denser than the equilibrium liquid and is therefore at the bottom of the calibrated narrower tube at the lower end of the sedimentation tube. In a few series however it happened — e.g. at the peak of the amyl alcohol curve in Fig. 1 —

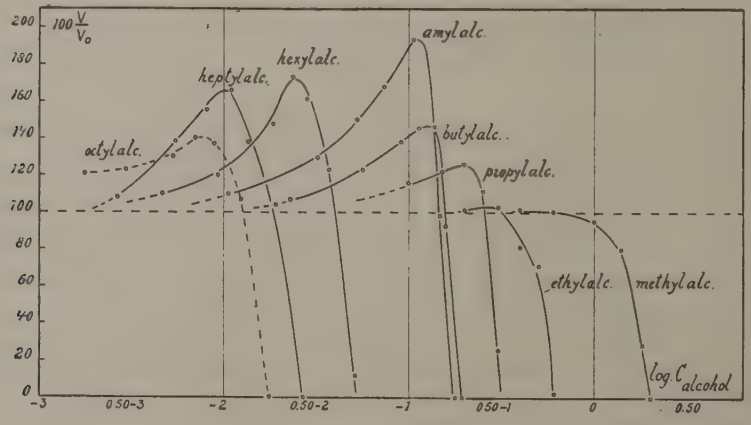

Fig. 1

that the coacervate layer was specifically lighter than the equilibrium liquid. In these cases we used sedimentation tubes which allow of reading the volumes when the coacervate is specifically heavier than the equilibrium as well as in the reverse case.

The results are given in Table 1, namely the volumes read in column 4, expressed in % of the blank series in column 5. Compare Fig. 1, where the latter values are set out against the logarithms of the alcohol concentrations (in mol pL).

From this we see that in sufficient concentration any alcohol finally neutralizes the coacervation, and that any successive term of the homologous series has a stronger effect than the one preceding it:

Octylalc. > heptylalc. > hexylalc. > amylalc. > butylalc. > propylalc. > aethylalc. > methylalc.

We must further point out that the "concentrations" of the alcohols are here the

TABEL I.

Alcohol	Alcohol-concentration		Coacervate-volume		Dryweight mgr/gr.		Coacerv. vol. calcul. from analysis data	
	millimol/L	log C	V in cc	$100\frac{V}{V_0}$	Coacervate	equilibr. liquid	V in cc	$100\frac{V}{V_0}$
Methylalcohol (dryweight of the shaken blank = 75.5 mgr/gr)	blank	— ∼	1.25	100	176.7	66.4	1.21	100
	400	0.60 —1	1.27	102	169.7	67.5	1.21	100
	600	0.78 —1	1.26	101	164.7	68.0	1.23	102
	1000	0.00	1.19	95	154.8	69.2	1.25	103
	1400	0.14^5	1.00	80	140.6	72.6	0.93	77
	1800	0.25^5	0.36	29	112.8	75.7	0.71	59
	2000	0.30	0	0	—	77.5	0	0
Ethylalcohol (dryweight of the shaken blank = 76.3 mgr/gr)	blank	— ∼	1.25	100	175.6	66.2	1.36	100
	200	0.30 —1	1.27	102	165.0	67.1	1.41	104
	300	0.48 —1	1.28	102	152.6	68.0	1.49	110
	400	0.60 —1	1.02	82	143.9	70.2	1.29	95
	500	0.70 —1	0.89	71	134.4	72.3	1.09	80
	600	0.78 —1	0.03	2	103.6	75.2	0.93	68
	700	0.84^5—1	0	0	—	77.2	0	0
n. Propylalcohol (dryweight of the shaken blank = 76.9 mgr/gr)	blank	— ∼	1.32	100	180.3	66.9	1.29	100
	100	0.00 —1	1.53	116	161.8	66.4	1.61	125
	150	0.18 —1	1.61	122	153.5	66.5	1.82	141
	200	0.30 —1	1.66	126	141.4	68.2	1.87	145
	250	0.40 —1	1.47	111	127.9	72.0	1.47	114
	300	0.48 —1	0.34	26	112.2	76.8	0.41	32
	350	0.54^5—1	0	0	—	77.9	0	0
n. Butylalcohol (dryweight of the shaken blank = 76.3 mgr/gr)	blank	— ∼	1.27	100	186.7	66.4	1.21	100
	22.8	0.36 —2	1.36	107	181.5	66.0	1.32	109
	57.0	0.75^6—2	1.56	123	163.0	65.9	1.62	134
	91.2	0.96 —2	1.75	138	150.8	65.9	1.88	155
	114	0.05^8—1	1.85	146	140.6	66.9	1.99	164
	137	0.13^6—1	1.86	147	136.3	68.0	1.93	160
	160	0.20^3—1	1.18	93	110.8	72.2	1.86	154
	171	0.23 —1	0.84	66	106.9	75.3	0.88	73
	194	0.28^7—1	0	0	—	77.3	0	0
n. Amylalcohol (dryweight of the shaken blank = 76.1 mgr/gr)	blank	— ∼	1.24	100	175.7	66.7	1.27	100
	10.6	0.02^6—2	1.36	110	174.6	65.9	1.38	109
	31.9	0.50^4—2	1.61	130	171.6	64.6	1.59	125
	53.1	0.72^6—2	1.86	150	160.0	64.2	1.84	145
	74.3	0.87^1—2	2.08	168	150.5	64.2	2.06	162
	106	0.02^6—1	2.40	194	139.7	63.1	2.53	199
	149	0.17^2—1	1.22	98	129.9	71.0	1.35	106
	181	0.25^6—1	—	—	—	76.5	0	0
Hexylalcohol (dryweight of the shaken blank = 75.8 mgr/gr)	blank	— ∼	1.22	100	179.7	66.0	1.27	100
	4.68	0.67 —3	1.34	110	185.8	64.8	1.35	106
	9.35	0.97 —3	1.47	120	169.5	64.2	1.65	130
	18.7	0.27^2—2	1.81	148	164.4	63.1	1.88	148
	23.4	0.37 —2	2.11	173	152.7	63.0	2.16	170
	28.1	0.44^8—2	1.96	161	157.1	63.0	2.07	163
	37.4	0.57^4—2	1.50	123	153.5	66.4	1.69	133
	51.5	0.71^2—2	0.15	12	123.1	76.4	0.09	7
	70.1	0.84^6—2	0	0	—	77.0	0	0
Heptylalcohol (dryweight of the shaken blank = 76.4 mgr/gr)	blank	— ∼	1.18	100	180.7	66.4	1.28	100
	2.72	0.43^5—3	1.27	108	181.5	65.3	1.41	110
	5.44	0.73^6—3	1.63	138	177.3	64.4	1.57	123
	8.16	0.91^2—3	1.83	155	164.7	63.5	1.89	148
	10.9	0.03^6—2	1.96	166	157.5	63.4	2.04	159
	13.6	0.13^4—2	1.63	138	160.1	65.3	1.75	137
	19.0	0.28 —2	1.23	104	152.2	69.4	1.28	100
	27.2	0.43^5—2	0	0	—	76.7	0	0
Octylalcohol (dryweight of the shaken blank = 76.2 mgr/gr)	blank	— ∼	1.22	100	181.5	66.6	1.23	100
	1.78	0.25 —3	1.48	121	180.8	66.0	1.30	106
	3.55	0.55 —3	1.50	123	176.5	64.2	1.57	128
	5.33	0.76^6—3	1.59	130	162.7	63.5	1.88	153
	7.10	0.85 —3	1.71	140	158.3	63.8	1.93	157
	8.88	0.94^8—3	1.67	137	158.1	64.5	1.84	150
	12.4	0.09^5—2	1.30	107	154.8	68.8	1.26	103
	17.8	0.25 —2	0	0	—	76.2	0	0

quantities of alcohol with reference to the volume of the total system (coacervate + equilibrium liquid). In consequence of the pronounced lipophily of the coacervate, the concentration of the alcohol in it will be greater, likewise the alcohol concentrations in the equilibrium liquid will be smaller than these "concentrations" in columns 2 and 3, and these differences will be the greater as the term is higher in the homologous series.

This is at once seen from the fact that the "concentrations" noted in column 2 as highest for hexyl, heptyl and octyl alcohol (70; 27.2 resp. 17.8 millimol pL) are many times higher than their solubility in water. This obliged us to adopt the method mentioned of adding the higher alcohols to the system in drops.

On account of all this we desist from discussing further in their mutual relations the "concentrations" with which there is neutralization. In order to answer the question whether for each successive term of the homologous series e.g. $^1/_3$ of the concentration is required, we should have to know the alcohol concentrations in the equilibrium liquid, and the concentrations used by us may not be employed for this purpose.

3. *Effect of the alcohols on the colloid percentage of coacervate and equilibrium liquid.*

Whereas the addition of methylalcohol practically only causes the coacervate volume to decrease from the level of the blank series, we already find with eathylalcohol a slight preliminary increase of the coacervate volume, which becomes greater with the following terms: propyl, butyl and amyl alcohol and is also present with the higher terms: hexyl, heptyl and octyl alcohol, although less than with amylalcohol.

We shall now discuss the question what change in condition the coacervate undergoes owing to the alcohols added.

As ultimately, under the decrease of the coacervate volume until zero, all alcohols neutralize the coacervation, it is very likely that along the descending branches of the curves the alcohols will have an "opening" (resp. "swelling") effect, i.e. decrease of the colloid percentage in the coacervate. The question arises what significance is to be attached to the increase of the coacervate volume which most alcohols cause in smaller concentrations.

For that purpose we determined the dryweights of the coacervates and equilibrium liquids (vaporization on the waterbath followed by 2 hours in an electric desiccator at 95°). The results are also given in Table I (columns 6 and 7). Column 6 at once provides the answer to the question asked above: the dryweight of the coacervate is always the highest with the blank series (in the order of 180 mgr per gram) [1]) and all the alcohols — also in the concentration section where the coacervate volume at first shows a noticeable increase — only cause a decrease of the dryweight.

So we arrive at the conclusion that all alcohols — also in smaller concentrations — have an opening (swelling) effect.

The occurrence of maximum curves for the coacervate volume must then be the consequence of the fact that the "solubility" of the coacervate in the lower alcohol-concentrations is not changed to such an extent that it becomes a determining factor for the magnitude of the coacervate volume. The opening (swelling) effect of the alcohols is then expressed by the preliminary increase of the coacervate volume. With higher alcohol concentrations on the other hand, the "solubility" of the coacervate must increase to such an extent that this factor becomes predominant, so that the coacervate volume rapidly falls to zero. As a matter of fact we see in column 7 that the dryweights of the equilibrium liquid with the higher alcohols in the smaller concentrations do not increase but even slightly decrease, after which a rise sets in. In the following section we shall discuss this in detail.

---

[1]) If the biborate should be divided equally over coacervate and equilibrium liquid, about 59 mgr out of the 180 mgr would come to the account of the biborate.

4. *Calculation of the course of the coacervate volume curves from dryweight analyses.*

We shall now show that the typical course of the coacervate volume curves of Fig. 1 may be actually calculated from the dryweight analyses.

If v = volume, d = density and p = dryweight (mgr dry substance per gram) and if we use indices t, c resp. e according as v, d and p refer to the total system (t) the coacervate (c) resp. the equilibrium liquid (e) then:

$$d_c v_c p_c + d_e v_e p_e = d_t v_t p_t.$$

Assuming that approximately

$$d_c = d_e = d_t$$

it follows that

$$v_c = \frac{p_t - p_e}{p_c - p_e} \cdot v_t$$

Value v_t was repeatedly determined direct in a calibrated tube for the blank mixtures and found to be averagely 14.68 cc at 40°.

We have *approximately* assumed this value for the other mixtures as well. Dryweights p_c and p_e (in mgr per gr) were determined in duplicate for the blanks and for each alcohol concentration, and are given in columns 6 and 7 of Table I. Value p_c was twice determined in duplicate when investigating each alcohol series, the first time for the corresponding blank, which macroheterogeneous system was vigorously shaken immediately before a sample was taken, the second time for the alcohol concentration, when the coacervation had just been neutralized, so that there is now a macrohomogeneous system.

For the alcohol concentrations between blank and these highest alcohol concentrations the corresponding p_t values were calculated by interpolation.

The p_t values interpolated thus, are indicated by an asterisk in Table II, which gives an instance of the calculation.

TABLE II. Butylalcohol.

Conc. m. mol p l.	Dryweights mgr p. gr			Coacerv. vol. calculated $14.68 \frac{p_t - p_e}{p_c - p_e}$	Coacerv. vol. experim.
	p_c	p_e	p_t		
blank	186.7	66.4	76.3	1.21	1.27
22.8	181.5	66.0	76.4*	1.32	1.36
57.0	163.0	65.9	76.6*	1.62	1.56
91.2	150.8	65.9	76.8*	1.88	1.75
114.0	140.6	66.9	76.9*	1.99	1.85
136.8	136.3	68.0	77.0*	1.93	1.86
159.6	110.8	72.0	77.1*	1.86	1.18
171.0	106.9	75.3	77.2*	0.88	0.84
193.8	—	77.3	77.3	0	0

As a comparison of the two last columns of the table shows, the course of the coacervate volume corresponds to the course found experimentally. The coacervate volume at first increases, reaches a maximum and then falls to zero. Although the order in value of the coacervate volumes calculated corresponds to those found in experiment, the fact that the correspondence is not absolute need not surprise us, in view of the simplifying assumptions employed. In the same way, from the analysis data the other coacervate

volumes have been calculated (Table I, column 8) and referred to the blanks (last column of Table I). The values obtained thus are set out in Fig. 2 against the logarithms of

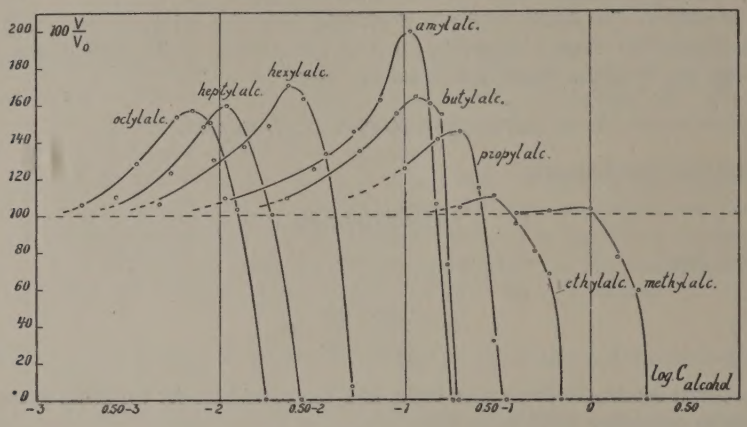

Fig. 2

the alcohol final concentrations. When we compare this figure with Fig. 1, it is seen that in general there is qualitative correspondence [1]). From this correspondence we may conclude that the assumption made at the end of § 3 concerning the shape of the curves in Fig. 1 is correct.

Summary.

1. In mixture of gelatine and oleate sols K salts cause coacervation, a gelatine and oleate containing coacervate separating, which possesses marked lipophile properties.

2. The effect of n-primary alcohols on these coacervates was examined. All these alcohols have a neutralizing effect, the stronger as the C chain is longer:

octylalc. > heptylalc. > hexylalc. > amylalc. > butylalc. > propylalc. > aethylalc. > methylalc.

3. In the smaller concentrations the alcohols increase the coacervate volume to a maximum, in the greater concentrations the coacervate volume rapidly decreases to zero. With methylalcohol this preliminary rise of the coacervate volume is absent.

4. From dryweight analyses it is seen that all alcohols have an "opening" (swelling) effect, also in the section of smaller concentrations.

5. With higher alcohols in the smaller concentrations there is hardly an increase, usually there is decrease of the colloid percentage of the equilibrium liquid; in the higher concentrations on the other hand there is a marked increase of the colloid percentage.

6. From the dryweight analyses the shape of the coacervate volume curves can be calculated qualitatively.

Leiden, Laboratory for Medical Chemistry.

---

[1]) In Fig. 1 the peak of the octylalcohol curve is relatively lower, however, than in Fig. 2. Possibly this is owing to an experimental error in the coacervate volume curve determined direct, e.g. of the blank, which would give the entire curve in Fig. 1 a wrong location. On account of this this curve is marked by a dotted line in Fig. 1.

Palæontology. — *An addition to "Smaller foraminifera from the lower Oligocene of Cuba".* By F. KEIJZER. (Communicated by Prof. L. RUTTEN.)

(Communicated at the meeting of May 30, 1942.)

In this article a number of smaller foraminifera is tabulated, which comes in addition to the faunal list as given some months ago by VAN BELLEN, DE WITTPUYT, RUTGERS and VAN SOEST (Proc. Ned. Akad. v. Wetensch., Amsterdam, **44**, 1140—1146 (1941), 1 plate). 26 Species are new to the fauna, while 2 are mentioned from new localities. These changes in the composition of the faunal list do not affect materially the age-determination of the fauna as a whole, and no specification of the occurrence of these forms in other formations is given here. As the manuscript of the above article had been finished quite a long time before the actual publication, a correction is given for some species, which in the meantime have changed name or have been described as new, but no complete revision of the list has been made, and changes have been made only when the writer stumbled upon them in connection with other work.

The following species are added to the fauna, or are mentioned from other localities:

Planularia westermanni PIJPERS. Loc. 2353 (no. 31).
Pseudoglandulina comatula (CUSHMAN). Loc. 2621, 2714, 3059 (no. 50).
Pseudoglandulina gallowayi CUSHMAN. Loc. 2353, 2393, 2397, 3052.
Pseudoglandulina ovata (CUSHMAN and APPLIN). Loc. 2396, 2397, 3052.
Guttulina irregularis (D'ORBIGNY). Loc. 3071.
Guttulina irregularis (D'ORBIGNY), var. *nipponensis* CUSHMAN and OZAWA. Loc. 3081.
Guttulina problema D'ORBIGNY. Loc. 2393.
Pyrulina fusiformis (ROEMER). Loc. 3059.
Globulina münsteri (REUSS). Loc. 3059.
Sigmomorphina bornemanni CUSHMAN and OZAWA. Loc. 3059, 3081.
Glandulina cubensis CUSHMAN and BERMUDEZ. Loc. 2354, 2621, 3058.
Glandulina laevigata D'ORBIGNY. Loc. 2396, 2622, 2720, 3052, 3059, 3071, 3321, 3323, 3530.
Pleurostomella alternans SCHWAGER. Loc. 2393.
Pleurostomella brevis SCHWAGER. Loc. 2397.
Pleurostomella obesa CUSHMAN and BERMUDEZ. Loc. 3058.
Siphogenerina mayi CUSHMAN and PARKER. Loc. 3321.
Siphogenerina multicostata CUSHMAN and JARVIS. Loc. 2392, 2394, 2395, 2397, 2398, 2399, 3303, 3321, 3323.
Siphogenerina multicostata CUSHMAN and JARVIS, var. *denticosta* n. var. Loc. 2393, 2399, 3303.
Plectofrondicularia cf. *floridana* CUSHMAN. Loc. 2393.
Ellipsoidina ellipsoides SEGUENZA. Loc. 3530.
Ellipsoglandulina velascoensis CUSHMAN. Loc. 3081.
Ellipsoglandulina labiata SCHWAGER. Loc. 3056.
Cassidulina pacifica CUSHMAN. Loc. 2395, 2396, 2397, 2621, 3050.
Cassidulina havanensis CUSHMAN and BERMUDEZ. Loc. 2359.
Chilostomella ovoidea REUSS. Loc. 3050, 3059.
Chilostomella oolina SCHWAGER. Loc. 2622.
Sphaeroidina bulloides D'ORBIGNY. Loc. 2354, 2397, 2695.
Globigerinella subcretacea LOMNICKI. Loc. 2353, 2392, 2396.

The following changes in the nomenclature should be made:

1. *Nodosaria* aff. *carinata* NEUGEBOREN (no. 39) = *Nodosari nuttalli* HEDBERG (Journ. of Pal. vol. 11, 1937, p. 673, pl. 91, f. 6).

2. *Uvigerina canariensis* D'ORBIGNY, var. NUTTALL 1932 (no. 79, p. 1142) = *Uvigerina nuttalli* CUSHMAN and EDWARDS (Contr. Cushm. Lab. vol. 14, pt. 4, 1938, p. 82, pl. 14, f. 3—5). Figures 27—30, referred in the text to this species, represent, however, *Uvigerina pygmea* D'ORBIGNY, var. NUTTALL 1928 of the list (no. 82), but in the writer's opinion they are much closer to *Uvigerina mexicana* NUTTALL (Journ. of Pal. vol. 6, 1932, p. 22, pl. 5, f. 12, 13), which is not mentioned in the list.

3. The name of *Eponides byramensis* (CUSHMAN), var. *cubensis* PALMER and BERMUDEZ 1936 (no. 94; Mem. Soc. Cub. Hist. Nat. vol. 10, p. 302, pl. 20, f. 4—6) cannot be maintained, as "cubensis" is already occupied by *Eponides cubensis* PALMER and BERMUDEZ (ibid., vol. 9, 1935, p. 252, pl. 21, f. 10—12). The variety differs so much from *Eponides byramensis* (CUSHMAN) (See PALMER and BERMUDEZ l.c. 1936), that it is better regarded as a distinct species. The name of *Eponides bermudezi* is proposed here.

4. *Siphonina cubensis* VAN BELLEN (no. 102, p. 1144, f. 1—3) = *Siphonina nuda* CUSHMAN and BERMUDEZ (Contr. Cushm. Lab. vol. 12, pt. 3, 1936, p. 62, pl. 11, f. 3—6).

Siphogenerina multicostata CUSHMAN and JARVIS, var. *denticosta* n. var. (text-fig. 1, 2).
Contr. Cushm. Lab. vol. 5, pt. 1, 1929, p. 14, pl. 3, f. 6.

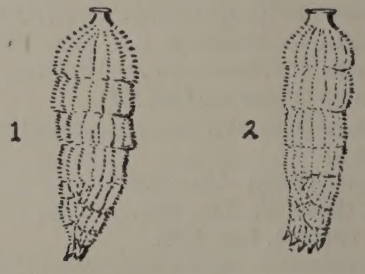

Variety differing only from the typical form in having the costae finely but distinctly denticulate.

Length up to 0.86 mm. Locs. 2393, 2399, 3303.

P. 1459/1.

Verantwoordelijk voor den geheelen inhoud: M. W. WOERDEMAN te Amsterdam. Uitgever: N.V. Noord-Hollandsche Uitgevers Maatschappij, N.Z. Voorburgwal 68–70, Amsterdam. Drukker: Drukkerij Holland N.V., N.Z. Voorburgwal 68–70, Amsterdam.